



Western Washington University  
Western CEDAR

---

WWU Graduate School Collection

WWU Graduate and Undergraduate Scholarship

---

Spring 2021

## Synthesis of guaipyridine alkaloids rupestines C, D and K with studies toward the synthesis of rupestines B, J, L and M

Briana J. Mulligan

Western Washington University, brimulligan1@gmail.com

Follow this and additional works at: <https://cedar.wwu.edu/wwuet>

 Part of the [Chemistry Commons](#)

---

### Recommended Citation

Mulligan, Briana J., "Synthesis of guaipyridine alkaloids rupestines C, D and K with studies toward the synthesis of rupestines B, J, L and M" (2021). *WWU Graduate School Collection*. 1036.  
<https://cedar.wwu.edu/wwuet/1036>

This Masters Thesis is brought to you for free and open access by the WWU Graduate and Undergraduate Scholarship at Western CEDAR. It has been accepted for inclusion in WWU Graduate School Collection by an authorized administrator of Western CEDAR. For more information, please contact [westerncedar@wwu.edu](mailto:westerncedar@wwu.edu).

**Synthesis of guaipyridine alkaloids rupestines C, D and K with studies toward the synthesis of rupestines B, J, L and M**

By

Briana J. Mulligan

Accepted in Partial Completion  
of the Requirements for the Degree  
Master of Science

ADVISORY COMMITTEE

Dr. James R. Vyvyan, Chair

Dr. Margaret Scheuermann

Dr. Mike Larsen

GRADUATE SCHOOL

David L. Patrick, Dean

## **Master's Thesis**

In presenting this thesis in partial fulfillment of the requirements for a master's degree at Western Washington University, I grant to Western Washington University the non-exclusive royalty-free right to archive, reproduce, distribute, and display the thesis in any and all forms, including electronic format, via any digital library mechanisms maintained by WWU.

I represent and warrant this is my original work, and does not infringe or violate any rights of others. I warrant that I have obtained written permissions from the owner of any third party copyrighted material included in these files.

I acknowledge that I retain ownership rights to the copyright of this work, including but not limited to the right to use all or part of this work in future works, such as articles or books.

Library users are granted permission for individual, research and non-commercial reproduction of this work for educational purposes only. Any further digital posting of this document requires specific permission from the author.

Any copying or publication of this thesis for commercial purposes, or for financial gain, is not allowed without my written permission.

Briana Mulligan

May 21st, 2021

**Synthesis of guaipyridine alkaloids rupestines C, D and K with studies toward the synthesis  
of rupestines B, J, L and M**

A Thesis  
Presented to  
The Faculty of  
Western Washington University

In Partial Fulfillment  
Of the Requirements for the Degree  
Master of Science

by  
Briana J. Mulligan  
June 2021

## Abstract

Hepatocellular carcinoma (HCC) is a type of primary liver cancer that is responsible for roughly 700,000 deaths around the world each year. While invasive treatment methods for HCC have proven to be limited, there are drug treatments available that show promising features. The structural elements of these drugs have given rise to an interest in guaipyridine alkaloids, specifically a family of naturally occurring guaipyridine alkaloids known as the rupestines. The rupestines have previously been isolated from the flowers of the plant *Artemisia rupestris*. This plant has been known for its reported antitumor, antiviral and antibacterial properties when used in traditional Chinese medicine. An additional guaipyridine alkaloid worth noting is cananodine, which has been isolated from the fruits of *Canaga odorata*. Cananodine has shown activity toward two lines of HCC cancer cells, with potency greater than the HCC drug treatment Sorafenib. This increase in bioactivity has made the core guaipyridine structure of cananodine an attractive synthetic target. Considering the rupestines contain this same bicyclic core, it is possible that they will reveal similar activity to that of cananodine. In this report, rupestines B-D and J-M are targeted for total synthesis. The synthesis of rupestine D has been reported in 6 steps from a picolyl bromide substrate in good to excellent step-wise yields. The formation of the 7-membered carbocycle to establish the key guaipyridine core is accomplished via an intramolecular Mizoroki-Heck cyclization. This forms in a mixture of rupestine D and epi-rupestine D in a 1:2 ratio. Isolation of rupestine D has proven to be difficult when using the initial synthetic route. Upon reversal of the final two synthetic steps, the separation of diastereomers was accomplished with ease, allowing for the synthesis of rupestine D as a single diastereomer. These methods were employed for the synthesis and isolation of rupestine C in 6 steps with poor to excellent step-wise yields. The methyl ketone-containing rupestine D and epi-rupestine D can then serve as the starting material for the

syntheses of rupestines J and K, as well as L and M. Rupestine K has been synthesized and isolated via a Rubottom oxidation of a silyl enol ether substrate. Progress is currently being made toward the synthesis of rupestine J, L and M.

## Acknowledgments

***Research Advisor:***

Dr. James R. Vyvyan

***Thesis Committee Members:***

Dr. Margaret Scheuermann

Dr. Mike Larsen

***Financial Support:***

WWU Office of Research and  
Sponsored Programs

***Instrument Technicians and Support:***

Dr. Hla Win-Piazza

Sam Danforth

## Table of Contents

<b>Abstract</b> .....	iv
<b>Acknowledgments</b> .....	vi
<b>List of Tables and Figures</b> .....	ix
<b>1. Introduction</b> .....	1
<b>1.1 Hepatocellular Carcinoma (HCC)</b> .....	1
<b>1.2 HCC treatment methods</b> .....	2
<b>1.3 Natural Products: Cananodine and Rupestines</b> .....	4
<b>1.4 Previous Synthetic Studies: Cananodine</b> .....	7
<b>1.5 Previous Synthetic Studies: Rupestines</b> .....	9
<b>2. Synthesis and isolation of Rupestine D</b> .....	17
<b>2.1 Initial synthetic route</b> .....	17
<b>2.2 Intramolecular Heck cyclization</b> .....	18
<b>2.3 Optimization of Grignard reaction</b> .....	21
<b>2.4 Alternative synthetic route</b> .....	22
<b>2.5 Separation of diastereomers</b> .....	25
<b>2.6 Hydrogenation: Diastereomeric ratios</b> .....	26
<b>3. Studies toward the synthesis of Rupestines J and K</b> .....	28
<b>3.1 Intended synthetic route</b> .....	28
<b>3.2 Benzoin condensation</b> .....	29

3.3	Alternative synthetic route.....	30
3.4	Optimization of silyl enol ether formation.....	32
3.5	Optimization of Rubottom oxidation.....	33
<b>4.</b>	<b>Studies toward the synthesis of Rupestines L and M.....</b>	<b>36</b>
4.1	Intended synthetic route.....	36
4.2	Optimization of Baeyer-Villiger oxidation.....	36
<b>5.</b>	<b>Alternative route to Starchman <i>et al.</i> synthesis of rupestines B and C... 40</b>	<b>40</b>
<b>6.</b>	<b>Conclusions.....</b>	<b>43</b>
<b>7.</b>	<b>Experimental.....</b>	<b>44</b>
<b>8.</b>	<b>References.....</b>	<b>61</b>
<b>9.</b>	<b>Supporting Information.....</b>	<b>64</b>

## List of Tables and Figures

<b>Figure 1.</b> Hydrogen-bonding interactions between the cysteine 531 residue of the B-Raf kinase and HCC drug treatments sorafenib and regorafenib.....	3
<b>Figure 2.</b> Natural products isolated from the fruits of <i>Cananga odorata</i> .....	5
<b>Figure 3.</b> Proposed hydrogen-bonding interactions between the cysteine 531 residue of the B-Raf kinase and cananodine.....	6
<b>Figure 4.</b> Rupestines A-M.....	7
<b>Figure 5.</b> Compounds synthesized and isolated by Büchi and van der Gen.....	8
<b>Figure 6.</b> Separation of rupestine D and epi-rupestine D via radial chromatography.....	25
<b>Figure 7.</b> Separation of nitriles <b>2.9</b> and <b>2.8</b> via radial chromatography.....	26
<b>Figure 8.</b> Major conformation of alkenes <b>2.1</b> and <b>2.2</b> .....	27
<b>Table 1.</b> Optimization of intramolecular Heck reaction.....	19
<b>Table 2.</b> <sup>1</sup> H NMR data comparison for rupestine D.....	24
<b>Table 3.</b> <sup>13</sup> C NMR data comparison for rupestine D.....	24
<b>Table 4.</b> Optimization of benzoin condensation on non-precious substrate <b>3.4</b> .....	30
<b>Table 5.</b> Optimization of silyl enol ether formation.....	32
<b>Table 6.</b> Optimization of the Rubottom oxidation.....	34
<b>Table 7.</b> <sup>1</sup> H NMR data comparison for rupestine K.....	34
<b>Table 8.</b> <sup>13</sup> C NMR data comparison for rupestine K.....	35
<b>Table 9.</b> Optimization of Baeyer-Villiger oxidation with non-precious substrate <b>4.5</b> .....	38
<b>Table 10.</b> Optimization of Baeyer-Villiger oxidation with substrates <b>1.18</b> and <b>2.0</b> .....	39
<b>Table 11.</b> <sup>1</sup> H NMR data comparison for rupestine C ( <b>1.17</b> ).....	41
<b>Table 12.</b> <sup>13</sup> C NMR data comparison for rupestine C ( <b>1.17</b> ).....	42

## **Introduction**

### **1.1 Hepatocellular carcinoma (HCC)**

Hepatocellular carcinoma (HCC) is the most common form of liver cancer that results in approximately 700,000 deaths around the world each year.<sup>1</sup> HCC has been reported to be the third most common cause of cancer-related death worldwide with diagnosis tripling in the last 40 years.<sup>1,2</sup> HCC cases are most prevalent in Sub-Saharan Africa and Southeast Asia, where hepatitis B and aflatoxin exposure are common.<sup>1</sup> Underlying liver diseases such as hepatitis B (HBV), hepatitis C (HCV) and cirrhosis of the liver are seen in a majority of HCC patients.<sup>3,4</sup> Cirrhosis is scarring of the liver tissue that prevents the cells from being functional again. This is most often seen in HBV and HCV patients, but is also seen in cases of chronic alcohol use.<sup>5</sup>

Recently, progress has been being made toward the treatment of HCV related HCC with direct-acting antiviral (DAA) agents. It was found the HCV related HCC patients had a 61.4% chance at a 5-year overall survival (OS, survival time after diagnosis) when using DAA agents, and a 24.2% chance of a 5-year OS without DAA agents.<sup>6</sup> Liver function can also decrease as a result of metastasis, where the cancer grows secondary tumors external to the primary tumor. The rate at which the liver loses its function after the time of diagnosis plays a crucial role in the ability to treat HCC. It was reported that 44% of patients diagnosed with HCC prior to loss in liver function have a 33% chance of a 5-year OS.<sup>7</sup> The chance of a 5-year OS decreases to 11% once the cancer has metastasized and 2% once the cancer has spread to another region in the body.<sup>7</sup> Significant progress has been made when it comes to potential treatments for HCC, however invasive methods including chemotherapy, radiation, and surgical resection have shown limited effectiveness. It has previously been reported that only 10-15% of cases show responses to chemotherapy and radiation, and less than 18% of patients are candidates for surgical resection.<sup>8</sup> While these invasive methods

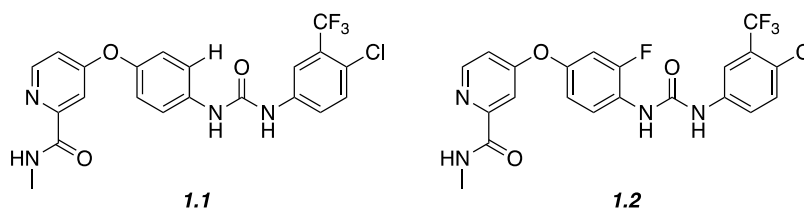
can be beneficial for a number of patients, it is crucial to continue investigating treatments that can impact a greater fraction of HCC patients.<sup>8</sup>

## 1.2 HCC treatment methods

A kinase is an enzyme that is responsible for phosphorylation of certain biomolecules. Small molecule kinase inhibitors are an attractive class of drugs because of their potential ability to treat cancer.<sup>9</sup> Kinase inhibitors function as competitors with adenosine triphosphate (ATP). When the binding of a kinase inhibitor is favored over the binding of ATP, phosphorylation of target proteins cannot occur.<sup>10</sup> Type I kinase inhibitors prevent phosphorylation by binding to the active site of the target enzyme, while type II kinase inhibitors will bind to the active site in a way that alters the conformation of the enzyme, forcing it into an inactive form.<sup>9</sup> In order to design effective type II kinase inhibitors, it is necessary to have an understanding of the SARs (structure activity relationships) that occur at the enzymes active site.

There are currently 37 FDA-approved kinase inhibitors that can be divided into groups based on their target kinases.<sup>10</sup> For HCC treatment, the active site residues responsible for tumor progression are serine and threonine kinases (Raf-1 and B-Raf).<sup>11</sup> Inhibition of these protein kinases has been achieved with a drug known as sorafenib (Nexavar<sup>®</sup> [1.1]) which was approved by the FDA in 2007 for HCC treatment.<sup>11</sup> While the average survival rate is increased by 2.8 months when taking sorafenib, the cost of treatment falls around \$15,000 per month.<sup>12</sup> A derivative of sorafenib known as regorafenib (Stivarga<sup>®</sup>, [1.2]) was approved by the FDA in 2017 for the treatment of HCC.<sup>13</sup> This derivative has been shown to have similar effectiveness to that of sorafenib, with a survival increase of 2.8 months compared to the placebo group.<sup>13</sup> The only

structural difference between **1.1** and **1.2** is the presence of a fluorine atom adjacent to the aryl urea in **1.2**.



Sorafenib has shown activity toward the Hep G<sub>2</sub> cell line of HCC, with a potency (IC<sub>50</sub> value) of 4.5 μM.<sup>11</sup> This results in the inhibition of the B-Raf and C-Raf protein kinases.<sup>11</sup> In order to understand how this inhibition process occurs, it is necessary to consider the functional groups present in both the drug and the active site residues. This interaction can be seen in **1.3** (Figure 1), where the pyridine head group of sorafenib (or regorafenib) interacts via hydrogen-bonding with the cystine 531 residue of the B-Raf kinase. As the drug approaches this active site, the inactive conformation of the B-Raf kinase is induced, preventing any further tumor growth. These hydrogen-bonding capabilities have made pyridine moieties a common feature among type II kinase inhibitors.<sup>14</sup> It should also be noted that the diaryl urea group present in sorafenib and regorafenib is a common functional group in type-II kinase inhibitors (interactions with other residues not shown).

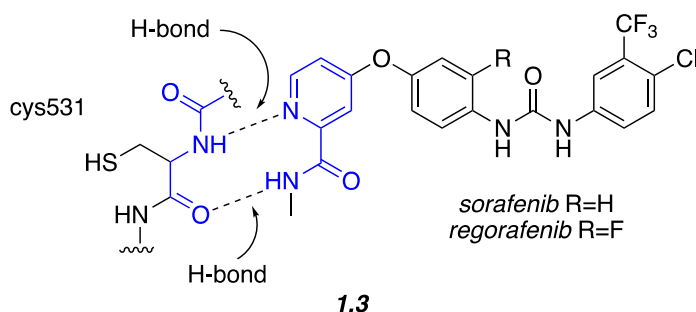
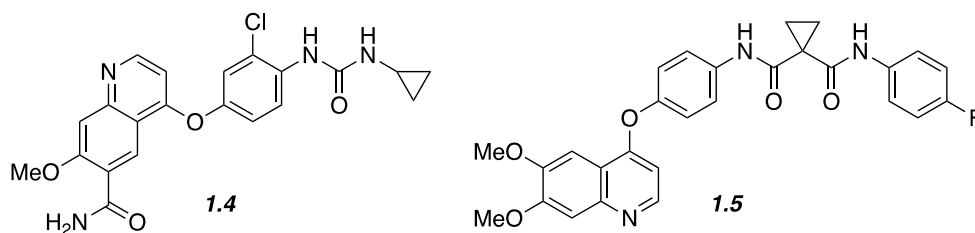


**Figure 1.** Hydrogen-bonding interactions between the cysteine 531 residue of the B-Raf kinase and HCC drug treatments sorafenib and regorafenib.

Similar derivations of these key structural features have recently been synthesized and utilized for HCC treatment. In 2018, the FDA approved lenvatinib (Lenvima<sup>®</sup> [**1.4**]) as an additional first line treatment.<sup>15,16</sup> It was found that lenvatinib was not statistically superior to sorafenib, however, it has become the new first line treatment because of its increase in progression-free survival.<sup>17</sup> In 2019 the FDA approved cabozantinib (Cabometyx<sup>®</sup> [**1.5**]) as a second line treatment for patients with little to no response to first line therapies.<sup>17,18</sup>



### 1.3 Natural Products: Cananodine and Rupestines

Natural products play a crucial role in drug development and cancer treatment. A naturally occurring guaipyridine alkaloid known as cananodine was isolated from the fruits of *Cananga odorata* (trivially known as the “ylang-ylang” tree).<sup>19</sup> Upon distillation of the ylang-ylang tree flowers, an essential oil is obtained and used in perfumes and for aromatherapy.<sup>20</sup> This plant belongs to the *Annonaceae* family which is known for treating malignant tumors.<sup>21</sup> *C. odorata* has been used in Taiwanese folk medicine, specifically for the topical treatment of asthma and malaria, and the oral treatment of stomach ulcers and fevers.<sup>22</sup> The discovery of cananodine began when Wu *et al.* successfully isolated eight different compounds from the fruits of *C. odorata*, a guaipyridine alkaloid, cananodine (**1.6**), three eudesmane sesquiterpenes, cryptomerediol 11- $\alpha$ -L-

rhamnoside (**1.7**),  $\gamma$ -eudesmol 11- $\alpha$ -L-rhamnoside (**1.8**) and  $\gamma$ -eudesmol (**1.9**) and four alkaloids, (+)-ushinsunine- $\beta$ -N-oxide (**1.10**), cleistopholine (**1.11**), *N*-*trans*-feruloyltyramine (**1.12**) and lyscamine (**1.13**).<sup>22</sup> Guaipyridine alkaloids like cananodine are attractive target compounds because they possess a unique structure consisting of a seven-membered carbocycle that is fused to a pyridine ring. Recall that the type II kinase inhibitors previously mentioned also contain this pyridine head group, making the family of guaipyridine alkaloids a promising group for potential HCC treatment.

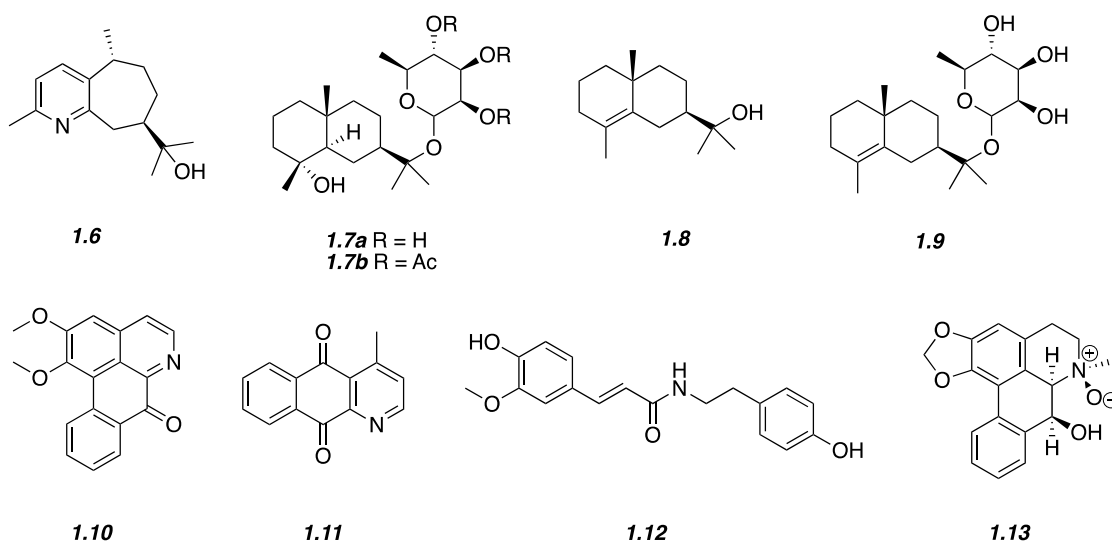


**Figure 2.** Natural products isolated from the fruits of *Cananga odorata*.

Cananodine was found to be biologically active, possessing activity toward two different cell lines in HCC.<sup>22</sup> An  $IC_{50}$  value of 0.94  $\mu$ M was shown toward the Hep G<sub>2</sub> cell line of HCC, which corresponds to a greater potency than the previously mentioned type II kinase inhibitors.<sup>22</sup> An  $IC_{50}$  value of 3.8  $\mu$ g/mL was shown toward the Hep 2,2,15 cell line, which was not seen in the previous drugs at all.<sup>22</sup> These results suggest that cananodine could be a more effective drug than sorafenib and regorafenib. The predicted binding sites of cananodine to the active site of the B-Raf kinase

(**1.14**) are shown in Figure 3, where the pyridine nitrogen remains a hydrogen-bond acceptor, and now a tertiary alcohol acts as the hydrogen bond donor (as opposed to the amide nitrogen of sorafenib/regorafenib).

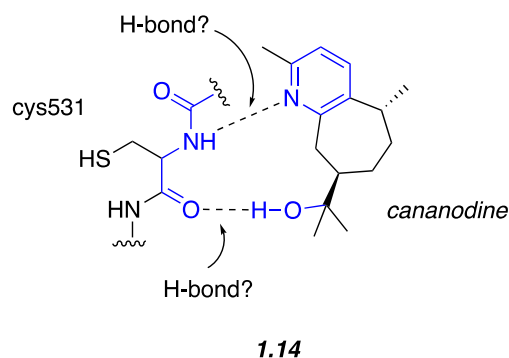


**Figure 3.** Proposed hydrogen-bonding interactions between the cysteine 531 residue of the B-Raf kinase and cananodine.

These promising results seen with cananodine have made guaipyridine alkaloids an interesting target for potential drug therapy. A group of guaipyridine alkaloids known as the rupestines (Figure 4) have previously been isolated from *Artemisia rupestris*. *A. rupestris* is a plant that has been used in traditional Chinese medicine for its antiviral, antibacterial and antitumor properties.<sup>23</sup> In 2010, Asia *et al.* isolated rupestines A-D (**1.15-1.18**), followed by rupestines F-M (**1.19-1.26**) in 2012 (Figure 4).<sup>23</sup> Each rupestone possesses the same bicyclic system that is present in cananodine. The differences between each of these alkaloids are seen at the 5- and 8-positions where there is varying stereochemistry. Additionally, the substituent at the 8-position varies, allowing a wide range of potential bioactivity via hydrogen bond donating and accepting. Both cananodine and the rupestines can only be isolated naturally in impractically small quantities, making them an attractive synthetic target.

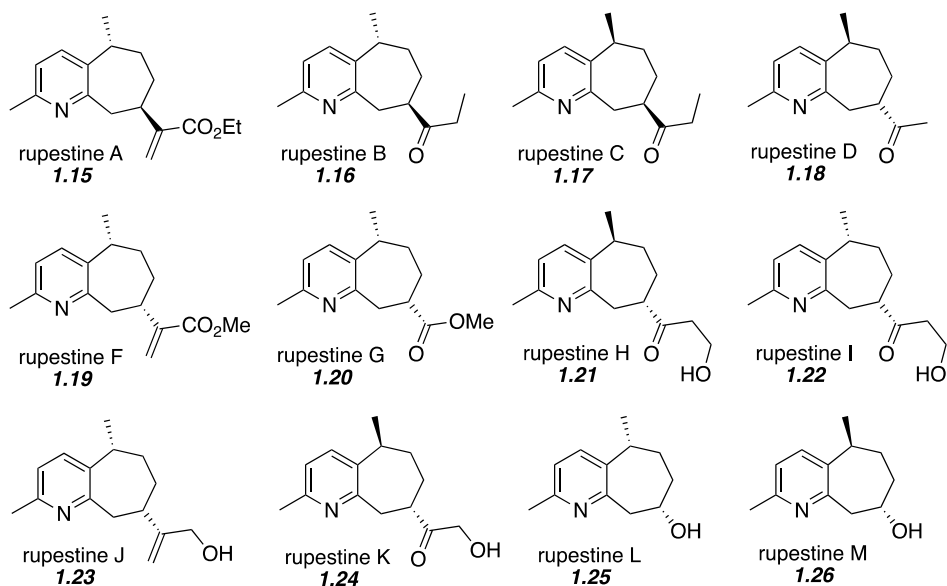


**Figure 4.** Rupestines A-M

#### 1.4 Previous Synthetic Studies: Guaipyridine Alkaloids

Before cananodine became a sought-after natural product, Büchi and van der Gen reported the first syntheses of guaipyridine alkaloids. Büchi *et al.* accomplished the isolation of two naturally occurring sesquiterpene alkaloids from patchouli oil, patchoulypyridine (**1.27**) and epiguaipyridine (**1.28**).<sup>24</sup> Upon investigation of these compounds by van der Gen *et al.*, it was found that a major component of patchouli oil, guaiol (**1.29**), revealed similar spectral properties to that of epiguaipyridine.<sup>25</sup> This was surprising considering guaiol (**1.29**) possesses *7R*, *10S* stereochemistry, and Büchi reported epiguaipyridine as a *7R*, *10R* structure.

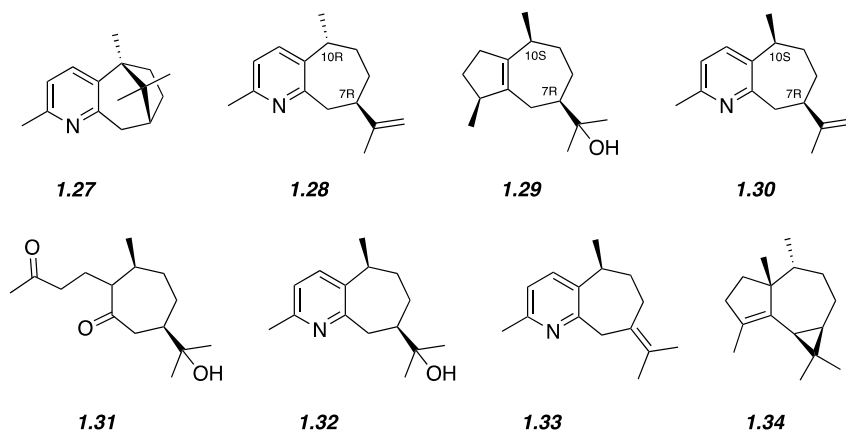
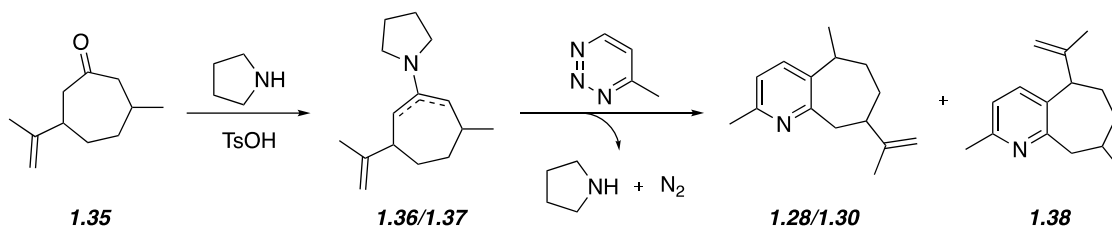


**Figure 5.** Compounds synthesized and isolated by Büchi and van der Gen.

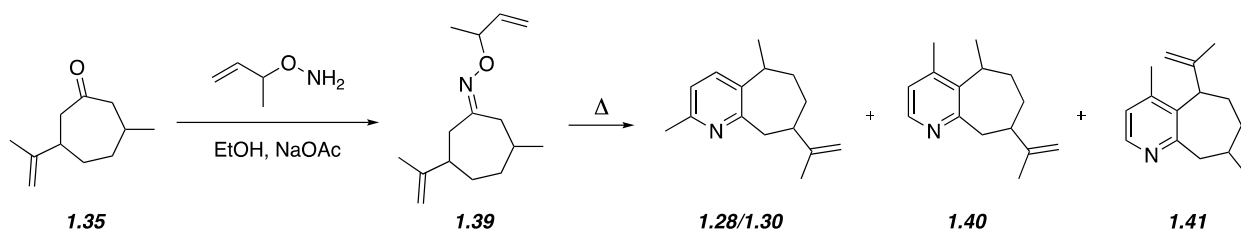
This led van der Gen to synthesize epiguaipyridine (**1.28**) and its C-10 epimer (**1.30**) from substrates with already established configurations. Guaiol was subjected to a palladium catalyzed alkene isomerization followed by ozonolysis to form the hydroxydiketone (**1.31**). Subsequent treatment with hydroxylamine hydrochloride in boiling ethanol lead to the hydroxy pyridine derivative (**1.32**). Upon dehydration with thionyl chloride, two alkene isomers were produced (**1.30** and **1.33**). Spectral analysis revealed that the *10S* epimer **1.30** was identical to the compound isolated from patchouli oil and the compound isolated by Büchi *et al.* The synthesis of epiguaipyridine (**1.28**) was accomplished from the sesquiterpene  $\alpha$ -gurjunene (**1.34**) via a diketone intermediate similar to the synthesis of the C-10 epimer. The isolated epiguaipyridine revealed spectral properties that differed from the C-10 epimer, proving that the configuration was initially misassigned by Büchi. Two additional syntheses of **1.28** and **1.30** were later reported by Okatani and Koyama *et al.*<sup>26</sup> The first synthesis was accomplished via a Diels-Alder reaction of 1,2,3-triazine with enamines which produced three isomeric products (**1.28**, **1.30** and **1.38**) (Scheme 1). The desired products, **1.28** and **1.30** were obtained in a 2:1 diastereomeric ratio. In the second synthesis, **1.35** was treated with O-( $\alpha$ -methylallyl)hydroxylamine to yield an oxime intermediate

(**1.39**). Subsequent thermal decomposition provided compounds **1.28**, **1.30**, **1.40** and **1.41** (Scheme 2).

**Scheme 1.** Synthesis of epiguaipyridine and its C-10 epimer via a Diels Alder pathway.<sup>26a</sup>



**Scheme 2.** Synthesis of epiguaipyridine and its C-10 epimer via an oxime intermediate.<sup>26b</sup>

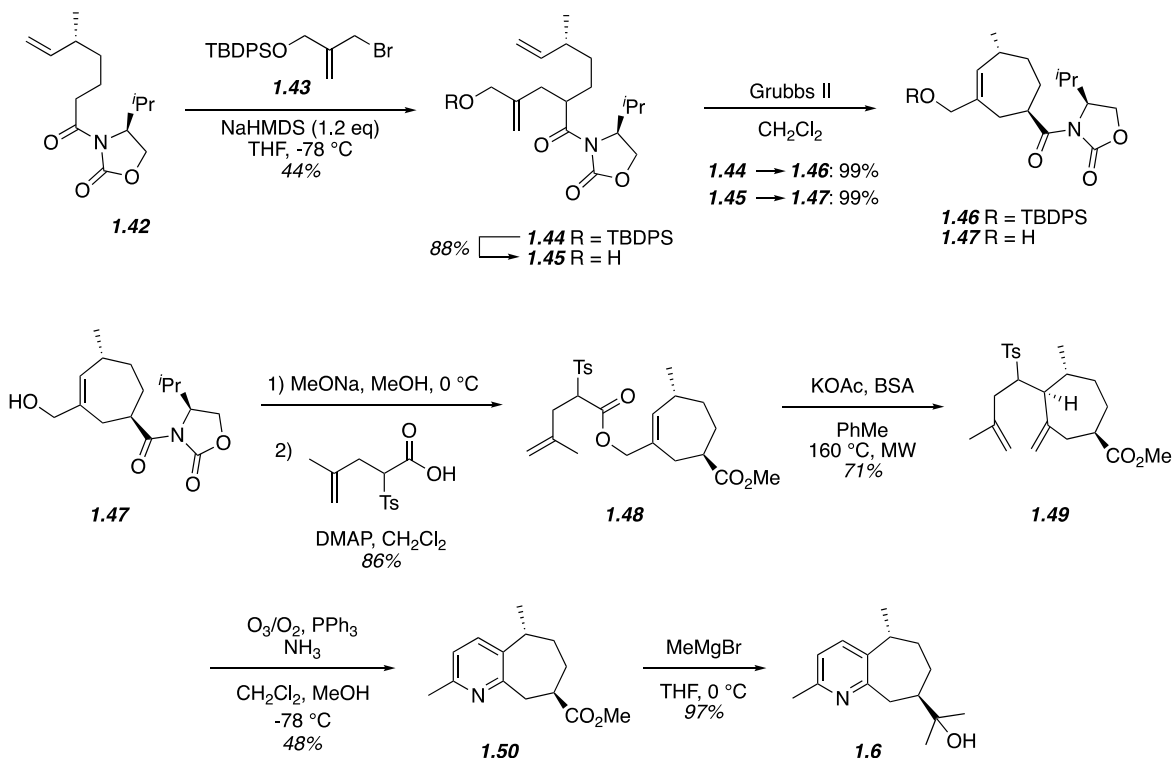


## 1.5 Previous Synthetic Studies: Cananodine

The first total synthesis of (+)-cananodine was reported by Craig and Henry in a total of 15 steps (Scheme 3).<sup>27</sup> This provided the single stereoisomer (**1.6**) in 4% yield. In order to set the stereochemistry, chiral auxiliaries were utilized. The desired auxiliary (**1.42**) was prepared in multiple steps using (*R*)-(-)-citronellene and (*S*)-valinol-derived oxazolidinone. Moving forward, the synthesis began with a diastereoselective allylation between the lithium enolate of the auxiliary and bromide (**1.43**) to provide the desired 1,7-diene (**1.44**). To form the cycloheptene ring of (**1.46**), a ring-closing olefin metathesis (RCM) was performed in the presence of the second-generation Grubbs catalyst. When attempting the subsequent desilylation in both acidic and basic conditions, decomposition occurred. To alleviate this issue, the RCM step was switched with the

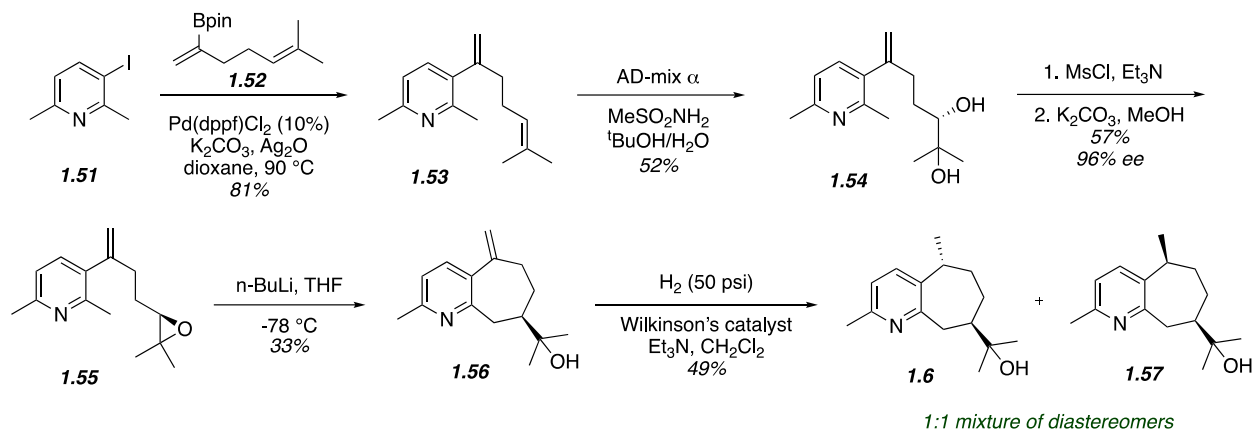
desilylation to provide the deprotected intermediate (**1.45**). Both intermediates **1.44** and **1.45** were able to be carried through the RCM in identical yields. After removal of the chiral auxiliary under basic conditions, esterification of the primary alcohol (**1.47**) with 4-methyl-2-(4-tolylsulfonyl)-4-pentenoic acid provided the desired alkene (**1.48**). This intermediate was then allowed to undergo a decarboxylative Claisen rearrangement to provide the desired 1,6-diene (**1.49**). Microwave-irradiation was implemented, and the resulting product was a mixture of two of the four possible diastereomers. In order to establish the pyridine ring of **1.50**, ozonolysis of **1.49** was followed by the addition of triphenylphosphine and ethanolic ammonia. The final step in the synthesis required reaction of (**1.50**) with excess methyl magnesium bromide to yield the final product, (+)-cananodine (**1.6**). This total synthesis provided promising results; however, due to the 4% over yield, it would not be practical to apply on an industrial scale.

**Scheme 3.** Synthesis of (+)-cananodine reported by Craig and Henry.<sup>27</sup>



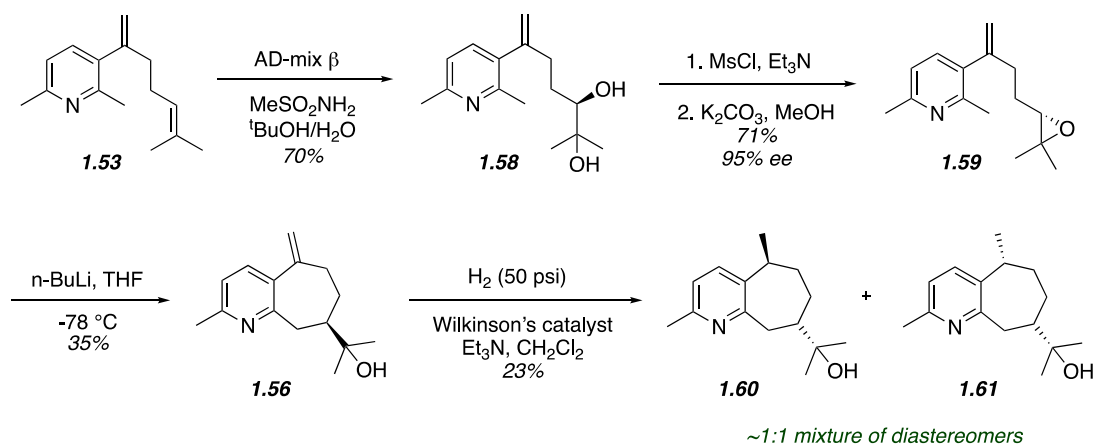
This led to the more recent total synthesis of (+)-cananodine which was accomplished in 2017 by Shelton *et al.* (Scheme 4).<sup>28</sup> The key step in this synthesis was an intramolecular epoxide opening reaction to form the seven-membered carbocycle of the guaipyridine core. The synthesis began with the pyridyl iodide substrate (**1.51**) undergoing a palladium catalyzed cross-coupling reaction with dienylboronate (**1.52**) in the presence of silver oxide. The diene intermediate (**1.53**) then underwent an asymmetric dihydroxylation to provide diol (**1.54**), which was converted to the epoxide (**1.55**) via a mesylate intermediate. The epoxide was then subjected to *n*-butyllithium which deprotonated the picolyl position of the pyridine ring and allowed for formation of the 7-membered carbocycle of **1.56**. The final step in the synthesis was a hydrogenation of the 1,1-disubstituted alkene in the presence of Wilkinson's catalyst to afford the desired (+)-cananodine (**1.6**) and its epimer (**1.57**) in a 1:1 ratio. While these results were encouraging, a downfall in the synthesis is seen in the step involving *n*-butyllithium. Since there are two possible sites of picolyl proton abstraction, there is roughly a 50% chance that the desired proton will be removed to form the cyclized product. Additionally, the non-diastereoselective hydrogenation led to an inseparable mixture of diastereomers.

**Scheme 4.** Synthesis of (+)-cananodine and its epimer by Shelton *et al.*<sup>28</sup>



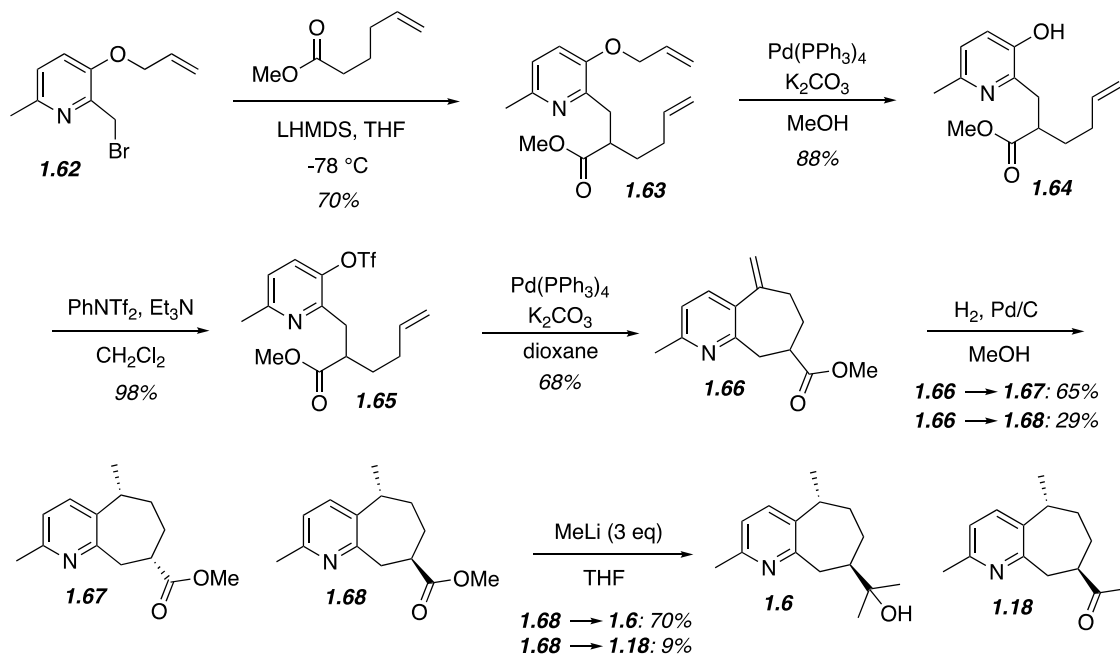
Shelton *et al.* also reported the synthesis of ent-canandine (**1.60**) starting from the same pyridyl iodide substrate (**1.51**). The key differing step is seen in the dihydroxylation of **1.53** with AD-mix  $\beta$  instead of the previously implemented AD-mix  $\alpha$  (Scheme 5). The subsequent steps were carried out similar to Scheme 4 and the resulting ent-canandine (**1.50**) and its epimer (**1.61**) were formed in a 1:1 ratio.

**Scheme 5.** Synthesis of ent-canandine and its epimer by Shelton *et al.*<sup>28</sup>



The most recently reported synthesis of cananodine by Shelton *et al.* was accomplished via an intramolecular Mizoroki-Heck cyclization (Scheme 6).<sup>29</sup> The synthesis began with the alkylation of picolyl bromide (**1.62**) with methyl 5-hexenoate using LHMDS. The allyl ether of intermediate **1.63** was then removed using a palladium(0) catalyst in the presence of potassium carbonate and methanol. After triflation of **1.64** with *N*-phenyltriflimide, **1.65** was reacted using the optimal Heck cyclization conditions. After a simple hydrogenation with palladium on carbon, the methyl ester diastereomers (**1.67** and **1.68**) were separated. Intermediate **1.68** was then exposed to 3 equivalents of methyl lithium to provide cananodine in a 70% yield. Rupestine D (**1.18**) was also obtained as a side product in a 9% yield.

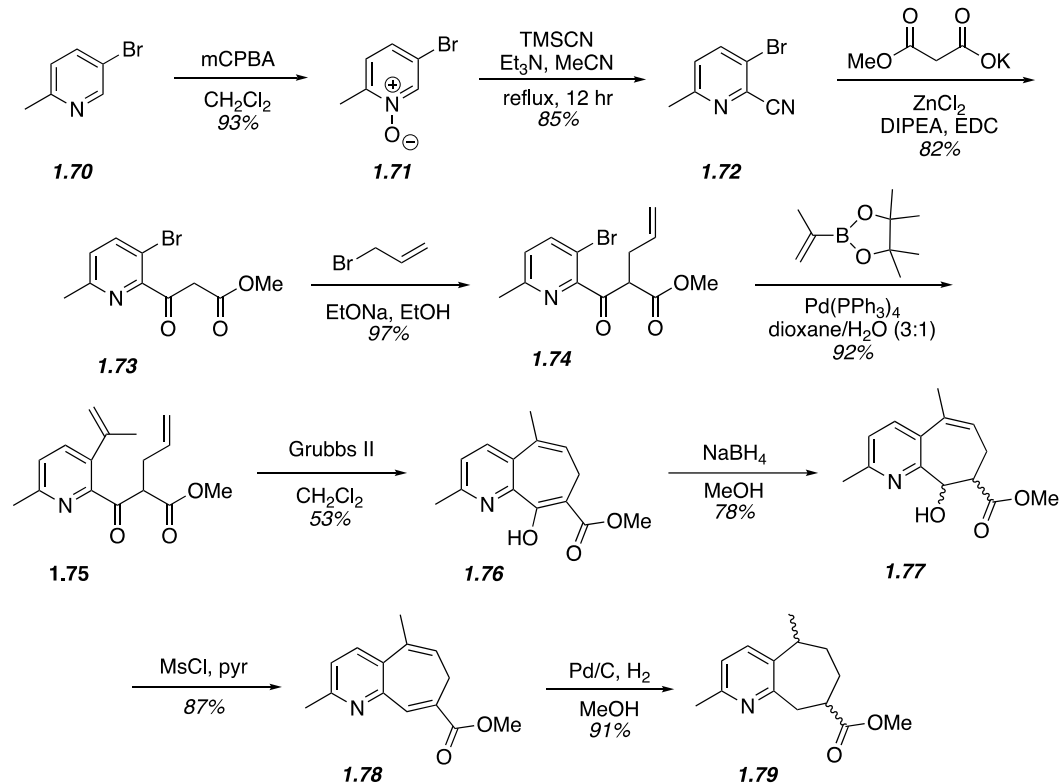
**Scheme 6.** Synthesis of cananodine by Shelton *et al.*<sup>29</sup>



## 1.6 Previous Synthetic Studies: Rupestines

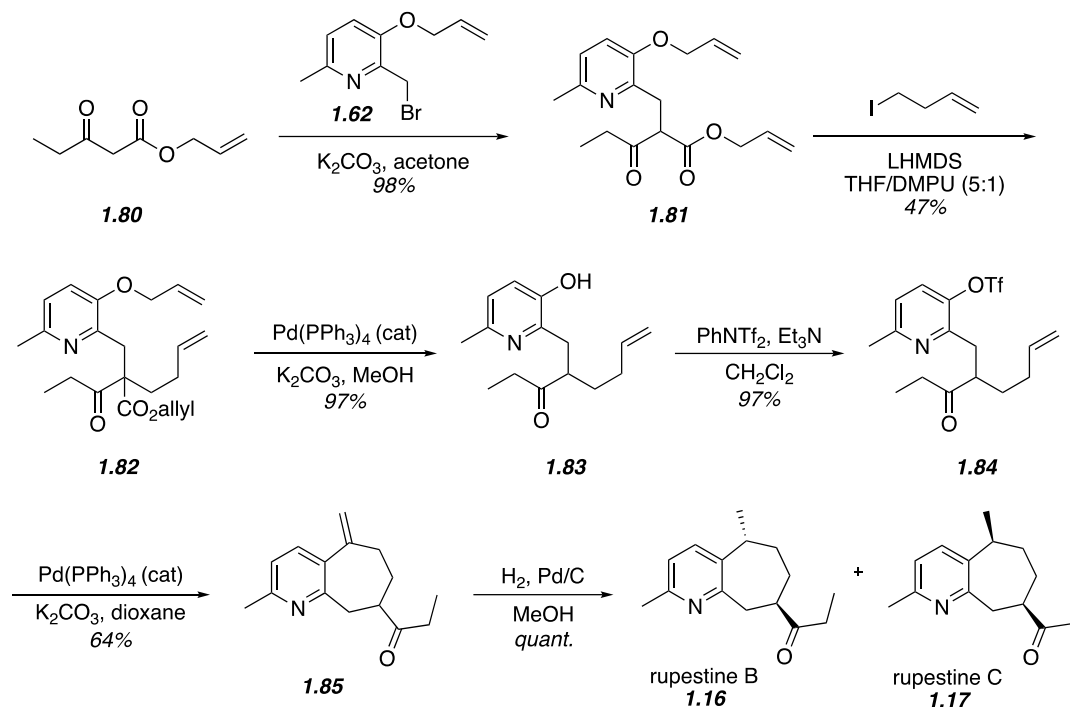
As previously mentioned, isolating the rupestines naturally is not a practical method for obtaining them for biological screening. This gave motivation for their syntheses, and led to the first synthesis of rupestine G in 2018 (Scheme 7).<sup>30</sup> The synthesis began with oxidation of the commercially available 5-bromo-2-picoline (**1.70**) to form the pyridine *N*-oxide (**1.71**). This was followed by a modified Reissert-Henze reaction to form the 2-cyanopyridine (**1.72**) and a decarboxylative Blaise reaction with potassium methyl malonate to provide **1.73**. This intermediate was alkylated with allyl bromide using sodium ethoxide as the base forming intermediate **1.74**. This set the stage for the Suzuki cross-coupling reaction which utilized isopropenylboronic acid pinacol ester to form intermediate **1.75**. This was followed by the key ring closing metathesis reaction which was catalyzed by the Grubbs II catalyst. Once the 7-membered carbocycle of **1.76** was formed, NMR analysis allowed for conclusion that the enol form was favored over the ketone. Intermediate **1.76** was then treated with sodium borohydride in methanol to afford the chiral alcohol (**1.77**). Dehydration of the alcohol with methanesulfonyl chloride to form diene (**1.78**) was followed by a simple hydrogenation reaction to provide rupestine G and its epimers (**1.79**) in an overall 18.9% yield.

**Scheme 7.** Synthesis of rupestine G and its epimers by Yusuf *et al.*<sup>30</sup>



More recently, rupestines B and C have been synthesized by Starchman *et al.* (Scheme 8).<sup>31</sup> This synthesis began with alkylation of picolyl bromide (**1.62**) with 3-oxopentanoate (**1.80**) to form intermediate **1.81**. This was followed by an additional alkylation with 4-iodo-1-butene to provide the keto ester intermediate **1.82**. The keto ester was then exposed to a palladium(0) catalyst with potassium carbonate and methanol to cleave both allyl groups, leaving intermediate **1.83**. In order to form the precursor for the key intramolecular Heck cyclization, the phenol type alcohol was converted to triflate **1.84**. When this intermediate was subjected to palladium(0) catalyst in basic dioxane at 130 °C, the desired 7-membered carbocycle of **1.85** was formed. Finally, a simple hydrogenation catalyzed by palladium on carbon lead to a 1:2 mixture of rupestines B (**1.16**) and C (**1.17**) which are separable using reverse phase chromatography.

**Scheme 8.** Synthesis of rupestines B and C reported by Starchman *et al.*<sup>31</sup>



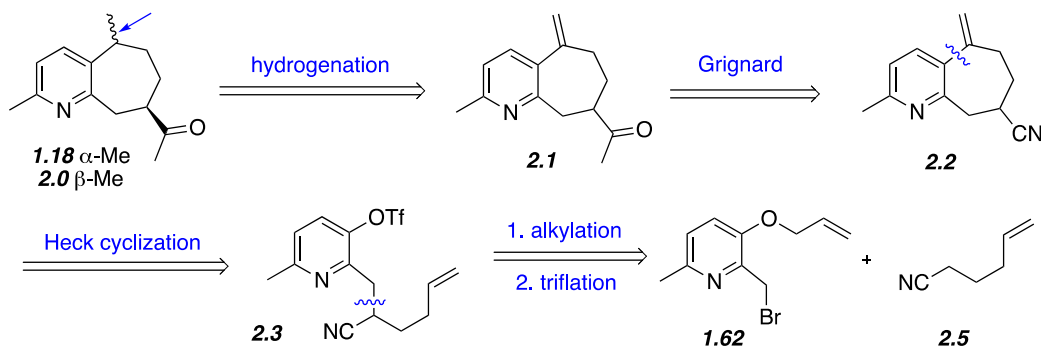
Together, all of these previous syntheses provide a solid foundation for exploring the syntheses of rupestines B-D and J-M. Specifically, the synthesis pathways reported by Shelton *et al.* and Starchman *et al.* will be carried out for the synthesis of rupestine D. The major difference in these syntheses is seen at the alkylation of picolyl bromide step. This will be adapted to better suit the desired rupestine D product, and can be further modified to provide an additional route toward rupestines B and C. Once the ketone-containing rupestines have been isolated, they can serve as the starting material for the syntheses of rupestines J-M. To obtain rupestines J and K, a Rubottom oxidation pathway will be used, and to obtain rupestines L and M, a Baeyer-Villiger oxidation pathway will be used. These strategies will be utilized in hopes of isolating the rupestines for bioactivity screening against HCC.

## 2.0 Synthesis of Rupestine D

### 2.1 Initial Synthetic Route

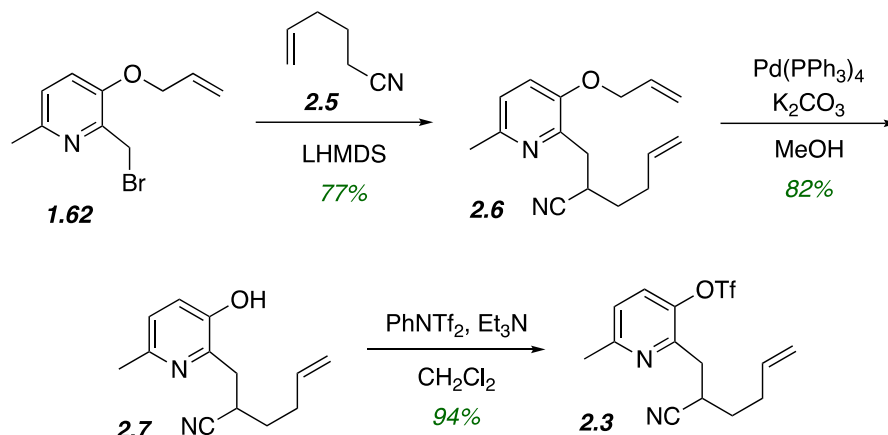
Using an adaptation of the pathway established by Shelton *et al.*, the first retrosynthetic route was designed (Scheme 9). To establish the methyl ketone diastereomers (**1.18** and **2.0**), a simple hydrogenation and Grignard reaction could be utilized. The guaipyridine core could then be accessed through an intramolecular Heck cyclization of triflate **2.3**. Finally, the triflate intermediate would be formed via alkylation of 5-hexenenitrile (**2.5**) and picolyl bromide (**1.62**).

**Scheme 9.** Proposed retrosynthesis of rupestine D (**1.18**)



Using this desired pathway, the synthesis began with the alkylation of **1.62** and **2.5** in the presence of LHMDS to provide intermediate **2.6** in a 77% yield after purification via flash chromatography (Scheme 10). Cleavage of the allyl ether protecting group of **2.6** was accomplished with a palladium(0) catalyst and  $K_2CO_3$  in methanol to provide the phenol-type intermediate (**2.7**) in an 82% yield. The crude mixture containing **2.7** was pure enough to move forward without purification and was immediately reacted with *N*-phenyltriflimide in the presence of triethylamine. This provided the Heck cyclization precursor (**2.3**) in a 94% yield after purification via flash chromatography.

**Scheme 10.** Synthesis of the Heck cyclization precursor (**2.3**) from 5-hexenenitrile (**2.5**) and picolyl bromide (**1.62**).



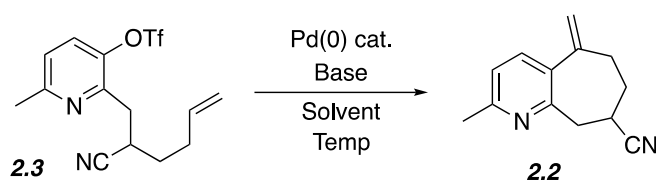
## 2.2 Optimization of Intramolecular Mizoroki-Heck Cyclization

The Mizoroki-Heck reaction is a coupling reaction between a vinyl or aryl halide and an alkene with the standard conditions being a base and palladium catalyst. While Richard F. Heck was awarded a 2010 Nobel Prize in Chemistry for this transformation, in 1971 Mizoroki *et al.* was the first to accomplish a palladium catalyzed reaction between alkenes and aryl iodides.<sup>32</sup> Heck *et al.* expanded on this report by incorporating benzyl and styryl halides as well as broadening the scope of successful palladium catalysts and bases.<sup>33</sup> The first intramolecular Heck cyclization for the formation of oxindole derivatives was reported by Heck *et al.* in 1979.<sup>34</sup> A decade later this work was expanded on by Shibasaki *et al.* to access *cis*-Decalin via an asymmetric Heck-type synthesis.<sup>35</sup> More recently, in 2003 Overman revealed the use of this transformation for natural product synthesis.<sup>36</sup> This led to Starchman *et al.* reporting a successful Mizoroki-Heck reaction

between a terminal mono-substituted alkene and an aryl triflate using a palladium(0) catalyst that allows access to the desired guaipyridine core of the rupestines.<sup>31</sup>

The investigation of the Mizoroki-Heck reaction on aryl triflate **2.3** began with Pd(PPh<sub>3</sub>)<sub>4</sub> catalyst and K<sub>2</sub>CO<sub>3</sub> in acetonitrile at 100 °C. Unfortunately, no cyclized material was formed, and the NMR spectrum revealed pyridyl alcohol (**2.7**). Similar results were obtained when Pd(OAc)<sub>2</sub> was utilized, the only difference being that reaction to pyridyl alcohol progressed much more slowly (Entry 2). Moving forward with the Pd(PPh<sub>3</sub>)<sub>4</sub> catalyst, a solvent investigation was done. It was concluded that DMF and acetonitrile were not suitable for the transformation when unwanted pyridyl alcohol **2.7** was formed. Finally, a temperature increase was made, resulting in the need for new solvents, toluene and dioxane. In toluene, the starting pyridyl triflate was never fully consumed and so the conditions were deemed impractical. In dioxane however, desired cyclized product was obtained after one day. After purification, it was concluded that the cyclized material was obtained in a 72% yield. Making entry 5 the most optimal set of conditions moving forward.

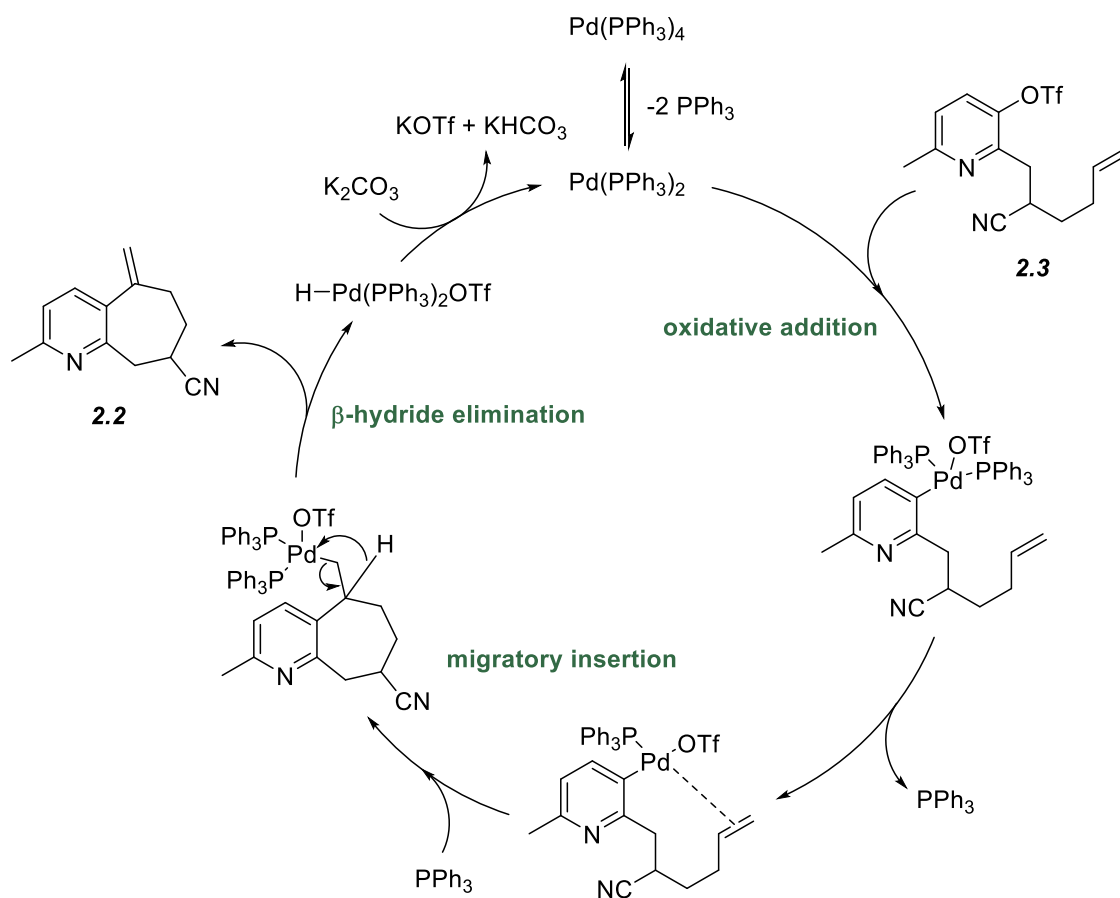
**Table 1.** Optimization of intramolecular Heck reaction



Entry	Catalyst	Base	Solvent	Temp (°C)	Reaction Time (days)	Yield (%)
1	Pd(PPh <sub>3</sub> ) <sub>4</sub>	K <sub>2</sub> CO <sub>3</sub>	CH <sub>3</sub> CN	100	7	0
2	Pd(OAc) <sub>2</sub>	K <sub>2</sub> CO <sub>3</sub>	CH <sub>3</sub> CN	100	>14	0
3	Pd(PPh <sub>3</sub> ) <sub>4</sub>	K <sub>2</sub> CO <sub>3</sub>	DMF	100	1	0
4	Pd(PPh <sub>3</sub> ) <sub>4</sub>	K <sub>2</sub> CO <sub>3</sub>	Toluene	130	>14	-
<b>5</b>	<b>Pd(PPh<sub>3</sub>)<sub>4</sub></b>	<b>K<sub>2</sub>CO<sub>3</sub></b>	<b>Dioxane</b>	<b>130</b>	<b>1</b>	<b>72</b>

The standard mechanism for the Mizoroki-Heck cyclization of triflate **2.3** is shown in Scheme 11. Upon loss of two triphenylphosphine ligands, the palladium catalyst undergoes an oxidative addition, inserting itself between the pyridine ring and the triflate group. An additional ligand is then lost to allow for coordination with the monosubstituted alkene, forming the desired seven-membered carbocycle. A  $\beta$ -hydride elimination then occurs to reestablish the alkene, relieving the desired product **2.2**. The final step requires a base to re-generate the palladium catalyst.

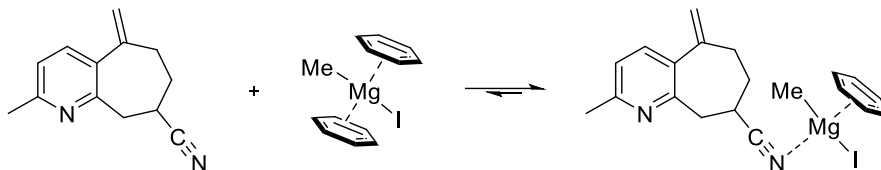
**Scheme 11.** Mizoroki-Heck reaction mechanism.



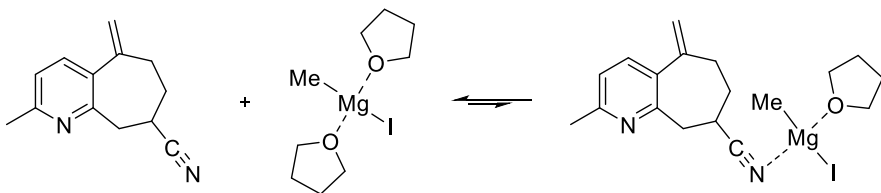
## 2.3 Optimization of Grignard reaction

The next step in the synthesis required conversion of the nitrile (**2.2**) to the methyl ketone of rupestine D. This was accomplished with methyl magnesium iodide in benzene. It should be noted that the reaction was not successful in THF due to solvent interactions with the nitrile.<sup>37</sup> These unfavorable solvent interactions were discussed in a 1980 report by Canonne *et al.* where benzene was shown to be the superior solvent in Grignard reactions of nitriles specifically.

**Scheme 12.** Proposed equilibrium between the free nitrile and the magnesium coordinated nitrile in the presence of benzene solvent.

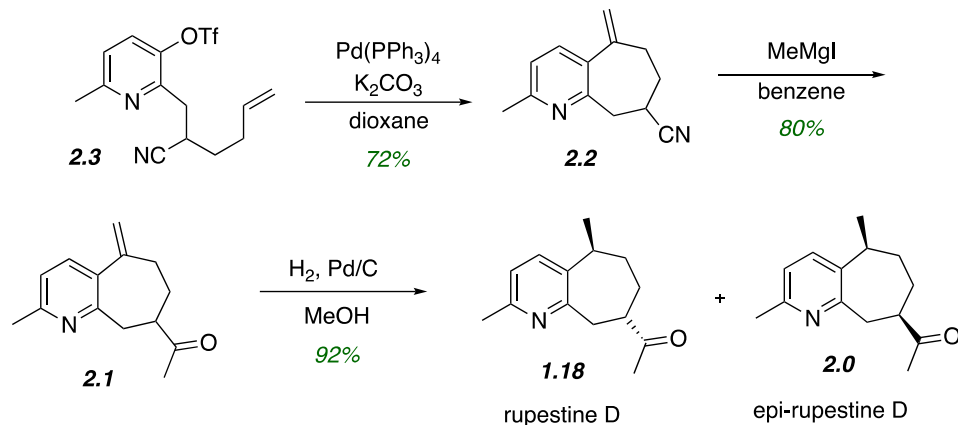


**Scheme 13.** Proposed equilibrium between the free nitrile and the magnesium coordinated nitrile in the presence of THF solvent.



After isolation of methyl ketone **2.1** in an 80% yield, the final step in the synthesis was a simple hydrogenation with palladium on carbon to provide rupestine D (**1.18**) and epi-rupestine D (**2.0**) in a 92% yield as a 1:2 ratio of diastereomers. Unfortunately, after multiple attempts it was concluded that the diastereomers were inseparable and rupestine D could not be isolated.

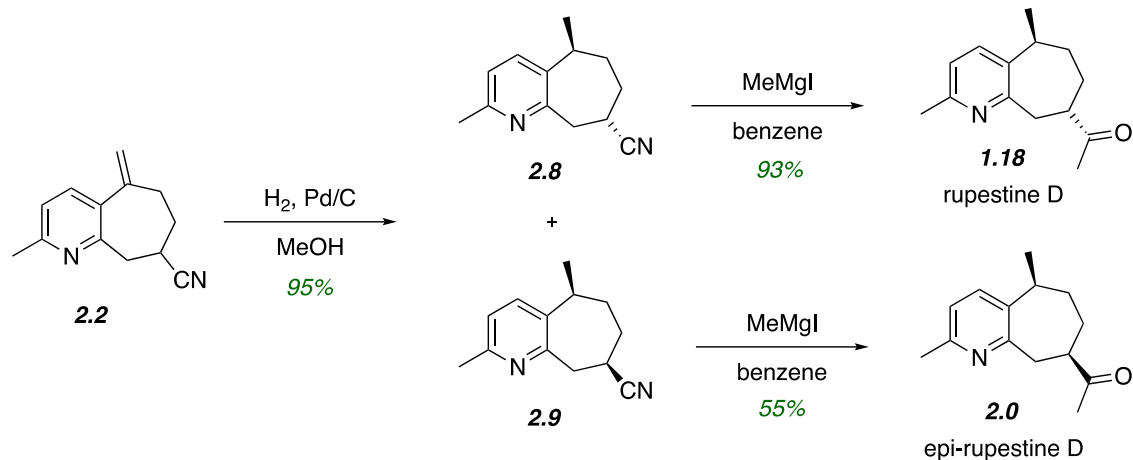
**Scheme 14.** Synthesis of rupestine D (**1.18**) and epi-rupestine D (**2.0**) from triflate (**2.3**).



## 2.4 Alternative Synthetic Route

In the initial synthesis of rupestine D, the second and final stereocenter was formed in the last step of the synthesis. When the simple hydrogenation was performed in the presence of the nitrile instead of the ketone, the diastereomers were obtained in a 95% yield as a 10:1 ratio of **2.9** to **2.8**. Interestingly, these diastereomers were completely separable and allowed for isolation of the rupestine D precursor (**2.8**) in a 15% yield which was carried through to rupestine D (**1.18**) in a 93% yield. The epi-rupestine D precursor was obtained in a 58% yield and was carried through to epi-rupestine D in a 55% yield. Not only did this alternative route allow for the isolation of rupestine D, but it also provided a key step in the synthesis where diastereomers could be separated.

**Scheme 15.** Alternative route toward isolation of rupestine D (**1.18**).



While the alternative route shown in Scheme 15 initially allowed for isolation of each diastereomer, reproducibility of the transformation proved to be difficult. It was found that at room temperature, there was a competing nucleophilic addition and deprotonation reaction occurring and a 1.3:1 ratio of **2.0** to **1.18** was obtained. As the temperature of the reaction was decreased to -78 °C, the desired nucleophilic addition was favored and only trace isomerization occurred. Tables 2 and 3 compare <sup>1</sup>H and <sup>13</sup>C NMR data for the naturally isolated rupestine D and the one synthesized in this experiment.

**Table 2.**  $^1\text{H}$  NMR data comparison for rupestone D.<sup>23</sup>

Position	Natural Product	This work
H—C(3)	7.00 (d, $J = 8.0$ )	7.37 (d, $J = 8.2$ )
H—C(4)	7.40 (d, $J = 8.0$ )	6.98 (d, $J = 8.2$ )
H—C(5)	2.94 – 3.04 (m)	2.90 – 3.04 (m)
H <sub>a</sub> —C(6)	1.23 – 1.30 (m)	1.20 – 1.35 (m)
H <sub>b</sub> —C(6)	1.82 – 1.94 (m)	1.75 – 2.00 (m)
H <sub>a</sub> —C(7)	1.82 – 1.94 (m)	1.75 – 2.00 (m)
H <sub>b</sub> —C(7)	2.04 – 2.11 (m)	2.00 – 2.15 (m)
H—C(8)	2.54 – 2.60 (m)	2.54 (tt, $J = 10.5$ , $J = 3.0$ )
H <sub>a</sub> —C(9)	3.13 – 3.28 (m)	3.22 (dd, $J = 14.1$ , $J = 10.0$ )
CH <sub>2</sub> (13) or Me(13)	2.23 (s)	2.22 (s)
H <sub>a</sub> —C(14) or Me(14)	2.51 (s)	2.50 (s)
Me(15)	1.35 (d, $J = 7.2$ )	1.34 (d, $J = 7.2$ )

**Table 3.**  $^{13}\text{C}$  NMR data comparison for rupestone D.<sup>23</sup>

Position	Natural Product	This work
C(2)	154.36	154.5
C(3)	121.24	121.1
C(4)	132.60	132.4
C(5)	34.76	34.7
C(6)	34.96	35.0
C(7)	32.92	32.9
C(8)	49.47	49.6
C(9)	39.43	39.6
C(10)	159.05	159.2
C(11)	137.90	137.7
C(12)	211.07	211.1
C(13)	28.49	28.4
C(14)	23.71	23.8
C(15)	20.32	20.3

## 2.5 Separation of Diastereomers

Many attempts were made to isolate rupepine D from its epimer via flash and radial chromatography. Results were initially promising when a separation was run in a 1:1 hexanes:ethyl acetate solvent system. As mentioned, the crude ratio of diastereomers **1.18** and **2.0** was 1:2, and after separation, one fraction was obtained that contained a 1:6 ratio of diastereomers, and a second fraction was obtained that contained a 1:2 ratio (Figure 6). This indicated that the isomers were at least semi-separable. Numerous different solvent systems were tested via TLC before resulting to an attempt at a reverse phase separation where a methanol:water solvent system was used. A gradient was run over 15 minutes starting with 40% MeOH in H<sub>2</sub>O and ending in 85% MeOH in H<sub>2</sub>O. Unfortunately, the diastereomers were still not isolated.

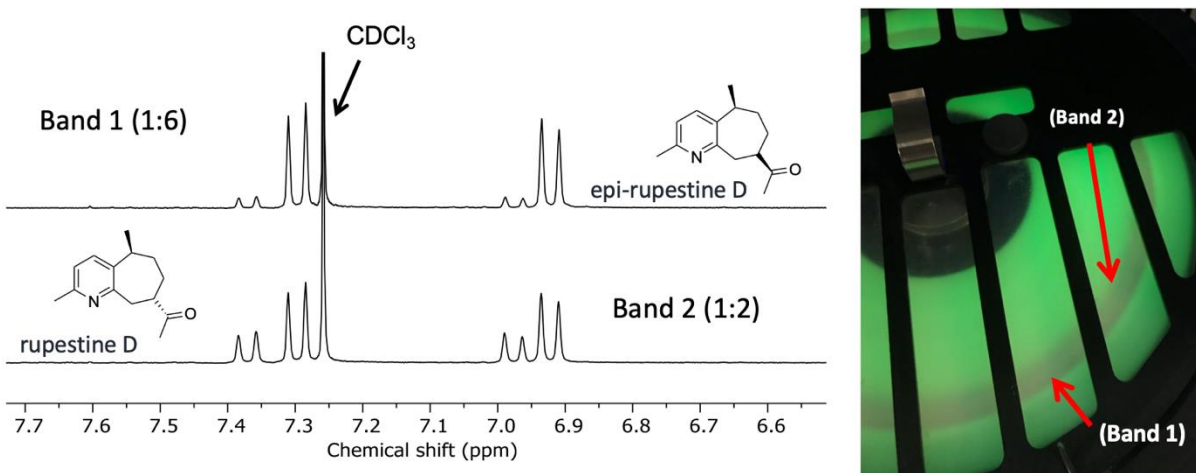


**Figure 6.** Separation of rupepine D and epi-rupepine D via radial chromatography (2mm, 1:1 hexanes:ethyl acetate).

When the hydrogenation was run in the presence of nitrile **2.2**, radial chromatography was an efficient method for separation (Figure 7). Directly upon <sup>1</sup>H NMR analysis of the crude

hydrogenated reaction, a 1:10 ratio of diastereomers **2.9** and **2.8** was obtained. After isolation of each compound, 1:3.9 ratio was obtained (determined via percent yield). It is proposed that the nitrile diastereomers are prone to isomerization on the slightly acidic silica gel of the radial chromatotron plate.

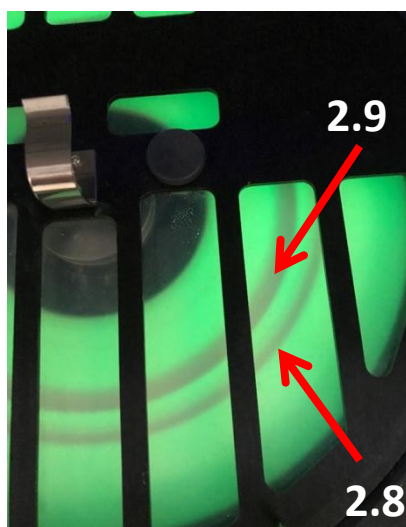


**Figure 7.** Separation of nitriles **2.9** and **2.8** via radial chromatography (2mm, 1:3 hexanes:ethyl acetate).

## 2.6 Hydrogenation: Diastereomeric ratios

The difference in the obtained diastereomeric ratios between ketone **2.1** and nitrile **2.2** upon hydrogenation was puzzling. Hydrogenation of **2.1** provided a 2:1 ratio of the *cis* isomer to the *trans* isomer, and hydrogenation of **2.2** lead to a 10:1 ratio of the *cis* to *trans*. Upon conformational analysis, it is proposed that the most stable conformation of the alkene substrates holds the C8 functional group in a pseudo-equatorial position. As seen in figure 8, these conformations result in the C7 and C9 pseudo-axial protons blocking the bottom face of the substrate, while the C8 pseudo-axial proton is blocking the top face. As the functional group at the C8 pseudo-equatorial position gets larger, the C8 pseudo-axial proton gets closer to the 1,1-disubstituted alkene, making

hydrogenation from the top face less favorable. This explains why the smaller nitrile-containing alkene results in a higher percentage of the *cis* isomer compared to the larger methyl ketone.

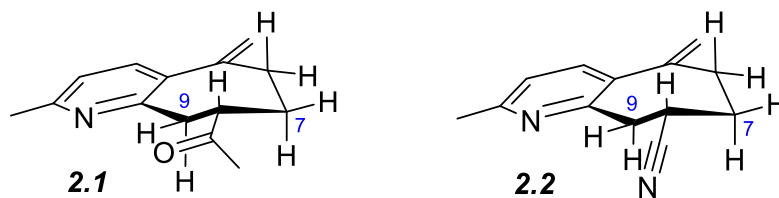
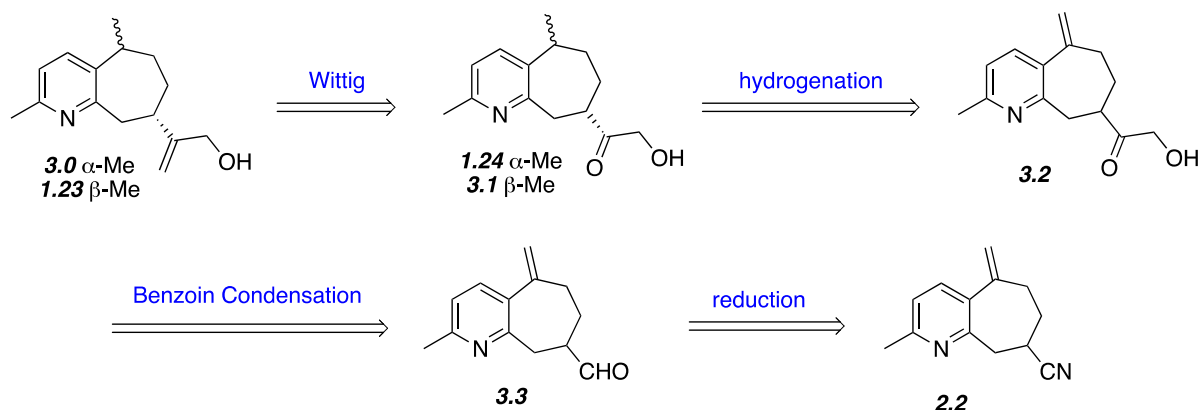


**Figure 8.** Major conformation of alkenes **2.1** and **2.2**.

### 3.0 Synthesis of rupestines J and K

It was initially proposed that the alpha hydroxy alkene of rupestine J (**1.23**) could be accessed through a Wittig reaction using epi-rupestine K (**3.1**) as the substrate. In order to form the  $\alpha$ -hydroxy ketone of rupestine K (**1.24**) and to establish the C5 stereocenter, a benzoin condensation followed by a simple hydrogenation would be utilized. Finally, the necessary aldehyde substrate (**3.3**) could be accessed through a reduction of nitrile **2.2**.

**Scheme 16.** Proposed retrosynthesis of rupestines J (**1.23**) and K (**1.24**).

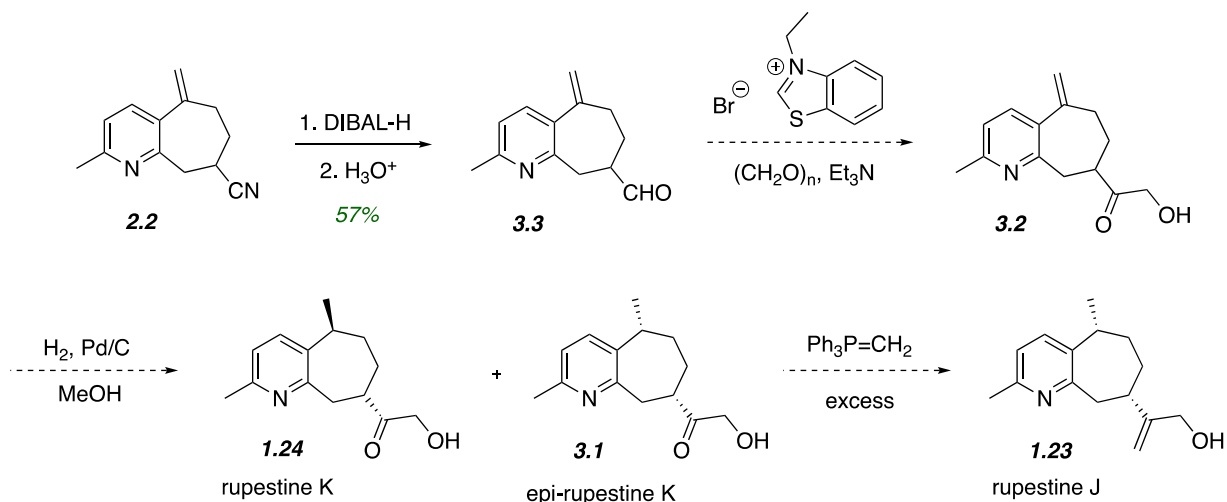


### 3.1 Initial synthetic route

The synthesis of rupestines J and K began with the previously synthesized nitrile **2.2** from the synthesis of rupestine D. This intermediate was reduced to aldehyde **3.3** in a 57% yield using DIBAL-H followed by an acidic work up. It was then anticipated to perform a benzoin condensation using an *N*-heterocyclic carbene catalyst, paraformaldehyde and triethylamine base. This would ideally establish the desired alpha hydroxy ketone and would be followed by a hydrogenation to form the final stereocenter. At this stage, separation of the diastereomers would be necessary in order to isolate rupestine K (**1.24**) and carry epi-rupestine K (**3.1**) through a Wittig

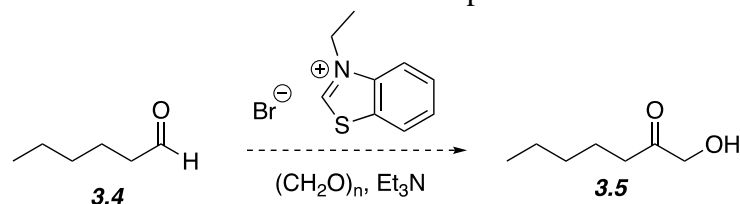
reaction to form rupestine J (**1.23**). Unfortunately, despite success in the literature, the synthesis never made it past the benzoin condensation step.

**Scheme 17.** Initial synthetic studies toward rupestines J and K.



### 3.2 Benzoin Condensation

Benzoin condensations require the use of an *N*-Heterocyclic carbene (NHC) which are known to be attractive organocatalysts for a number of transformations.<sup>38</sup> The NHC catalyst chosen for this synthesis was 3-ethylbenzothiazolium bromide which has been shown to be successful in the microwave-assisted synthesis reported by Nikolaou *et al.*<sup>39</sup> In order to preserve the precious aldehyde substrate **3.3**, a non-precious aldehyde substrate hexanal (**3.4**) was used for reaction optimization. This was an especially attractive model substrate because Nikolaou *et al.* had successfully achieved this transformation with heptanal.

**Table 4.** Optimization of benzoin condensation on non-precious substrate **3.4**.

Entry	Catalyst (mol %)	Base	Base (mol %)	Paraformaldehyde (equiv)	MW (Y/N)	Conversion (%) <sup>*</sup>
1	10	Et <sub>3</sub> N	20	3	N	25
2	10	Et <sub>3</sub> N	50	3	N	trace
3	10	Et <sub>3</sub> N	300	3	N	trace
4	10	DIPEA	20	3	N	7
5	10	DIPEA	20	3	Y	trace

<sup>\*</sup>% conversion was determined via GCMS

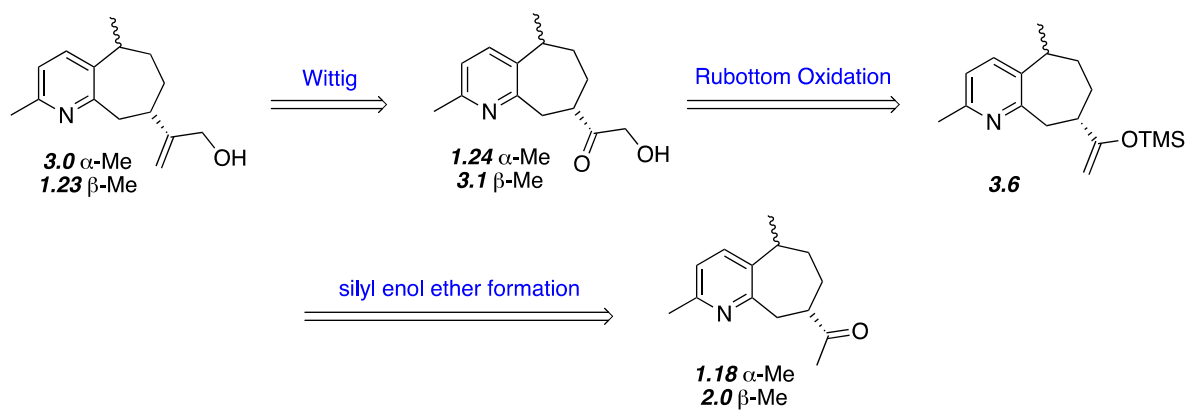
The reaction investigation began with the relative molar equivalents established by Nikolaou *et al.* (Table 4, Entry 1). GCMS did reveal product formation, however the reaction profile was unfortunately complex and isolation was not accomplished. In attempt to increase the percent conversion, the mol % of base was increased. It was proposed that since the end groups of paraformaldehyde are alcohols, the base could be deprotonating the hydroxy group first. Entries 2 and 3 reveal that increasing the base mol % did not increase the percent conversion. Moving back to the established molar equivalents reported by Nikolaou *et al.*, DIPEA base was incorporated. Without microwave radiation (entry 4), a 7% conversion was obtained. When microwave radiation was employed (50 Watts, 100 °C), a trace conversion to the product was obtained.

### 3.3 Alternative synthetic route

A second approach to the synthesis of rupestines J and K was proposed (Scheme 18). The final step toward rupestine J would remain the same as the initial synthesis (Scheme 16), where excess Wittig reagent would allow for conversion of ketone **3.1** to alkene **1.23**. In order to access the alpha hydroxy ketone of rupestine K and its epimer, the methyl ketone of rupestine D would

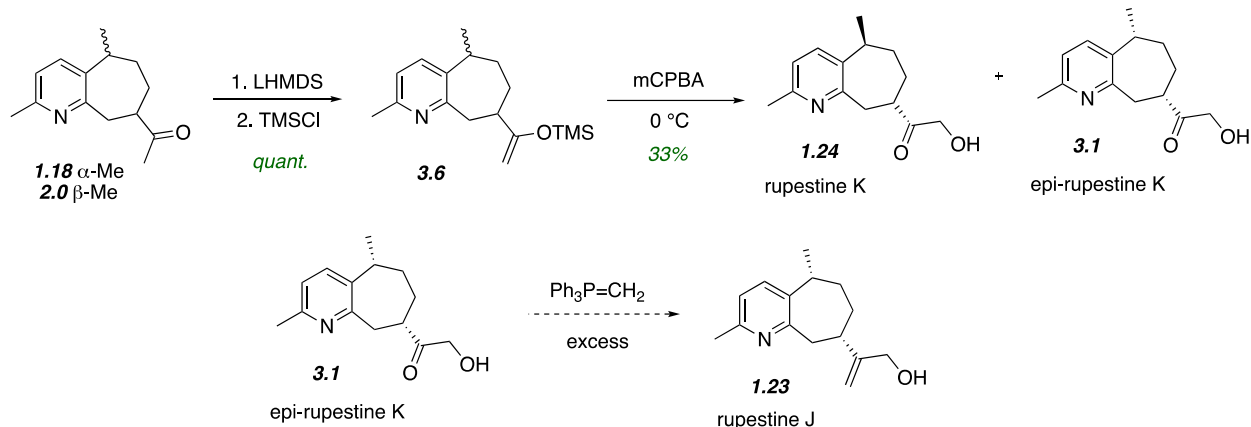
be converted to a silyl enol ether (**3.6**) and could be subsequently oxidized using a Rubottom oxidation.

**Scheme 18.** Alternative proposed retrosynthesis of rupestines J and K.



Starting from a mixture of ketones **1.18** and **2.0**, silyl enol ether **3.6** was formed in a quantitative yield using 3 equivalents of LHMDS followed by 6-9 equivalents of TMSCl (Scheme 19). Purification of **3.6** via flash chromatography resulted in a significant amount of product converting back to the substrate ketone. To avoid this, the silyl enol ether was not purified and was instead carried straight through to the Rubottom oxidation.

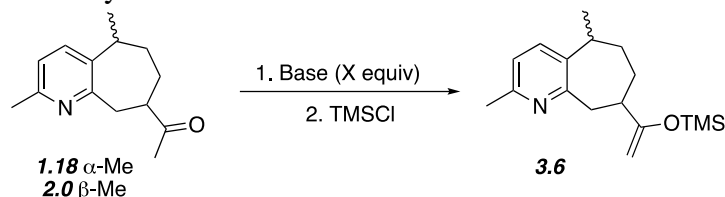
### Scheme 19. Alternative synthesis of rupestines J and K.



### 3.4 Optimization of silyl enol ether formation

Initial studies for the transformation began with a slight excess of LDA followed by an excess of TMS chloride. A small excess of base was used in anticipation of the picolyl methyl group being deprotonated. Fortunately, since the reaction was kept at -78 °C, the undesired deprotonation did not pose a problem. This allowed for a continuous increase in base equivalents until the substrate was fully consumed.

**Table 5.** Optimization of silyl enol ether formation



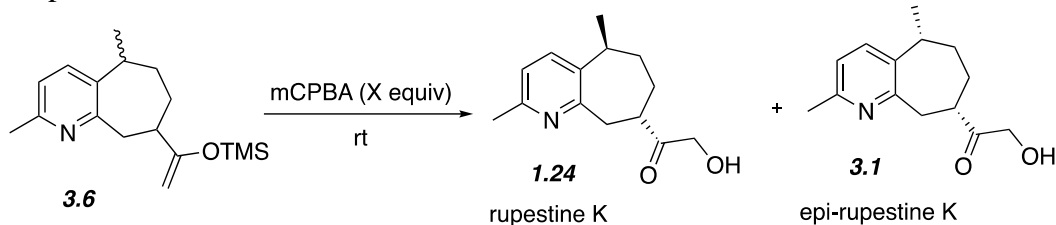
Entry	Base	Base equiv.	% conversion*
1	LDA	1.1	trace
2**	LHMDS	1.5	50
3**	LHMDS	2.1	92
4	LHMDS	3.1	100

\*% conversions determined via GCMS

\*\*substrate used was non-precious methyl undecyl ketone

### 3.5 Optimization of Rubottom Oxidation

The Rubottom oxidation is a reaction between trimethylsilyl enol ethers and mCPBA that was first reported in 1974.<sup>40</sup> This reaction was used more recently in 2008 for a scalable synthesis of 2*S*-hydroxymutilin, making it a promising transformation for the synthesis of potentially biologically active rupestines J and K.<sup>41</sup> For the substrate in question (**3.6**) it is important to consider the reaction between the pyridine nitrogen and mCPBA which results in an undesired pyridine *N*-oxide. Upon the addition of mCPBA to a solution of the substrate, the most electron rich functional group will react first. This means that with careful consideration of mCPBA equivalents, the pyridine *N*-oxide can be avoided. Table 6 highlights the different ratios obtained with varying equivalents of mCPBA. It was found that when 1.5 equivalents of mCPBA is exceeded, the pyridine *N*-oxide begins to form and cannot be reduced back to the neutral pyridine. However, when the mCPBA equivalents are less than or equal to 1.5, the starting enol ether substrate is not fully consumed. Since the reaction work-up allows for conversion of any remaining substrate **3.6** back to ketones **1.18** and **2.0**, it was concluded that it was more practical to under-oxidize **3.6** rather than over-oxidize. This leaves entry 2 as the optimal set of conditions. Upon purification of a previous crude reaction batch, a pure fraction of rupestine K was isolated and fully characterized. Tables 7 and 8 compare the <sup>1</sup>H and <sup>13</sup>C NMR obtained for the natural product and this experiment.

**Table 6.** Optimization of the Rubottom oxidation

Entry	mCPBA (equiv)	S.M.:Product*	Product: <i>N</i> -Oxide*
1	1.25	2:1	-
2	<b>1.5</b>	<b>1:1</b>	-
3	1.8	-	2:1
4	3	-	1:1

\*Relative ratios were determined via GC-MS

**Table 7.**  $^1\text{H}$  NMR data comparison for rupestone K.<sup>23</sup>

Position	Natural Product	This work
H—C(3)	7.02 (d, $J = 8.0$ )	7.00 (d, $J = 7.9$ )
H—C(4)	7.41 (d, $J = 8.0$ )	7.40 (d, $J = 7.8$ )
H—C(5)	3.02 (m)	3.00 (m)
H <sub>a</sub> —C(6)	1.97 (m)	1.97 (m)
H <sub>b</sub> —C(6)	1.31 (m)	1.30 (m)
H <sub>a</sub> —C(7)	1.97 (m)	1.97 (m)
H <sub>b</sub> —C(7)	2.03 (m)	2.02 (m)
H—C(8)	2.58 (m)	2.56 (m)
H <sub>a</sub> —C(9)	3.35 (dd, $J = 14$ , $J = 10.8$ )	3.32 (dd, $J = 11.0$ , $J = 14.0$ )
H <sub>b</sub> —C(9)	3.12 (d, $J = 14$ )	3.11 (d, $J = 14.0$ )
H <sub>a</sub> —C(13)	4.39 (s)	4.37 (s)
Me(15)	2.51 (s)	2.49 (s)
H—(16)	1.37 (d, $J = 7.2$ )	1.36 (d, $J = 7.0$ )

**Table 8.**  $^{13}\text{C}$  NMR data comparison for rupestine K.<sup>23</sup>

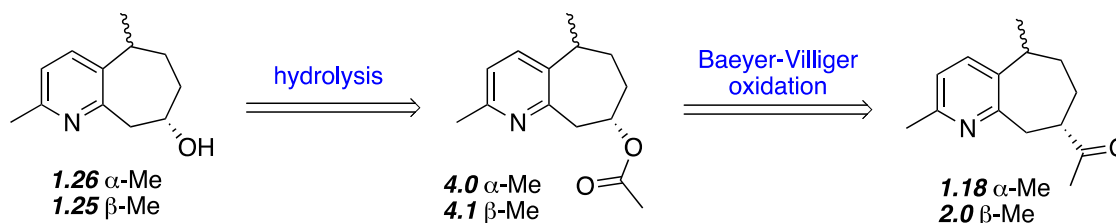
Position	Natural Product	This work
C(2)	154.2	154.7
C(3)	121.5	121.4
C(4)	132.6	132.7
C(5)	34.8	34.8
C(6)	34.8	34.8
C(7)	33.3	33.3
C(8)	45.2	45.2
C(9)	39.5	39.5
C(10)	159.3	158.5
C(11)	137.7	137.7
C(12)	208.9	212.0
C(13)	66.8	66.8
C(15)	23.6	23.8
C(16)	20.4	20.3

## 4.0 Synthesis of rupestines L and M

### 4.1 Intended synthetic route

Moving forward from the previously synthesized methyl ketone of rupestine D and epi-rupestine D, a new rupestine synthesis was proposed. The first step in the synthesis of rupestines L and M was a Baeyer-Villiger oxidation (BVO) to form esters **4.0** and **4.1**. This would be followed by a hydrolysis step to form the desired hydroxyl diastereomers rupestine L (**1.25**) and rupestine M (**1.26**) (Scheme 20). Should the hydroxyl diastereomers be inseparable, the syntheses of rupestines L and M could ideally be started from the previously isolated nitriles (**2.8** and **2.9**).

**Scheme 20.** Proposed retrosynthesis of rupestines L and M.

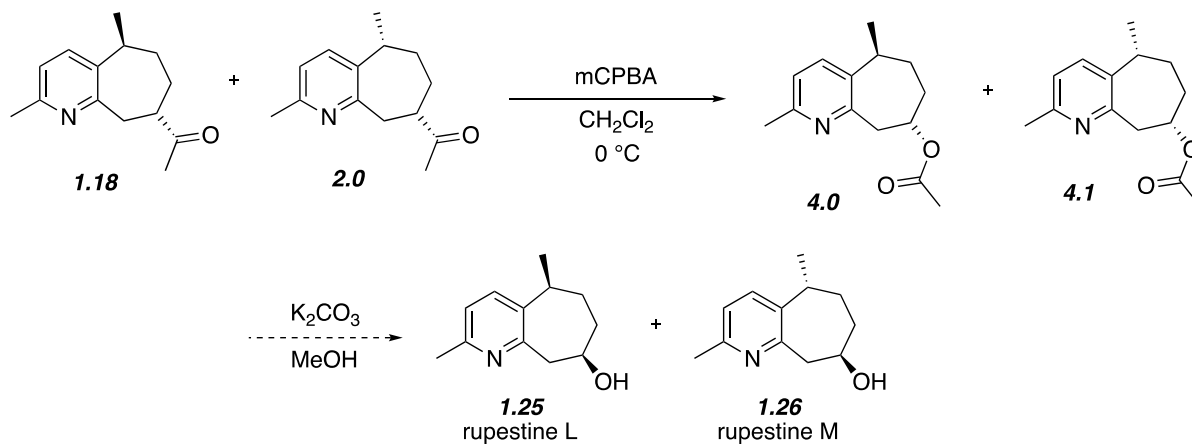


### 4.2 Studies on Baeyer-Villiger oxidation

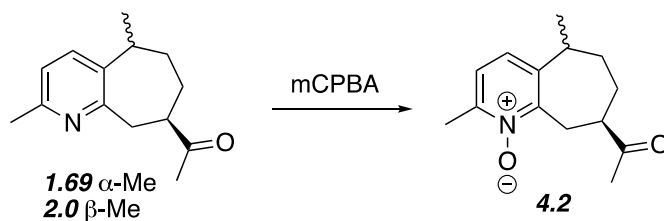
The studies for this synthesis began with the Baeyer-Villiger oxidation, where an oxygen is inserted on the more substituted side of a ketone, forming the desired ester **4.0** (Scheme 21). Initial attempts with the standard Baeyer-Villiger oxidant mCPBA were unsuccessful due to the favorability of pyridine *N*-oxide formation (Scheme 22). The presence of the pyridine *N*-oxide was confirmed via mass spectrometry and FTIR spectroscopy. Initially, the MS data was promising when the  $M^+$  ion corresponded to a mass of 233.31 which is the mass of desired ester **4.0**.

However, the FTIR spectrum revealed a carbonyl C=O stretch around 1710 cm<sup>-1</sup>, indicating the presence of a ketone.

**Scheme 21.** Proposed synthesis of rupestines L and M (**1.25**, **1.26**).



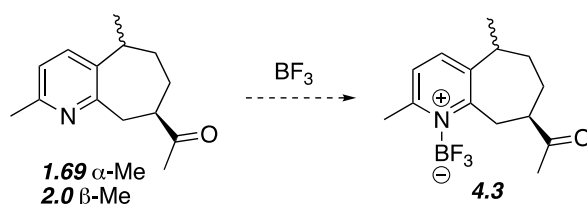
**Scheme 22.** Formation of the undesired pyridine *N*-oxide.



Further attempts were made toward the formation of esters **4.0** and **4.1** with a new oxidant, oxone. A Baeyer-Villiger oxidation with oxone in ionic solvents was reported by Chrobok *et al.*<sup>42</sup> Unfortunately, the formation of the pyridine *N*-oxide was still occurring in presence of oxone. After further literature searching, a new oxidant was found that has been used in Baeyer-Villiger oxidations, boron trifluoride etherate with hydrogen peroxide.<sup>43</sup> This reagent would not only

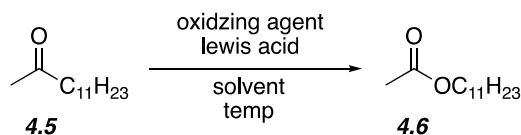
provide an oxidant for the desired transformation, but ideally it would also allow the pyridine nitrogen to complex with the boron trifluoride, inhibiting *N*-oxide formation (Scheme 23).

**Scheme 23.** Protection of the pyridine nitrogen with boron trifluoride.



Moving forward, a non-precious ketone substrate was utilized in order to conserve the precious ketone substrates (**1.18** and **2.0**). Table 9 provides a summary of all attempted conditions. After no desired product was obtained from entries 1 and 2, the standard BVO conditions were re-employed. It was determined that the temperature played an important role when the % conversion increased as the temperature was increased. When the reaction was attempted in ether, no product was obtained. It was concluded that the optimal conditions were mCPBA in DCM at 70 °C (entry 5).

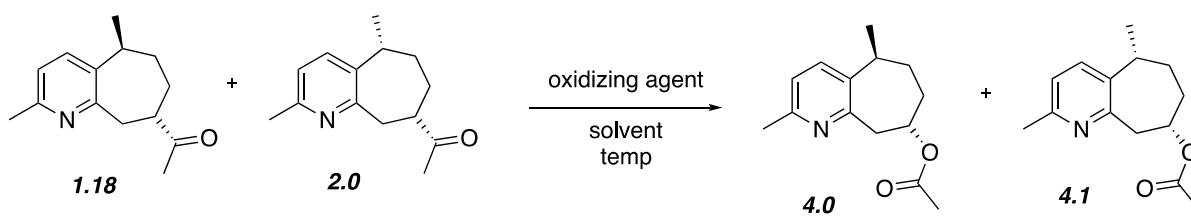
**Table 9.** Optimization of Baeyer-Villiger oxidation with non-precious substrate **4.5**.



Entry	Oxidant	Lewis Acid	Solvent	Temp (°C)	% Conversion*
1	mCPBA	BF <sub>3</sub> -etherate	ether	reflux	0
2	H <sub>2</sub> O <sub>2</sub>	BF <sub>3</sub> -etherate	ether	reflux	0
3	mCPBA	-	DCM	25	trace
4	mCPBA	-	DCM	60	~70
<b>5</b>	<b>mCPBA</b>	-	<b>DCM</b>	<b>70</b>	<b>~90</b>
6	mCPBA	-	ether	70	0

Unfortunately, when using the optimal conditions from Table 9 in the presence of the precious ketone substrate mixture (**1.18** and **2.0**), only the pyridine *N*-oxide was recovered. Since the formation of the pyridine *N*-oxide was inevitable, it was then proposed that it could be reduced back to the neutral pyridine in a later step. A method for the removal of *N*-oxides with triphenylphosphine was reported in 1959 by Howard *et al.*<sup>44</sup> When the ketone substrates were reacted in the presence of excess mCPBA at 70 °C for 3 days, only the pyridine *N*-oxide was recovered. The temperature was then increased to 110 °C in benzene and 150 °C in dioxane and no desired product was formed. It was finally concluded that the methyl ketone of **1.18** and **2.0** are not reactive enough for this transformation and different routes will have to be explored.

**Table 10.** Optimization of Baeyer-Villiger oxidation with substrates **1.18** and **2.0**.



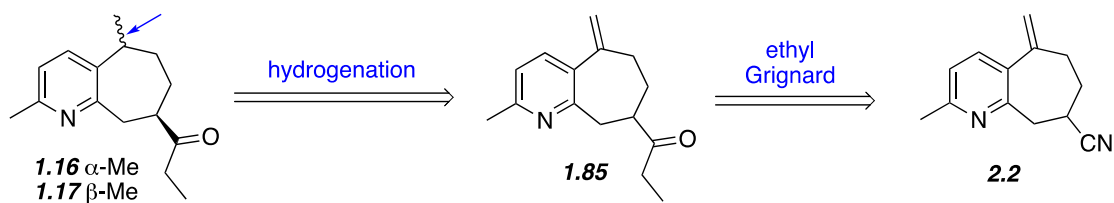
The reaction scheme shows two ketone substrates, **1.18** and **2.0**, reacting with an oxidizing agent in a solvent at a specific temperature to yield two lactam products, **4.0** and **4.1**. The structures of **1.18** and **2.0** are bicyclic systems with a pyridine ring fused to a seven-membered ring, and a methyl ketone group attached to the seven-membered ring. The methyl group in **1.18** is on the pyridine ring, while in **2.0** it is on the seven-membered ring. The products **4.0** and **4.1** are the corresponding lactams, where the methyl ketone group has been converted to a lactam ring.

Entry	Oxidant	Solvent	Temp (°C)	C=O IR stretch (cm <sup>-1</sup> )
1	mCPBA	DCM	70	1710
2	mCPBA	benzene	110	1709
3	mCPBA	DMF	150	1709

## 5.0 Alternative synthesis to Starchman *et al.*'s synthesis of rupestines B and C

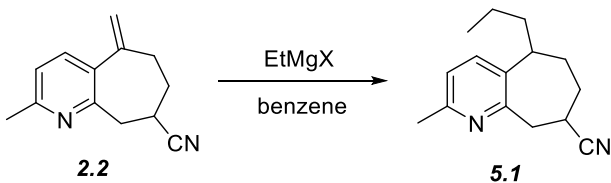
Ketone-containing guaipyridine alkaloids rupestines B and C differ from rupestine D and epi-rupestine D by one methylene group. It was initially proposed that the ethyl ketone of rupestines B and C could be accessed using the same initial synthesis of rupestine D and epi-rupestine D, with the exception of the methyl Grignard step. Instead, an ethyl Grignard would be utilized to establish the ethyl ketone. This would be followed by a simple hydrogenation to form the C5 stereocenter.

**Scheme 24.** Retrosynthesis of rupestines B and C from intermediate **2.2**.



The intended path for the synthesis of rupestines B and C began with the previously synthesized alkene nitrile **2.2**. It was our hope that the ethyl ketone of **1.85** could be accessed through an ethyl Grignard reaction (Scheme 24), however attempts were unsuccessful due to reaction of the Grignard reagent and the 1,1-disubstituted alkene (Scheme 25).

**Scheme 25.** Undesired reaction with 1,1-disubstituted olefin of **2.2**.



This issue was alleviated when the alternative synthesis of rupestine D was employed, where nitrile **2.9** was carried through to rupestine C in a 36% percent yield. Due to the fact that reflux was required to accomplish this transformation, isomerization did occur, and a 55% yield of a semi-separable mixture of rupestines B and C was obtained. Tables 11 and 12 reveal the  $^1\text{H}$  and  $^{13}\text{C}$  data comparison for rupestine C between the natural product and this experiment.

**Scheme 26.** Desired reaction for the formation of rupestine C.

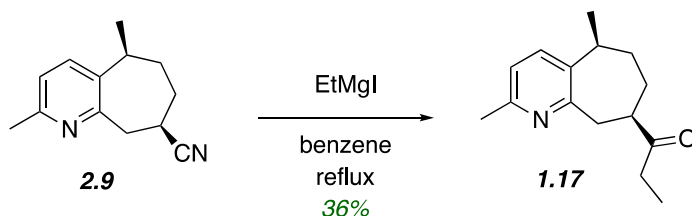


**Table 11.**  $^1\text{H}$  NMR data comparison for rupestine C (**1.17**).<sup>23</sup>

Position	Natural product (400 MHz)	This work (300 MHz)
H—C(3)	6.94 (d, $J = 7.6$ )	6.92 (d, $J = 7.7$ )
H—C(4)	7.33 (d, $J = 7.6$ )	7.30 (d, $J = 7.6$ )
H—C(5)	2.95 – 3.04 (m)	2.94 – 3.04 (m)
H <sub>a</sub> —C(6)	1.72 – 1.88 (m)	1.73 – 1.89 (m)
H <sub>a</sub> —C(7)	1.72 – 1.88 (m)	1.73 – 1.89 (m)
H <sub>b</sub> —C(7)	2.00 – 2.10 (m)	1.97 – 2.10 (m)
H—C(8)	2.67 – 2.75 (m)	2.65 – 2.72 (m)
H <sub>a</sub> —C(9)	3.16 – 3.24 (m)	3.17 (dd, $J = 2.7, J = 14.7$ )
H <sub>b</sub> —C(9)	3.31 – 3.41 (m)	3.28 – 3.36 (m)
CH <sub>2</sub> (13) or Me(13)	2.60 (q, $J = 7.2$ )	2.57 (q, $J = 7.3$ )
H <sub>a</sub> -C(14) or Me(14)	1.02 (t, $J = 7.2$ )	1.02 (t, $J = 7.3$ )
Me(15)	2.50 (s)	2.47 (s)
Me(16)	1.31 (d, $J = 7.6$ )	1.30 (d, $J = 7.3$ )

**Table 12.**  $^{13}\text{C}$  NMR data comparison for rupestine C (**1.17**).<sup>23</sup>

position	Natural product (400 MHz)	This work (300 MHz)
C(2)	154.63	154.67
C(3)	121.42	121.25
C(4)	136.59	136.26
C(5)	37.65	37.70
C(6)	32.11	32.18
C(7)	28.40	28.28
C(8)	48.50	48.66
C(9)	39.57	39.97
C(10)	157.63	157.75
C(11)	138.14	137.84
C(12)	213.38	213.56
C(13)	34.29	34.26
C(14)	7.76	7.78
C(15)	23.56	23.85
C(16)	18.85	18.79

## 6.0 Conclusions

In conclusion, the synthesis and isolation of rupestine D as a single diastereomer has been reported in 6 total steps from picolyl bromide **1.62** in a 6.3% overall yield. The key step in the synthesis was an intramolecular Mizoroki-Heck cyclization to form the desired bicycle guaipyridine core. Upon the initial synthesis of rupestine D and epi-rupestine D, a 1:2 ratio of inseparable diastereomers was obtained. This obstacle was overcome by forming the diastereomers with the nitrile functional group still intact, providing a separable mixture. This established synthetic route was used to synthesize and isolate rupestine C in 6 steps with an overall yield of 2.4%. It is proposed that rupestine B can also be isolated via this route with careful consideration of the temperature and Grignard equivalents.

The resulting methyl ketone of rupestine D and epi-rupestine D then served as the starting material for the synthesis of rupestine K and J respectively. In order to access the alpha hydroxy ketone of rupestine K, a silyl enol ether was formed and carried through a Rubottom oxidation. Rupestine K was synthesized and isolated as a single diastereomer in 8 steps from picolyl bromide **1.62** with low to excellent yields. The formation of rupestine J from epi-rupestine K using a Wittig reaction is currently in progress.

The synthesis of rupestines L and M was studied but not accomplished. The proposed synthetic route required a Baeyer-Villiger oxidation of rupestine D and epi-rupestine D. It was determined that the methyl ketone was not reactive enough for oxygen insertion, and only the pyridine *N*-oxide of the substrate was recovered. New synthetic routes for the synthesis of rupestines L and M are currently being explored by other members of the Vyvyan research group.

## 7.0 Experimental

### General Experimental Methods

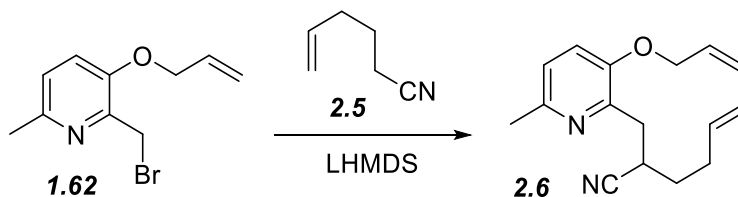
All reactions were carried out in oven-dried glassware. Air sensitive reactions were run under argon or nitrogen gas. Dry solvents were either freshly distilled or obtained from an Innovative Technology Pure-Solv™ 400 Solvent Purification System. Anhydrous 1,4-dioxane was purchased from Alfa Aesar.

Purification of compounds was accomplished via flash or radial chromatography in hexanes/ethyl acetate solvent systems unless otherwise noted. Silica gel (40-63  $\mu\text{m}$ ) was used in the hand-packed flash columns and 2 mm - 4 mm silica gel rotors were used in radial chromatography. 200  $\mu\text{m}$  thick silica plates from Sorbtech were used for TLC.

$^1\text{H}$  and  $^{13}\text{C}$  NMR data was acquired on a Varian MercuryPlus (300 MHz) or a Bruker Avance III (500 MHz) spectrometers. All NMR samples were prepared in  $\text{CDCl}_3$ .  $^1\text{H}$  NMR spectra were referenced to tetramethylsilane (TMS) at 0.00 ppm and  $^{13}\text{C}$  NMR spectra were referenced to  $\text{CDCl}_3$  at 77.0 unless otherwise noted. All spectra were processed using MestreNova software where chemical shifts are in units of ppm and coupling constants are reported in Hz.

All infrared spectra were acquired on a Thermo iS10 FT-IR with a diamond ATR at 16-32 scans with a resolution of  $1\text{ cm}^{-1}$ . Large scale characterization was accomplished by placing the compound directly on the ATR while small scale characterization was often done by placing a drop of the NMR sample on the ATR and allowing the  $\text{CDCl}_3$  to evaporate.

## Preparation of (3-(allyloxy)-2-(2-cyano-hex-5-enyl)-6-methyl)pyridine (2.6).



Notebook Entries: BJMA013, BJMA065, BJMA089

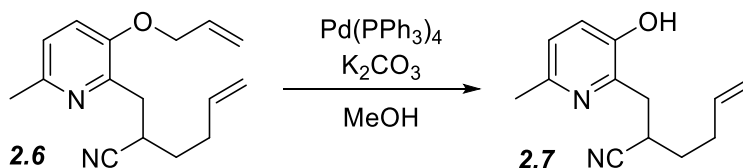
A flask was put under argon and charged with dry THF and placed over a dry ice/isopropyl alcohol slush bath. LHMDS (1 M, 12.0 mL, 12.0 mmol) was added followed by drop-wise addition of 5-hexenenitrile (**2.5**) (1.30 mL, 10.2 g, 11.6 mmol) diluted in THF (1.5 mL). Pyridyl bromide (**1.62**) (2.6164 g, 10.8 mmol) dissolved in THF (10 mL) was added drop-wise and the flask was allowed to stir overnight. The reaction was quenched with sat.  $\text{NH}_4\text{Cl}$  and diluted in ether (100 mL). The layers were separated and the aqueous layer was extracted with ether and the organic layers were combined. The organic layer was washed with brine and dried over  $\text{Na}_2\text{SO}_4$  for 1 hr. Flash chromatography (3:1 hexanes:EtOAc) gave **2.6** (2.118 g, 8.26 mmol, 77%) as a colorless oil.

FT-IR: 3056, 2965, 2926, 2867, 2238, 1642, 1581, 1257, 1125, 993, 916, 816, 732, 703  $\text{cm}^{-1}$ .

$^1\text{H}$  NMR (300 MHz,  $\text{CDCl}_3$ )  $\delta$  7.02 (d,  $J = 8.4$  Hz, 1H), 6.96 (d,  $J = 8.4$  Hz, 1H), 6.04 (dddd,  $J = 5.15, 10.43, 15.69, 17.26$  Hz, 1H), 5.77 (dddd,  $J = 6.21, 7.02, 10.18, 13.24$  Hz, 1H), 5.39 (dq,  $J = 1.64, 17.27$  Hz, 1H), 5.30 (dq,  $J = 1.42, 10.53$  Hz, 1H), 4.53 (dt,  $J = 1.57, 5.15$  Hz, 2H), 3.34-3.19 (m, 2H), 3.06-2.94 (m, 1H), 2.5-2.1 (m, 5H), 1.85-1.6 (m, 2H) ppm.

$^{13}\text{C}$  NMR (75 MHz,  $\text{CDCl}_3$ )  $\delta$  150.5, 149.3, 145.7, 136.5, 132.6, 121.94, 121.91, 199.2, 117.7, 115.8, 68.9, 34.3, 31.01, 30.98, 29.5, 23.2 ppm.

## Preparation of (3-hydroxy-2-(2-cyano-hex-5-enyl)-6-methyl)pyridine (2.7).



Notebook Entries: BJMA019, BJMA067, BJMA091

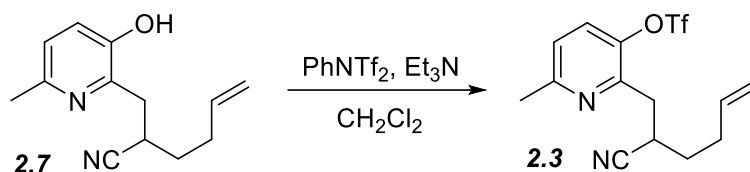
Allyl ether (**2.6**) (1.954 g, 7.622 mmol) was added to a flask with  $\text{Pd}(\text{PPh}_3)_4$  (0.1053 g, 0.0911 mmol) and  $\text{K}_2\text{CO}_3$  (3.1430 g, 22.7 mmol) and placed under argon.  $\text{MeOH}$  (40 mL) was added and the reaction was allowed to stir at room temperature (rt). The solution was left stirring overnight before being taken up in  $\text{CH}_2\text{Cl}_2$  (50 mL) and washed with sat.  $\text{NH}_4\text{Cl}$ . The layers were separated and the aqueous layer was extracted twice with  $\text{CH}_2\text{Cl}_2$  (20 mL) and all of the organic layers were combined and dried over  $\text{NaSO}_4$ . Crude product would not completely dissolve for purification. Flash chromatography on dissolved product (2:1 hexanes:EtOAc) gave **2.7** (0.511 g, 2.36 mmol, 31%) as a white solid. Subsequent product loss resulted from flask shattering. A second flash column was run (2:1 hexanes:EtOAc) and combined with the previously purified product to give **2.7** (0.622 g, 2.88 mmol, 37.7%) as a white solid.

FT-IR: 2921, 2455(br), 2239, 1640, 1577, 1280, 1123, 1004, 929, 842  $\text{cm}^{-1}$ .

$^1\text{H}$  NMR (300 MHz,  $\text{CDCl}_3$ )  $\delta$  7.02 (dd,  $J = 8.2$ , 1H), 6.90 (dd,  $J = 8.2$ , 1H), 5.85-5.65 (m, 1H), 5.15-4.95 (m, 1H), 4.2-4.0 (m, 2H), 3.30-3.15 (m, 2H), 3.05-2.93 (m, 1H), 2.45 (s, 3H) ppm.

$^{13}\text{C}$  NMR (300 MHz,  $\text{CDCl}_3$ )  $\delta$  150.0, 147.9, 144.1, 136.4, 123.9, 123.4, 121.7, 116.1, 34.2, 31.2, 31.1, 30.0, 22.4 ppm.

## Preparation of (2-(2-cyano-hex-5-enyl)-6-methyl-3-(((trifluoromethyl)sulfonyl)oxy))pyridine (**2.3**).



Notebook Entries: BJMA023, BJMA053, BJMA073, BJMA093

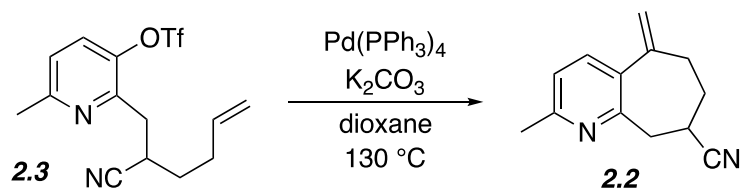
Phenol (**2.7**) (0.6235 g, 2.88 mmol) and PhNTf<sub>2</sub> (1.0202 g, 2.85 mmol) were placed in a flask under nitrogen and dissolved in dry CH<sub>2</sub>Cl<sub>2</sub> (17 mL). The reaction mixture was placed over an ice bath before subsequent addition of Et<sub>3</sub>N (0.500 mL, 0.363 g, 3.59 mmol). The reaction progress was checked by TLC (3:1 hexanes:EtOAc) 2.5 hr later and revealed unreacted starting material. An additional portion of Et<sub>3</sub>N (0.061 mL, 0.0443 g, 0.438 mmol) and PhNTf<sub>2</sub> (0.1630 g, 0.4563 mmol) were added and the solution was allowed to stir overnight. TLC revealed slight unreacted starting material so additional Et<sub>3</sub>N (0.100 mL, 0.0726 g, 0.717 mmol) and PhNTf (0.0563 g, 0.158 mmol) were added. After 1 hr, no starting material remained so the reaction mixture was diluted in ether and washed with sat. NH<sub>4</sub>Cl, 10% NaOH and then brine. The layers were separated and the organic layer was dried over Na<sub>2</sub>SO<sub>4</sub>. Flash chromatography (6:1 hexanes:EtOAc) gave **2.3** (0.818 g, 2.35 mmol, 77%) as a clear yellow oil.

FT-IR: 3081, 2930, 2241, 1643, 1594, 1210, 1136, 1083, 918, 865, 830, 703 cm<sup>-1</sup>.

<sup>1</sup>H NMR (300 MHz, CDCl<sub>3</sub>) δ 7.49 (dd, *J* = 8.53 Hz, 1H), 7.13 (d, *J* = 8.71 Hz, 1H), 5.79 (dddd, *J* = 6.28, 7.05, 10.2, 13.4 Hz, 1H) 5.19-5.02 (m, 2H), 3.49-3.35 (m, 1H), 3.24 (dd, *J* = 15.3, 8.55 Hz, 1H), 3.05 (dd, *J* = 15.2, 6.41 Hz, 1H) 2.59 (s, 3H) ppm.

<sup>13</sup>C NMR (300 MHz, CDCl<sub>3</sub>) δ 158.6, 148.6, 143.1, 136.1, 129.4, 129.3, 123.1, 121.2, 118.4 (q, *J* = 320 Hz), 116.3, 33.9, 30.99, 30.96, 28.9, 23.9 ppm.

## Preparation of 2-Methyl-5-methylene-6,7,8,9-tetrahydro-5H-5-cyclohepten[b]pyridine-8-carbonitrile (2.2, table 1, entry 6).



Notebook Entries:

BJMA031, BJMA039, BJMA061, BJMA075, BJMA095, BJMA105, BJMB047

Triflate (**2.3**) (0.865 g, 2.483 mmol) was added to a screw cap culture tube with  $\text{K}_2\text{CO}_3$  (1.7324 g, 12.53 mmol) and  $\text{Pd}(\text{PPh}_3)_4$  (0.1445 g, 0.1250 mmol) and placed under nitrogen. Dry dioxane (30 mL) was then added and the septa was quickly exchanged with a screw cap. The reaction tube was placed on a heating mantel at  $130\text{ }^\circ\text{C}$  and allowed to stir overnight. The reaction was monitored by TLC (3:1 hexanes:EtOAc) until no starting material remained (24 hr). The solution was filtered through a fritted funnel with silica gel and rinsed (x3) with EtOAc. The filtrate was concentrated on the rotavap and purified via radial chromatography (1:1 hexanes:EtOAc). A white solid (0.24 g, 1.21 mmol, 49% yield, mp =  $78.5\text{-}80.1\text{ }^\circ\text{C}$ ) was obtained.

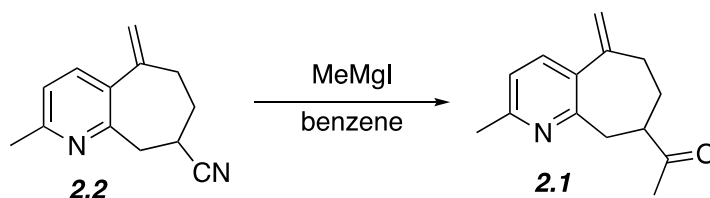
FT-IR: 3080, 2926, 2858, 2236, 1629, 1589, 1563, 911, 839  $\text{cm}^{-1}$ .

$^1\text{H}$  NMR (300 MHz,  $\text{CDCl}_3$ ):  $\delta$  7.41 (d,  $J = 7.74\text{ Hz}$ , 1H), 7.02 (d,  $J = 7.74\text{ Hz}$ , 1H), 5.24 (s, 1H), 5.09 (s, 1H) 3.28 (d,  $J = 5.88\text{ Hz}$ , 2H), 3.04 (quintet,  $J = 5.87, 11.72\text{ Hz}$ , 1H) 2.73-2.41 (m, 2H) 2.52 (s, 3H), 2.18-2.12 (m, 2H) ppm.

$^{13}\text{C}$  NMR (300 MHz,  $\text{CDCl}_3$ ):  $\delta$  156.89, 153.45, 147.28, 136.37, 135.25, 122.07, 121.28, 116.71, 40.79, 33.29, 32.97, 27.65, 24.04 ppm.

HRMS (ESI, TOF)  $m/z$ : calcd for  $\text{C}_{13}\text{H}_{14}\text{N}_2\text{Na}$  221.1055; found 221.1050

## Preparation of 1-(2-methyl-5-methylene-6,7,8,9-tetrahydro-5H-cyclohepta[b]pyridine-8-yl)ethan-1-one (**2.1**).



Notebook Entries: BJMA049, BJMA081

Preparation of Grignard reagent (MgMeI). An oven dried flask with stir bar equipped with water cooling reflux condenser was charged with crushed Mg turnings (0.2493 g, 10.26 mmol). The reaction flask was put under nitrogen and methyl iodide (0.65 mL, 1.148 g, 10.44 mmol) was added drop wise over the course of 30 minutes. The presence of unreacted Mg turnings required additional methyl iodide (0.2 mL, 0.456 g, 3.21 mmol) Once all Mg turnings were reacted, the flask was placed over an ice bath.

A separate oven dried flask with stir bar was charged with nitrile (**2.2**) and put under nitrogen. Distilled benzene (3 mL) was transferred to the flask and the reaction was allowed to stir. The synthesized Grignard reagent (3 mL, 3.418 M) was added to the reaction flask drop wise and allowed to stir overnight. Reaction was quenched by adding pH=5.2 acetic acid/sodium acetate buffer solution dropwise while reaction was kept stirring. The crude mixture was transferred to a 125-mL separatory funnel with 25 mL of ether and 25 mL of water. The aqueous layer was extracted with ether (20 mL, x3). The organic layers were combined and washed with H<sub>2</sub>O (20 mL, x2) and brine (20 mL, x2) and dried over Na<sub>2</sub>SO<sub>4</sub>. The crude reaction mixture was purified via radial chromatography (2 mm, EtOAc, 4.8 mL/min) to provide the product **2.1** as a yellow oil (0.022 g, 0.102 mmol, 53% yield).

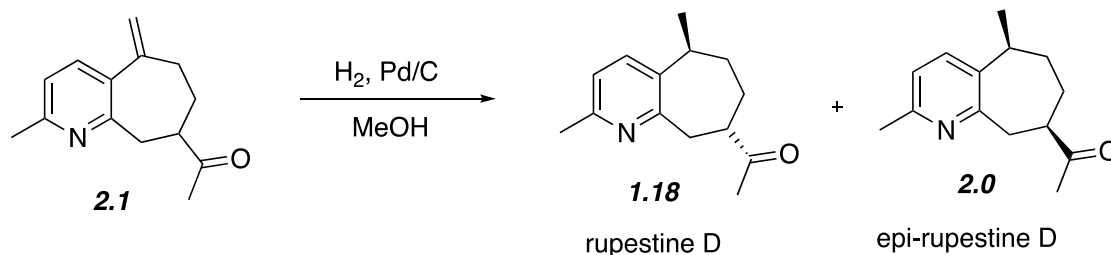
FT-IR: 3079, 2927, 2855, 1709, 1630, 1599, 1563 cm<sup>-1</sup>.

<sup>1</sup>H NMR (300 MHz, CDCl<sub>3</sub>) δ 7.38 (d, *J* = 7.7 Hz, 1H), 6.96 (d, *J* = 7.7 Hz, 1H), 5.15 (d, *J* = 1.13 Hz, 1H), 5.04 (d, *J* = 1.6 Hz, 1H), 3.18-3.02 (m, 2H), 2.83-2.59 (m, 2H) 2.49 (s, 3H), 2.36-2.26 (m, 1H), 2.20 (s, 3H), 2.06-1.99 (m, 2H), 1.94-1.82 (m, 1H) ppm.

<sup>13</sup>C NMR (300 MHz, CDCl<sub>3</sub>) δ 210.38, 156.4, 156.2, 148.4, 136.0, 135.2, 121.3, 115.5, 49.3, 39.7, 33.7, 31.9, 28.4, 24.1 ppm.

HRMS (ESI, TOF) *m/z*: calcd for C<sub>14</sub>H<sub>17</sub>NONa 238.1208; found 238.1215

**Preparation of 1-(2,5-dimethyl-6,7,8,9-tetrahydro-5H-cyclohepta[b]pyridine-8-yl)ethan-1-one (1.69, 2.0).**



Notebook Entries: BJMA063, BJMA085,

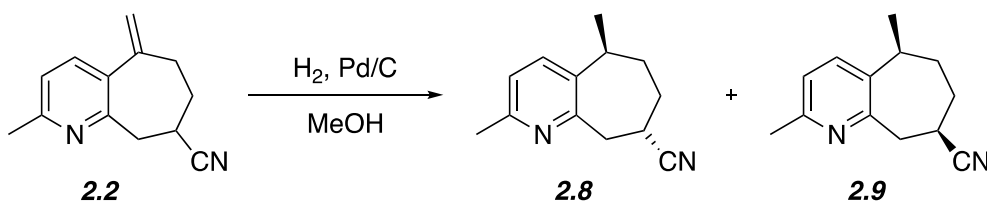
A flask containing the substrate (**2.1**) was charged with a stir bar, Pd/C (0.0103 g, mmol) and methanol (1.6 mL). The flask was flushed with argon and an balloon filled with H<sub>2</sub> was obtained. The first H<sub>2</sub> balloon was used to flush the reaction flask and the second balloon was left to react overnight. After removal of the H<sub>2</sub> balloon, the reaction flask was purged with argon. The crude product was filtered through a celite pipette and rinsed (x3) with EtOAc. Concentration of filtrate via rotary evaporation gave the crude product as a yellow oil of mass 0.0205 g (0.1 mmol 92%).

FT-IR: 2961, 2923, 2853, 1709, 1591, 1574, 1463 cm<sup>-1</sup>.

<sup>1</sup>H NMR (300 MHz, CDCl<sub>3</sub>) δ 7.36 (d, *J* = 7.85 Hz, 1H), 7.29 (d, *J* = 7.72 Hz, 1H), 6.97 (d, *J* = 7.87 Hz, 1H), 6.91 (d, *J* = 7.72 Hz, 1H), 3.35-3.09 (m, 4H), 3.03-2.91 (m, 2H), 2.72-2.64 (m, 1H), 2.49 (s, 3H), 2.47 (s, 3H), 2.21, (s, 3H), 2.20 (s, 3H), 2.08-1.69 (m, 2H), 1.92-1.70 (m, 6H) 1.34-1.24 (m, 7H) ppm.

<sup>13</sup>C NMR (300 MHz, CDCl<sub>3</sub>) δ 211.09, 210.81, 159.18, 157.52, 154.67, 154.46, 137.89, 137.85, 132.52, 132.52 121.36, 121.21, 49.55, 49.55, 39.52, 39.52, 35.03, 35.03, 34.79, 34.79, 32.95, 32.20, 28.60, 28.48, 28.21, 23.78, 20.35, 18.93 ppm.

## Preparation of 2,5-dimethyl-6,7,8,9-tetrahydro-5H-cyclohepta[b]pyridine-8-carbonitrile (**2.8** and **2.9**).



Notebook Entries: BJMB031, BJMB039, BJMB075, BJMB079, BJMB087, BJMB135, BJMB177,

A single neck 25-mL round bottom flask equipped with a stir bar was charged with substrate **2.2** (0.084 g, 0.42 mmol), 10 % w/w Pd/C (0.046 g, 0.432 mmol) and methanol (6.2 mL). The reaction mixture was allowed to stir and flushed N<sub>2</sub> (g) for 5 minutes, after which the N<sub>2</sub> was removed and an H<sub>2</sub> balloon was added. The reaction flask was flushed with the first H<sub>2</sub> balloon. The second H<sub>2</sub> balloon was allowed to react overnight at room temperature. The crude reaction mixture was filtered over a 3 cm plug of Celite and rinsed with 5 mL portions of EtOAc (x3). The filtrate was collected in a round bottom flask and concentrated via rotary evaporation to provide a clear yellow oil in a 94% yield. The product mixture was separated via radial chromatography (2mm, 1:3 hexanes/ethyl acetate) and two fractions were isolated.

Fraction 1 (**2.8**) was obtained as a clear yellow oil (0.013 g, 0.065 mmol, 15%).

FT-IR: 2961.75, 2923.2, 2854.5, 2238.1, 1591.7, 1573.2, 1463 cm<sup>-1</sup>.

<sup>1</sup>H NMR (300 MHz, CDCl<sub>3</sub>): δ 7.38 (d, *J* = 7.88 Hz, 1H), 7.01 (d, *J* = 7.87 Hz, 1H), 3.38 (d, *J* = 6.45 Hz, 2H), 2.99 (ddq, *J* = 1.61, 6.59, 8.67 Hz, 1H), 2.73 (dddd, *J* = 3.53, 6.29, 6.29, 9.8 Hz, 1H), 2.49 (s, 3H), 2.28-2.17 (m, 1H) 2.13-2.05 (m, 1H), 2.00-1.91 (m, 2H), 1.34 (d, *J* = 7.11 Hz, 3H) ppm.

<sup>13</sup>C NMR (300 MHz, CDCl<sub>3</sub>): δ 157.48 154.17, 137.43, 131.80, 121.97, 121.94, 41.04, 35.10, 33.67, 33.05, 28.79, 22.26, 17.35 ppm.

GCMS *m/z* 200.2 (M<sup>+</sup>, 52.32%)

HRMS (ESI, TOF) *m/z*: calcd for C<sub>13</sub>H<sub>16</sub>N<sub>2</sub> 200.1313; found 201.1392

Fraction 2 (**2.9**) was obtained a white semi-solid in a (0.049 g, 0.24 mmol, 58%, mp = 77.0-78.8 °C).

FT-IR: 2962, 2954, 2881, 2236, 1589, 1577, 1462 cm<sup>-1</sup>.

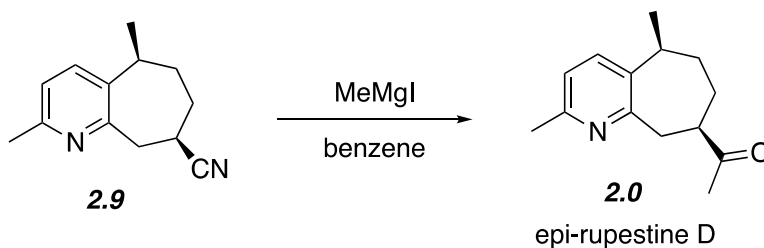
<sup>1</sup>H NMR (300 MHz, CDCl<sub>3</sub>): δ 7.39 (d, *J* = 7.87 Hz, 1H), 7.01 (d, *J* = 7.86 Hz, 1H), 3.35 (d, *J* = 5 Hz, 2H), 3.07 (apparent quintet, *J* = 4.94 Hz, 1H), 2.94 (ddq, *J* = 2.32, 6.87, 9.19 Hz, 1H), 2.52 (s, 3H), 2.30-2.20 (m, 1H) 2.12-2.02 (m, 1H), 1.86-1.81 (m, 2H), 1.36 (d, *J* = 7.13 Hz, 3H) ppm.

<sup>13</sup>C NMR (300 MHz, CDCl<sub>3</sub>): δ 155.75, 155.12, 137.56, 134.19, 121.97, 120.64, 40.36, 36.07, 32.60, 32.25, 27.83, 23.85, 19.84 ppm.

GCMS: *m/z* 200.2 (M<sup>+</sup>, 64.02%).

HRMS (ESI, TOF) *m/z*: calcd for C<sub>13</sub>H<sub>16</sub>N<sub>2</sub> 200.1313; found 201.1392

## Preparation of 1-((5S,8R)-2,5-dimethyl-6,7,8,9-tetrahydro-5H-cyclohepta[b]pyridin-8-yl)ethan-1-one (**2.0**).



Notebook Entries: BJMB037, BJMB043, BJMB179,

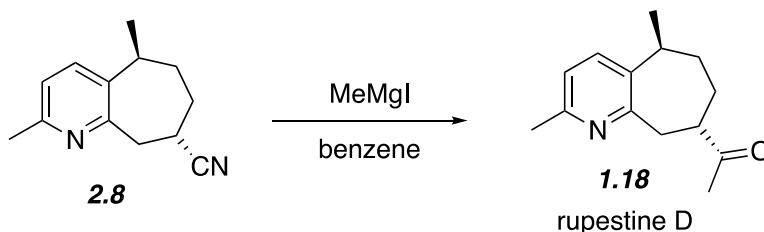
An oven dried flask equipped with a water-cooling reflux condenser and stir bar was charged with crushed magnesium turnings (0.247 g, 10.2 mmol) and two small iodine crystals. The flask was put under nitrogen and the solids were covered in anhydrous ether (1.5 mL). Methyl iodide (0.63 mL, 1.43 g, 10.1 mmol) was added drop-wise over the course of 30 minutes, after which the flask was placed over an ice bath. A separate oven dried flask containing a stir bar and the nitrile substrate (**11b**, 0.010 g, 0.05 mmol) was put under nitrogen and dissolved in distilled benzene (1.3 mL). This flask was then placed over an ice bath and allowed to stir. The entire solution containing the Grignard reagent was added to the nitrile solution and the reaction mixture was allowed to warm to room temperature overnight. The solution was quenched with 3 mL of pH = 5.2 acetic acid buffer and transferred to a 125-mL separatory funnel with 25 mL of ether and 15 mL of water. The aqueous layer was extracted with 25 mL of ether (x2). The organic layers were combined and washed with 25 mL brine (x2). The resulting organic layers were dried over sodium sulfate. The solution was then concentrated under vacuum and the crude mixture was purified via radial chromatography (2 mm, ethyl acetate). The purified product was obtained as a clear/white semi-solid (0.006 g, 0.03 mmol, 55%).

FT-IR: 2960, 2925, 1707, 1591, 1574, 1463, 1354, 1160, 1035, 825  $\text{cm}^{-1}$ .

$^1\text{H}$  NMR (300 MHz,  $\text{CDCl}_3$ ):  $\delta$  7.34 (d,  $J = 7.76$  Hz, 1H), 6.95 (d,  $J = 7.76$  Hz, 1H), 3.38-3.21 (m, 2H), 3.05-2.94 (m, 1H), 2.75-2.67 (m, 1H), 2.49 (s, 3H), 2.21 (s, 3H), 2.10-1.98 (m, 2H), 1.91-1.82 (m, 2H), 1.80-1.70 (m, 2H), 1.31 (d,  $J = 7.28$  Hz, 3H) ppm.

$^{13}\text{C}$  NMR (300 MHz,  $\text{CDCl}_3$ ):  $\delta$  159.3, 154.4, 136.9, 135.4, 120.8, 73.5, 47.3, 43.5, 39.1, 36.5, 33.6, 27.4, 26.4, 26.1, 23.7, 18.4 ppm.

## Preparation of 1-((5S,8S)-2,5-dimethyl-6,7,8,9-tetrahydro-5H-cyclohepta[b]pyridin-8-yl)ethan-1-one (1.18).



Notebook Entry: BJMB083, BJMB181

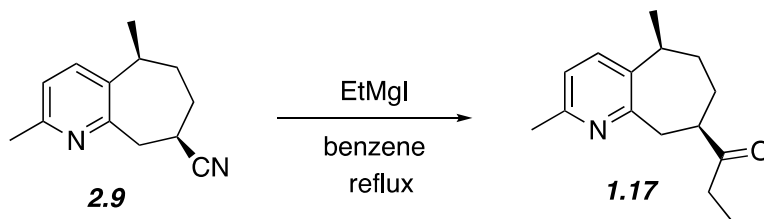
An oven dried flask equipped with a water-cooling reflux condenser and stir bar was charged with crushed magnesium turnings (0.232 g, 9.5 mmol) and two small iodine crystals. The flask was put under argon and the solids were covered in anhydrous ether (1.2 mL). Methyl iodide (0.60 mL, 1.368 g, 9.6 mmol) was added drop-wise over the course of 20 minutes, after which the flask was placed over an ice bath. A separate flask containing a stir bar and the nitrile substrate (B075\_F2 and B079\_F2, 0.029 g, 0.145 mmol) was put under argon and dissolved in distilled benzene (2.4 mL). This flask was then placed over an ice bath and allowed to stir. The entire solution containing the Grignard reagent was added to the nitrile solution and the reaction mixture was allowed to warm to room temperature overnight. The solution was quenched with 1 mL of pH = 5.2 acetic acid buffer and transferred to a 125-mL separatory funnel with 20 mL of ether and 20 mL of water. The aqueous layer was extracted with 25 mL of ether (x3). The organic layers were combined and washed with 25 mL brine (x2). The resulting organic layer was dried over sodium sulfate. The solution was then concentrated under vacuum and the crude mixture was purified via radial chromatography (2 mm, 1:3 hexanes/ethyl acetate). The purified product was obtained as a white crystalline solid (0.028 g, 0.129 mmol, 93%).

FTIR: 2960, 2922, 1709, 1591, 1462, 1354, 1159, 830, 813  $\text{cm}^{-1}$ .

$^1\text{H}$  NMR (300 MHz,  $\text{CDCl}_3$ ):  $\delta$  7.37 (d,  $J = 8.2$  Hz, 1H), 6.98 (d,  $J = 8.2$  Hz, 1H), 3.22 (dd,  $J = 14.1, 10.0$  Hz, 1H), 3.13 (dt,  $J = 14.1, 2.0$  Hz, 1H), 3.04-2.90 (m, 1H), 2.54 (tt,  $J = 10.5, 3.0$  Hz, 1H), 2.50 (s, 3H), 2.22 (s, 3H), 2.15-2.00 (m, 1H), 2.00-1.75 (m, 2H), 1.34 (d,  $J = 7.2$  Hz, 3H), 1.35-1.20 (m, 1H) ppm.

$^{13}\text{C}$  NMR (300 MHz,  $\text{CDCl}_3$ ):  $\delta$  211.1, 159.2, 154.5, 137.7, 132.4, 121.1, 49.6, 39.6, 35.0, 34.7, 32.9, 28.4, 23.8, 20.3 ppm.

## Preparation of 1-((5*S*,8*R*)-2,5-dimethyl-6,7,8,9-tetrahydro-5*H*-cyclohepta[*b*]pyridin-8-yl)propan-1-one (**1.17**)



Notebook Entry: BJMB133

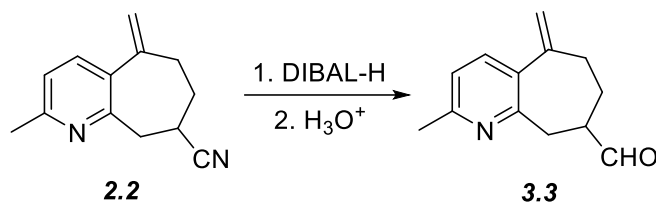
An oven dried flask equipped with a water-cooling reflux condenser and stir bar was charged with crushed magnesium turnings (0.2467 g, 10.15 mmol) and two small iodine crystals. The flask was put under nitrogen and the solids were covered in anhydrous ether (0.5 mL). Ethyl iodide (0.79 mL, 1.53 g, 9.8 mmol) was added drop-wise over the course of 30 minutes, after which the flask was placed over an ice bath. A separate oven dried flask containing a stir bar and the nitrile substrate (**2.9**, 0.0190 g, 0.095 mmol) was put under nitrogen and dissolved in distilled benzene (2.5 mL). This flask was then allowed to stir. The entire solution containing the Grignard reagent was added to the nitrile solution and the reaction mixture was brought to reflux and allowed to react overnight. The solution was quenched with 5 mL of pH = 5.2 acetic acid buffer and transferred to a 50-mL separatory funnel with 20 mL of ether and 15 mL of water. The aqueous layer was extracted with 20 mL of ether (x2). The organic layers were combined and washed with 25 mL brine (x2). The resulting organic layers were dried over sodium sulfate. The solution was then concentrated under vacuum and the crude mixture was purified via radial chromatography (2 mm, 1:2 hexanes:ethyl acetate). The purified product was obtained as a white solid (0.008 g, 0.035 mmol, 36%). An additional fraction containing a 1:1 ratio of rupestone B and rupestone C was obtained in a 53% yield.

FTIR: 2962, 2922, 1708, 1590, 1574, 1460, 142, 1375, 1348, 1280, 1164, 1110, 1026, 987, 972, 923, 825, 772, 731, and 690  $\text{cm}^{-1}$ .

$^1\text{H}$  NMR ( $\text{CDCl}_3$ , 300 MHz):  $\delta$  7.29 (d,  $J = 7.7$ , 1H), 6.91 (d,  $J = 7.7$ , 1H), 3.36-3.28 (m, 1H), 3.19 (dd,  $J = 14.0$ , 10.8, 1H), 3.04-2.96 (m, 1H), 2.67-2.72 (m, 1H), 2.56 (q,  $J = 7.3$ , 2H), 2.46 (s, 3H), 2.10-1.97 (m, 1H), 1.88-1.72 (m, 3H), 1.30 (d,  $J = 7.3$ , 3H), and 1.02 (t,  $J = 7.3$ , 3H) ppm.

$^{13}\text{C}$  NMR ( $\text{CDCl}_3$ , 75 MHz):  $\delta$  213.6, 157.8, 154.7, 137.8, 136.3, 121.2, 48.7, 40.0, 37.7, 34.3, 32.2, 28.3, 23.9, 18.8, and 7.8 ppm.

## Preparation of 2-methyl-5-methylene-6,7,8,9-tetrahydro-5H-cyclohepta[b]pyridine-8-carbaldehyde (3.3).



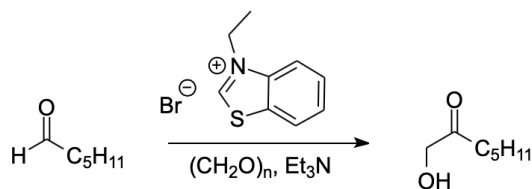
Notebook Entries: BJMB023, BJMB051

An oven dried culture tube with stir bar was charged with 2-methyl-5-methylene-6,7,8,9-tetrahydro-5H-cyclohepta[b]pyridine-8-carbonitrile (0.051 g, 0.257 mmol) and put under nitrogen. Dry dichloromethane (2.5 mL) was added and the solution was allowed to stir. The reaction flask was then cooled over a dry ice/isopropanol slush and DIBAL-H (1.0 M, 0.3 mL, 0.3 mmol) was added dropwise. The reaction was allowed to proceed for 3 hours and was subsequently quenched with saturated ammonium chloride (4 mL) followed by pH = 5.2 acetic acid/acetate buffer (1 mL). The reaction was allowed to warm to room temperature before being transferred to a 125-mL separatory funnel with ether (20 mL) and saturated ammonium chloride (20 mL). The aqueous layer was extracted with ether (20 mL, x2). The organic layers were combined and washed with pH = 5.2 acetic acid/acetate buffer (20 mL, x2), saturated sodium bicarbonate (25 mL, x2), and brine (25 mL, x2). The organic layer was then dried over magnesium sulfate and then concentrated under vacuum.

$^1\text{H}$  NMR (300 MHz,  $\text{CDCl}_3$ ):  $\delta$  9.74 (s, 1H), 7.40 (d,  $J = 7.72$  Hz, 1H), 6.98 (d,  $J = 7.7$  Hz, 1H), 5.18 (s, 1H), 5.06 (s, 1H), 3.36 (d,  $J = 13.33$  Hz, 1H), 3.01 (dd,  $J = 10.32, 14.66$  Hz, 1H), 2.67-2.59 (m, 2H), 2.51 (s, 3H), 2.37-2.29 (m, 1H), 2.22-2.13 (m, 1H), 1.90-1.77 (m, 1H) ppm.

$^{13}\text{C}$  NMR (300 MHz,  $\text{CDCl}_3$ ):  $\delta$  202.70, 156.45, 155.72, 148.22, 136.24, 135.33, 121.45, 115.86, 48.61, 37.54, 33.64, 29.47, 24.01 ppm.

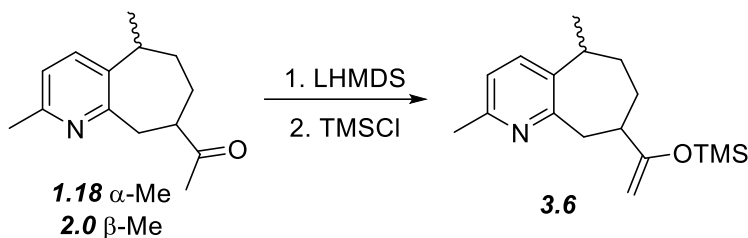
## Preparation of 1-hydroxyheptan-2-one



Notebook Entries: BJMB067, BJMB101

A 15-mL oven dried culture tube with stir bar was charged with distilled hexanal (0.12 mL, 0.100 g, 1.0 mmol) and dry THF (0.6 mL). The culture tube was then sequentially charged with paraformaldehyde (0.099 g, 3.3 mmol), 3-ethylbenzothiazolium bromide (0.028 g, 0.11 mmol) and triethylamine (0.04 mL, 0.029 g, 0.29 mmol). The reaction tube was flushed with argon and then quickly capped and placed on a heat block at 60 °C. The reaction was allowed to proceed for 4 days. On day 3, 1 mL of THF was added. The reaction was allowed to cool to room temperature and was then transferred to a 125-mL separatory funnel with water (15 mL) and DCM (20 mL). The aqueous layer was extracted with DCM (20 mL, x3) and the combined organic layers were washed with brine (25 mL). The resulting organic layer was dried over sodium sulfate and then concentrated under vacuum. GCMS analysis revealed a 25% desired product however isolation was never accomplished.

## Preparation of 2,5-dimethyl-8-(1-((trimethylsilyl)oxy)vinyl)-6,7,8,9-tetrahydro-5H-cyclohepta[*b*]pyridine (3.6)



A single neck oven dried flask with stir bar was charged with ketone (0.058 g, 0.267 mmol), put under argon and dissolved in dry THF (2.0 mL). A separate oven dried flask with stir bar was put under argon and charged with dry THF (2.0 mL) and LHMDS (0.82 mL, 0.82 mmol, 3 equiv). Both reaction flasks were cooled to  $-78\text{ }^{\circ}\text{C}$  in dry ice/isopropanol baths. The solution containing the ketone was added dropwise to the LHMDS solution over the course of 20 minutes. The combined solution was allowed to stir at  $-78\text{ }^{\circ}\text{C}$  for 30 minutes, after which TMSCl (0.30 mL, 0.26 g, 2.4 mmol, 9.0 equiv) was added. The reaction mixture was allowed to stir for 45 minutes at  $-78\text{ }^{\circ}\text{C}$  and then for 15 minutes at  $0\text{ }^{\circ}\text{C}$ . The reaction solution was transferred to a single neck flask and concentrated under vacuum. Hexanes (6 mL) was added and the solution was allowed to stir for 5 minutes at room temperature. The solution was then filtered over 1 cm of celite in a pipet and rinsed with 20 mL of hexanes. The filtrate was concentrated under vacuum and a crude yellow liquid was obtained (0.086 g, 112%).

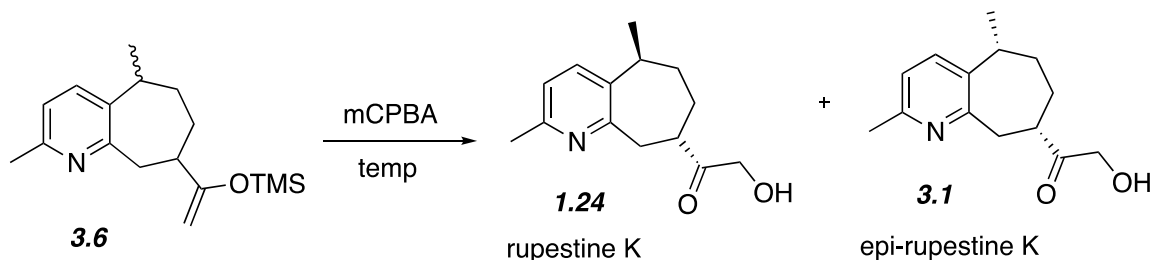
\*\*\*\*Having trouble tabulating the NMR data for the crude mixture

FT-IR: 2960, 2924, 1626, 1591, 1575, 2462, 1252, 1017, 919, 846  $\text{cm}^{-1}$ .

$^1\text{H}$  NMR (500 MHz,  $\text{CDCl}_3$ ):  $\delta$  7.35 (d,  $J = 7.6$  Hz, 1H), 7.27 (d,  $J = 7.9$  Hz, 1H), 6.94 (d,  $J = 7.8$  Hz, 1H), 6.89 (d,  $J = 7.6$  Hz, 1H), 3.89 (s, 2H), 3.79 (s, 2H), 3.07-2.88 (m, 4H), 2.83-2.75 (m, 2H), 2.31 (s, 3H), 2.30 (s, 3H), 1.91-1.55 (m, 8H), 1.15-1.10 (m, 8H) ppm.

$^{13}\text{C}$  NMR (500 MHz,  $\text{CDCl}_3$ ):  $\delta$  163.6, 163.5, 160.4, 158.9, 154.5, 154.1, 137.9, 137.7, 136.5, 132.0, 120.8, 120.7, 87.7, 87.6, 43.43, 43.32, 42.71, 42.71, 38.19, 36.06, 35.81, 35.06, 32.56, 30.13, 23.93, 23.88, 20.51, 18.59 ppm.

**Preparation of 1-((5*S*,8*S*)-2,5-dimethyl-6,7,8,9-tetrahydro-5*H*-cyclohepta[*b*]pyridin-8-yl)-2-hydroxyethan-1-one and 1-((5*R*,8*S*)-2,5-dimethyl-6,7,8,9-tetrahydro-5*H*-cyclohepta[*b*]pyridin-8-yl)-2-hydroxyethan-1-one**



Reaction procedure at 0 °C: An oven-dried flask with stir bar was charged with silyl enol ether **3.6** (0.072 g, 0.249 mmol) and 2.0 mL of dry CH<sub>2</sub>Cl<sub>2</sub> and allowed to stir at 0 °C. Solid mCPBA (0.056g, 0.325, 1.3 equivalents) was dissolved in 1.0 mL of dry CH<sub>2</sub>Cl<sub>2</sub> and added to the flask containing the substrate dropwise over 30 minutes. The resulting solution was transferred to a 125-mL separatory funnel with 20 mL of saturated NH<sub>4</sub>Cl solution. The organic layer was washed with saturated NH<sub>4</sub>Cl (20 mL, x2), saturated Na<sub>2</sub>S<sub>2</sub>O<sub>3</sub> (20 mL, 2x) and saturated Na<sub>2</sub>CO<sub>3</sub> (20 mL, 2x) before being dried over Na<sub>2</sub>SO<sub>4</sub>. The resulting solution was decanted from the drying agent and allowed to stir with TBAF (0.072 g, 0.275 mmol) at room temperature for 1 hour to remove the TMS protecting group. The mixture was then concentrated under vacuum and purified via flash chromatography in 20% MeOH in EtOAc. One test tube containing a white solid was isolated and confirmed to be rupestone K (**1.24**) (0.002 g, 0.0086 mmol, 3.4% yield). A yellow oil containing a 1:1 mixture of **1.24** and **3.1** was isolated (0.019 g, 0.081 mmol, 33% yield). Further attempts were made toward the isolation of each diastereomer using radial chromatography (12% MeOH in DCM, 2 mm plate, 6.3 mL/min) however both diastereomers were lost during the purification.

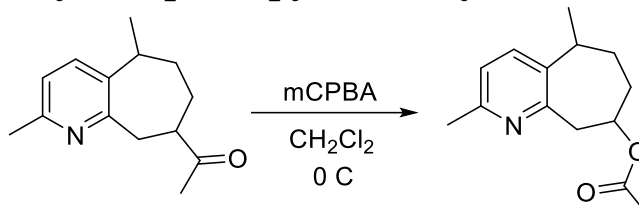
Rupestone K:

FT-IR: 3196(br), 2956, 2917, 2872, 2849, 1716, 1592, 1577, 1460, 1415 cm<sup>-1</sup>.

<sup>1</sup>H NMR (300 MHz, CDCl<sub>3</sub>): δ 7.40 (d, *J* = 7.8 Hz, 1H), 7.00 (d, *J* = 7.9 Hz, 1H), 4.37 (s, 2H), 3.32 (dd, *J* = 11.0, 14.0 Hz, 1H), 3.11 (d, *J* = 14.0 Hz, 1H), 3.03-2.97 (m, 1H), 2.56 (m, 1H), 2.49 (s, 3H), 2.04-1.90 (m, 3H), 1.36 (d, *J* = 7.0 Hz, 3H), 1.40-1.24 (m, 3H) ppm.

<sup>13</sup>C NMR (CDCl<sub>3</sub>, 500 MHz): δ 212.0, 158.5, 154.7, 137.7, 132.7, 121.4, 66.8, 45.2, 39.5, 34.8, 34.8, 33.3, 23.8, 20.3 ppm.

## Preparation of 2,5-dimethyl-6,7,8,9-tetrahydro-5H-cyclohepta[b]pyridine-8-yl acetate



Notebook Entries: BJMA121, BJMA139, BJMB025

A round bottom flask containing a stir bar was charged with pyridyl ketone (0.1176 g, 0.5412 mmol) and dissolved in DCM (5 mL). The reaction flask was then placed over an ice bath and allowed to stir, after which the mCPBA (0.1670 g, 0.9677 mmol) was added. The reaction flask was allowed to warm to room temperature overnight. Due to unreacted starting material (verified by TLC, 1:2 hexanes/EtOAc), an additional portion of mCPBA was added (0.0188 g, 0.109 mmol). A new ice bath was placed under the reaction flask before the addition of mCPBA. The reaction was monitored by TLC 2 hours later and starting material still remained. The next day, TLC confirmed that all starting material was consumed. Saturated Na<sub>2</sub>S<sub>2</sub>O<sub>3</sub> (3 mL) was added dropwise to the reaction flask followed by Na<sub>2</sub>CO<sub>3</sub> (25 mL). The solution was transferred to a separatory funnel and extracted with 50 mL ether (x3). The organic layers were combined and washed with 25 mL Na<sub>2</sub>CO<sub>3</sub> (x2) and 50 mL brine (x2). The organic layers were combined and dried over sodium sulfate. The crude product was concentrated via rotary evaporation and purified by radial chromatography (2 mm plate, 20% MeOH in EtOAc). A colorless oil was obtained in a 66% yield.

GC-MS m/z (% relative intensity, ion) 233.2 (100, M<sup>+</sup>).

FTIR revealed a C=O stretch at 1700 cm<sup>-1</sup>, indicating the presence of a ketone and not an ester.

## 8.0 References

1. Thomas, M.B.; Zhu, A.X. Hepatocellular Carcinoma: The Need for Progress. *J. Clin. Oncol.* **2005**, *23*, 2892-2899. DOI: [10.1200/JCO.2005.03.196](https://doi.org/10.1200/JCO.2005.03.196)
2. Ferlay J.; Shin H.R.; Bray F.; Forman D.; Mathers C.; Parkin D.M. Estimates of worldwide burden of cancer in 2008: GLOBOCAN 2008. *Int. J. Cancer* **2010**, *127*, 2893–917. DOI: [10.1002/ijc.25516](https://doi.org/10.1002/ijc.25516)
3. Zhang, B.H.; Yang, B.H.; Tang, Z.Y. Randomized controlled trial of screening for hepatocellular carcinoma. *J. Cancer Res. Clin. Oncol.* **2004**, *130*, 417-422. DOI: [10.1007/s00432-004-0552-0](https://doi.org/10.1007/s00432-004-0552-0)
4. Singal, A.; Volk, M.L.; Waljee, A.; Salgia, R.; Higgins, P.; Rogers, M.A.; Marrero, J.A. Meta-analysis: surveillance with ultrasound for early-stage hepatocellular carcinoma in patients with cirrhosis. *Pharmacol. Ther.* **2009**, *30*, 37-47. DOI: [10.1111/j.1365-22036.2009.04014](https://doi.org/10.1111/j.1365-22036.2009.04014)
5. El-Serag, H.B.; Kanwal, F. Epidemiology of Hepatocellular Carcinoma in the United States: Where Are We? Where Do We Go? DOI: [10.1002/hep.27222](https://doi.org/10.1002/hep.27222)
6. Lin, W.C.; Lin, Y.S.; Chang, C.W.; Chang, C.W., Wang, T.E.; Wang, H.Y.; Chen, M.J. Impacts of direct-acting antiviral therapy for hepatitis C-related hepatocellular carcinoma. *PLOS ONE* **2020**, *15* (5), 1-12. DOI: [10.1371/journal.pone.0233212](https://doi.org/10.1371/journal.pone.0233212)
7. <https://www.cancer.net/cancer-types/liver-cancer/statistics> (Accessed June 13th, 2020).
8. Ruff, P. Therapeutic Options in Hepatocellular Carcinoma. *Am. J. Cancer* **2004**, *3* (2), 119-131. DOI: [10.2165/00024669-200403020-00004](https://doi.org/10.2165/00024669-200403020-00004)
9. Zhang, J.; Gray, N.S. Targeting cancer with small molecule kinase inhibitors. *Nature Rev.* **2009**, *9*, 28-39. DOI: [10.1038/nrc2559](https://doi.org/10.1038/nrc2559)
10. Jeon, J.Y.; Sparreboom, A.; Baker, S.D. Kinase inhibitors: the reality behind the success. *Clin. Pharmacol. Ther.* **2017**, *102*, 726-730. DOI: [10.1002/cpt.815](https://doi.org/10.1002/cpt.815)
11. Keating, G.M.; Santoro, A. Sorafenib: a review of its use in advanced hepatocellular carcinoma. *Drugs* **2009**, *69*, 223-240. DOI: [10.2165/00003495-200969020-00006](https://doi.org/10.2165/00003495-200969020-00006)
12. Parsons, H. M.; Chu, Q.; Karlitz, J. J.; Stevens, J. L.; Harlan, L. C. Adoption of Sorafenib for the Treatment of Advanced-Stage Hepatocellular Carcinoma in Oncology Practices in the United States. *Liver Cancer* **2017**, *6*, 216-226. DOI: [10.1159/000473862](https://doi.org/10.1159/000473862)
13. Heo, Y.-A.; Syed, Y. Y. Regorafenib: A Review in Hepatocellular Carcinoma. *Drugs*, **2018**, *78*, 951-958. DOI: [10.1007/s40265-018-0932-4](https://doi.org/10.1007/s40265-018-0932-4)
14. Barford, D.; Marais, R. Mechanism of activation of the RAF-ERK signaling pathway by oncogenic mutations of B-RAF. *Cell* **2004**, *116*, 855-867. DOI: [10.1016/S0092-8674\(04\)00215-6](https://doi.org/10.1016/S0092-8674(04)00215-6)
15. Al-Salama, Z. T.; Syed, Y. Y.; Scott, L. J. Lenvatinib: A Review in Hepatocellular Carcinoma. *Drugs* **2019**, *79*, 665-674. DOI: [10.1007/s40265-019-01116-x](https://doi.org/10.1007/s40265-019-01116-x)
16. Bteich, F.; Di Bisceglie, A. M. Current and Future Systemic Therapies for Hepatocellular Carcinoma. *Gastroenterol. and Hepatol* **2019**, *15*, 266-272. PMID: [PMC6589844](https://pubmed.ncbi.nlm.nih.gov/36589844/)
17. Baxter, M. A.; Glen, H.; Evans, T. R. J. Lenvatinib and its use in the treatment of unresectable hepatocellular carcinoma. *Future Oncol.* **2018**, *14*, 2021-2029. DOI: [10.2217/fon-2017-0689](https://doi.org/10.2217/fon-2017-0689)
18. Peters, M. L. B.; Miksad, R. A. Caocantini in the treatment of hepatocellular carcinoma. *Future Oncol.* **2017**, *13*, 1915-1929. DOI: [10.2217/fon-2017-0169](https://doi.org/10.2217/fon-2017-0169)

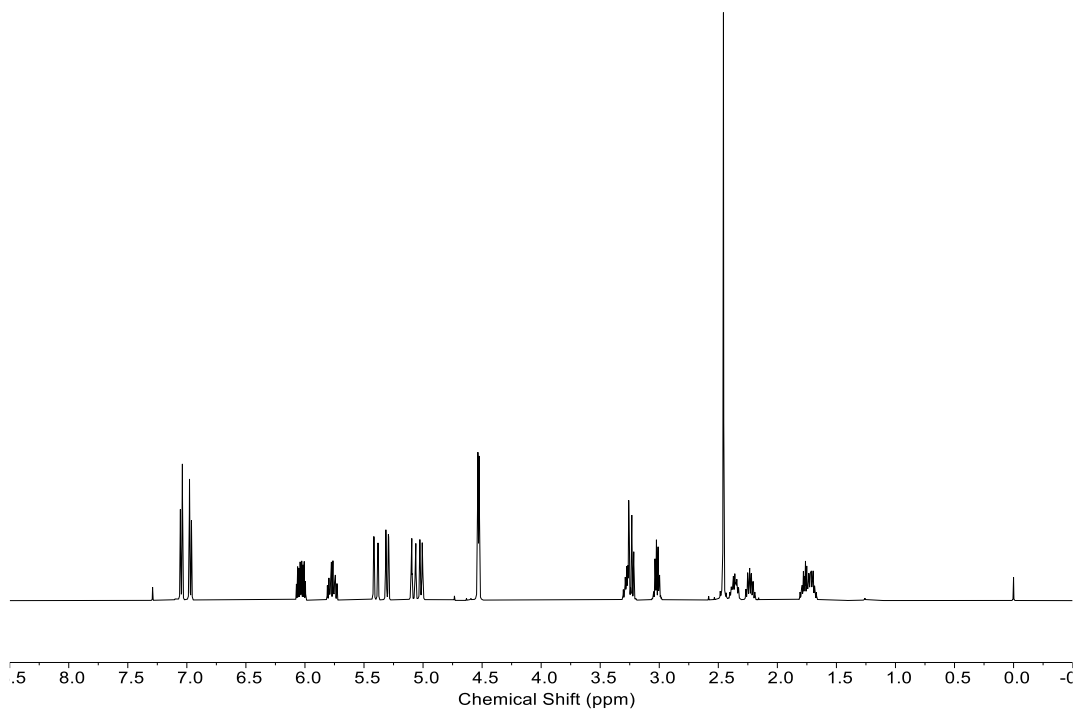
19. Hartwell, J. L. *Plants Used Against Cancer*, Quarterman Publications, Lawrence, MA, **1982**, pp 406.
20. Olivero, J.; Garcia, T.; Payares, P.; Vivas, R.; Diaz, D.; Daza, E.; Geerliger, P. Molecular structure and gas chromatographic retention behavior of the components of ylang-ylang oil. *J. Pharm. Sci.* **1997**, *86*, 625-630. DOI: [10.1021/js960196u](https://doi.org/10.1021/js960196u)
21. Farnsworth, N. R.; Graham, J. G.; Quinn, M. L.; Fabricant, D. S. J. Plants used against cancer – an extension of the work of Jonathan Hartwell. *Ethnopharm.* **2000**, *73*, 347-377. DOI: [10.1016/s0378-8741\(00\)00341-x](https://doi.org/10.1016/s0378-8741(00)00341-x)
22. (a) Hsieh, T.-J.; Chang, F.-R.; Chia, Y.-C.; Chen, C.-Y.; Chiu, H.-F.; Wu, Y.-C. Cytotoxic Constituents of the Fruits of *Cananga odorata*. *J. Nat. Prod.* **2001**, *64*, 616-618. DOI: [10.1021/np0005208](https://doi.org/10.1021/np0005208)  
(b) Wu, Y. C.; Hsieh, T. J.; Chang, F. R.; Chia, Y. C.; Chiu, H. F. The constituents of *Cananga odorata*. *J. Chin. Chem. Soc.* **1999**, *46*, 607-611. DOI: [10.1002/jccs.199900084](https://doi.org/10.1002/jccs.199900084)
23. (a) Aisa, H. A.; Su, Z.; Wu, F. H.; Slukan, U. New Guaipyridine Sesquiterpene Alkaloids from *Artemisia rupestris* L. *Helv. Chim. Acta* **2010**, *93*, 33-38. DOI: [10.1002/hlca.200900125](https://doi.org/10.1002/hlca.200900125)  
(b) Aisa, H. A.; He, F.; Nugroho, A. E.; Wong, C. P.; Hirasawa, Y.; Shiota, O.; Morita, H. Rupestines F-M, new guaipyridine sesquiterpene alkaloids from *Artemisia rupestris*. *Chem. Pharm. Bull.* **2012**, *60*, 213-218. DOI: [10.1248/cpb.60.213](https://doi.org/10.1248/cpb.60.213)
24. Büchi, G.; Goldman, M.; Mayo, D. W. The total synthesis of (-)-aromadendrene. *J. Am. Chem. Soc.* **1966**, *88*, 3109-3113. DOI: [10.1021/ja00969a053](https://doi.org/10.1021/ja00969a053)
25. van der Gen, A.; Van der Linde, L. M.; Witteveen, J. G. Synthesis of guaipyridine and some related sesquiterpene alkaloids. *Rec. Trav. Chim. Pays-Bas.* **1972**, *91*, 1433-1440. DOI: [10.1002/recl.19720911207](https://doi.org/10.1002/recl.19720911207)
26. (a) Okatani, T.; Koyama, J.; Tagahara, K.; Suzuta, Y. Synthesis of sesquiterpene alkaloids, guaipyridine, epiguaipyridine, and related compounds. *Heterocycles* **1987**, *26*, 595-597.  
(b) Koyama, J.; Okatani, T.; Tagahara, K.; Suzuta, Y.; Irie, H. Synthesis of guaipyridine, epiguaipyridine, and related compounds. *Heterocycles* **1987**, *26*, 925-927.
27. Craig, D.; Henry, G. D. Eur. Total synthesis of the cytotoxic guaipyridine sesquiterpene alkaloid (+)-cananodine. *J. Org. Chem.* **2006**, *16*, 3558-3561. DOI: [10.1002/ejoc.200600414](https://doi.org/10.1002/ejoc.200600414)
28. Shelton, P.; Ligon, T. J.; Dell (née Meyer), J. M.; Yarbrough, L.; Vyvyan, J. R. Synthesis of cananodine by intramolecular epoxide opening. *Tetrahedron Lett.* **2017**, *58*, 3478-3481. DOI: [10.1016/j.tetlet.2017.07.080](https://doi.org/10.1016/j.tetlet.2017.07.080)
29. Shelton, P.M.; Grosslight, S.M.; Mulligan, B.J.; Spargo, H.V.; Saad, S.S.; Vyvyan, J.R. Synthesis of guaipyridine alkaloids ( $\pm$ )-cananodine and ( $\pm$ )-rupestines D and G using an intramolecular Mizoroki-Heck reaction. *Tetrahedron.* **2020**, *76* (41), 131500. DOI: [10.1016/j.tet.2020.131500](https://doi.org/10.1016/j.tet.2020.131500)
30. Yusuf, A.; Zhao, J.; Wang, B.; Aibibula, P.; Aisa, H.; Huang, G. Total synthesis of rupestrine G and its epimers. *Royal. Soc. Open Sci.* **2018**, *5*, 172037/1-172037/9. DOI: [10.1098/rsos.172037](https://doi.org/10.1098/rsos.172037)

31. Starchman, E. S.; Marshall, M. S.; Vyvyan, J. R. Synthesis of ( $\pm$ )-rupestines B and C by intramolecular Mizoroki-Heck cyclization. *Tetrahedron Lett.* **2020**, *61*, 151837. DOI: [10.1016/j.tetlet.2020.151837](https://doi.org/10.1016/j.tetlet.2020.151837)
32. Mizoroki, T.; Mori, K.; Ozaki, A. Arylation of olefin with aryl iodide catalyzed by palladium. *Bull. Chem. Soc. Jpn.* **1971**, *4*, 581. DOI: [10.1246/BCSJ.44.581](https://doi.org/10.1246/BCSJ.44.581)
33. Heck, R. F.; Nolley, Jr., J. P. Palladium-catalyzed vinylic hydrogen substitution reactions with aryl, benzyl, and styryl halides. *J. Org. Chem.* **1972**, *37*, 2320-2322. DOI: [10.1021/jo00979a024](https://doi.org/10.1021/jo00979a024)
34. Heck, R. F.; Terpkko, M. O. Rearrangement in the palladium-catalyzed cyclization of  $\alpha$ -substituted N-acryloyl-*o*-bromoanilines. *J. Am. Chem. Soc.* **1979**, *101*, 5281-5283. DOI: [10.1021/ja00512a028](https://doi.org/10.1021/ja00512a028)
35. Shibasaki, M.; Sato, Y.; Sodeoka, M. Catalytic asymmetric carbon-carbon bond formation: asymmetric synthesis of cis-decalin derivatives by palladium-catalyzed cyclization of prochiral alkenyl iodides. *J. Org. Chem.* **1989**, *54*, 4738. DOI: [10.1021/jo00281a007](https://doi.org/10.1021/jo00281a007)
36. Overman, L. E.; Dounay, A. B. The Asymmetric Intramolecular Heck Reaction in Natural Product Total Synthesis. *Chem. Rev.* **2003**, *103*, 2945-2963. DOI: [10.1021/cr020039h](https://doi.org/10.1021/cr020039h)
37. Canonne, P.; Foscolos, G.B.; Lemay, G. Effet Du Benzene Dans La Reaction De Grignard Sur Les Nitriles. *Tetrahedron Lett.* **1980**, *21*, 155-158.
38. Hopkinson, M.N.; Richter, C.; Schedler, M.; Glorius, F. An overview of N-heterocyclic carbenes. *Nature* (510), **2014**, 485-496. DOI: [10.1038/nature13384](https://doi.org/10.1038/nature13384)
39. Nikolaou, A.; Kokotos, G.; Magrioti, V. Efficient microwave-assisted synthesis of hydroxymethyl ketones using NHC organocatalysts. *Tetrahedron* **2016**, *72*, 7628-7632. DOI: [10.1016/j.tet.2017.11.024](https://doi.org/10.1016/j.tet.2017.11.024)
40. Rubottom, G.M.; Vazquez, M.A.; Pelegriana, D.R. Peracid Oxidation of Trimethylsilyl Enol Ethers: A Facile  $\alpha$ -Hydroxylation Procedure. *Tetrahedron Lett.* **1974**, *49-50*, 4319-4322. DOI: [10.1016/S0040-4039\(01\)92153-7](https://doi.org/10.1016/S0040-4039(01)92153-7)
41. Rubottom ref: Wang, H.; Andemichael, Y.W., Vogt, F.G. A Scalable Synthesis of 2S-Hydroxymutilin via a Modified Rubottom Oxidation. *J. Org. Chem.* **2009**, *74* (1), 478 – 481. DOI: [10.1021/jo801969e](https://doi.org/10.1021/jo801969e)
42. Chrobok, A. The Baeyer-Villiger oxidation of ketones with Oxone® in the presence of ionic liquids as solvents. *Tetrahedron*, **2010**, *66*, 6212-6216. DOI: [10.1016/j.tet.2010.05.091](https://doi.org/10.1016/j.tet.2010.05.091)
43. McClure, J.D.; Williams, P.H. Hydrogen Peroxide-Boron Trifluoride Etherate, a New Oxidizing Agent. *J. Org. Chem.* **1962**, *27* (1), 24-26. DOI: [10.1021/jo01048a005](https://doi.org/10.1021/jo01048a005)
44. Howard, E.; Olszewski, W.F. The Reaction of Triphenylphosphine with Some Aromatic Amine Oxides. *J. Am. Chem. Soc.* **1959**, *81* (6), 1483-1484. DOI: [10.1021/ja01515a050](https://doi.org/10.1021/ja01515a050)

## 9.0 Supporting Information

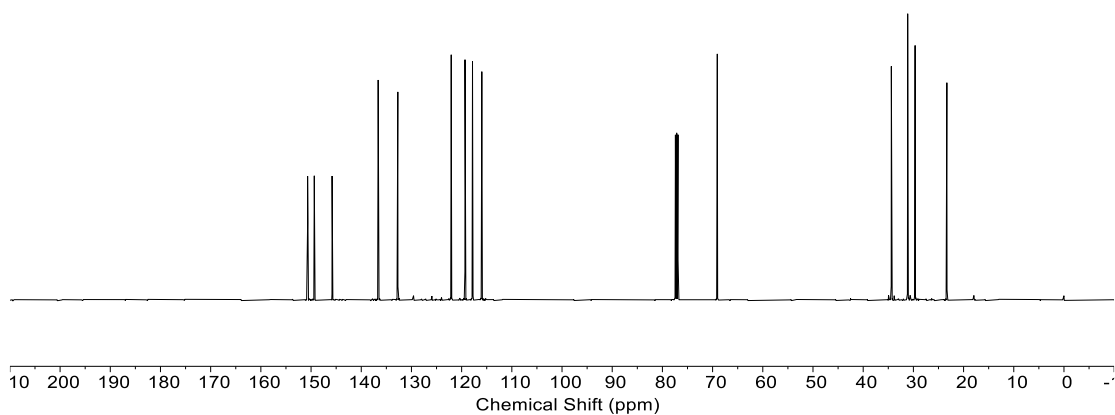
### S1. $^1\text{H}$ NMR spectrum of nitrile 2.6

Alkylated nitrile (2.6)



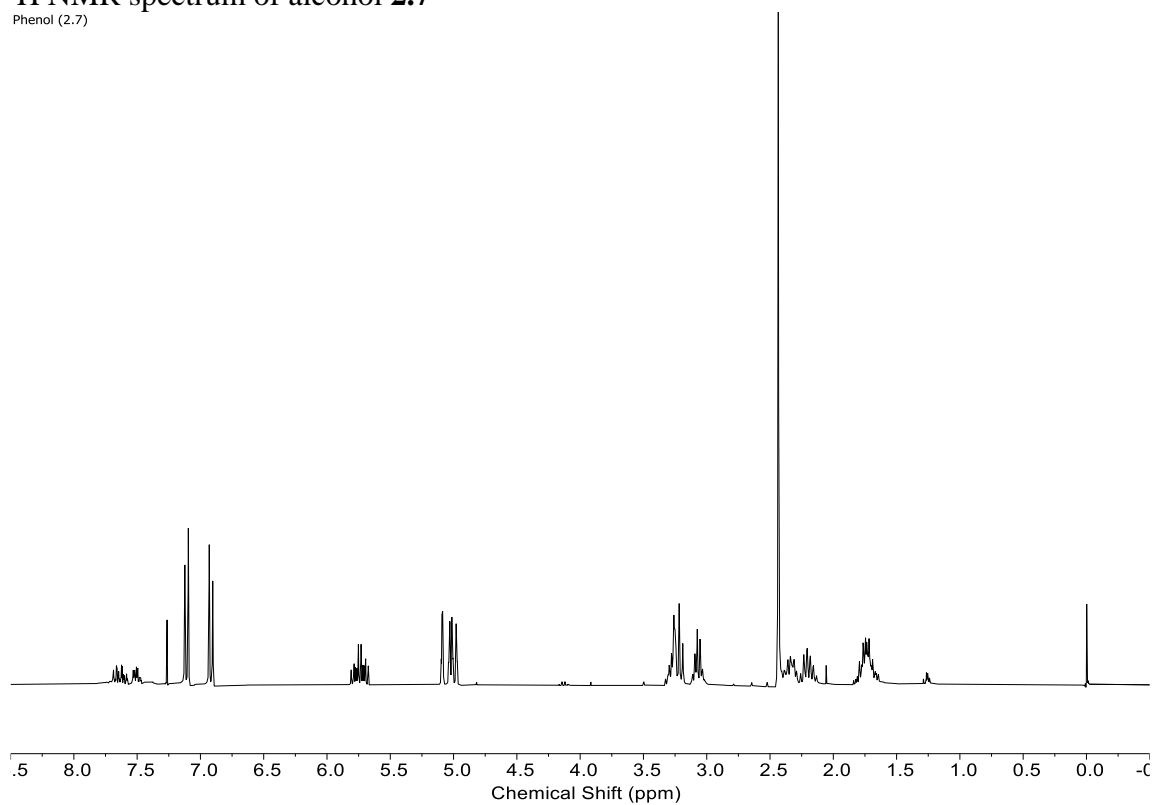
### S2. $^{13}\text{C}$ NMR spectrum of nitrile 2.6

Alkylated nitrile (2.6)



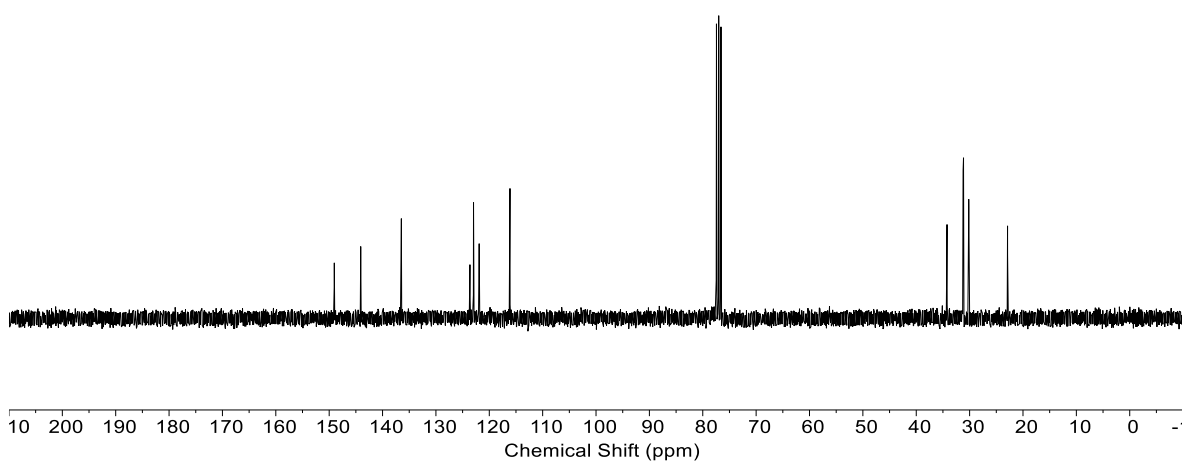
**S3.  $^1\text{H}$  NMR spectrum of alcohol 2.7**

Phenol (2.7)



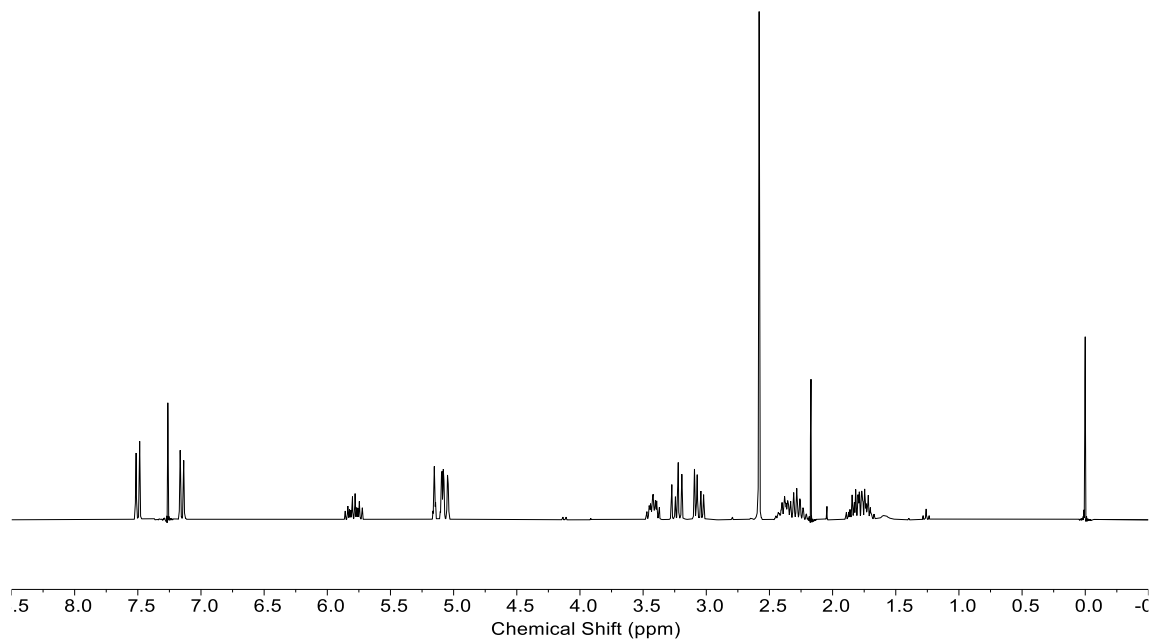
**S4.  $^{13}\text{C}$  NMR spectrum of alcohol 2.7**

Phenol (2.7)



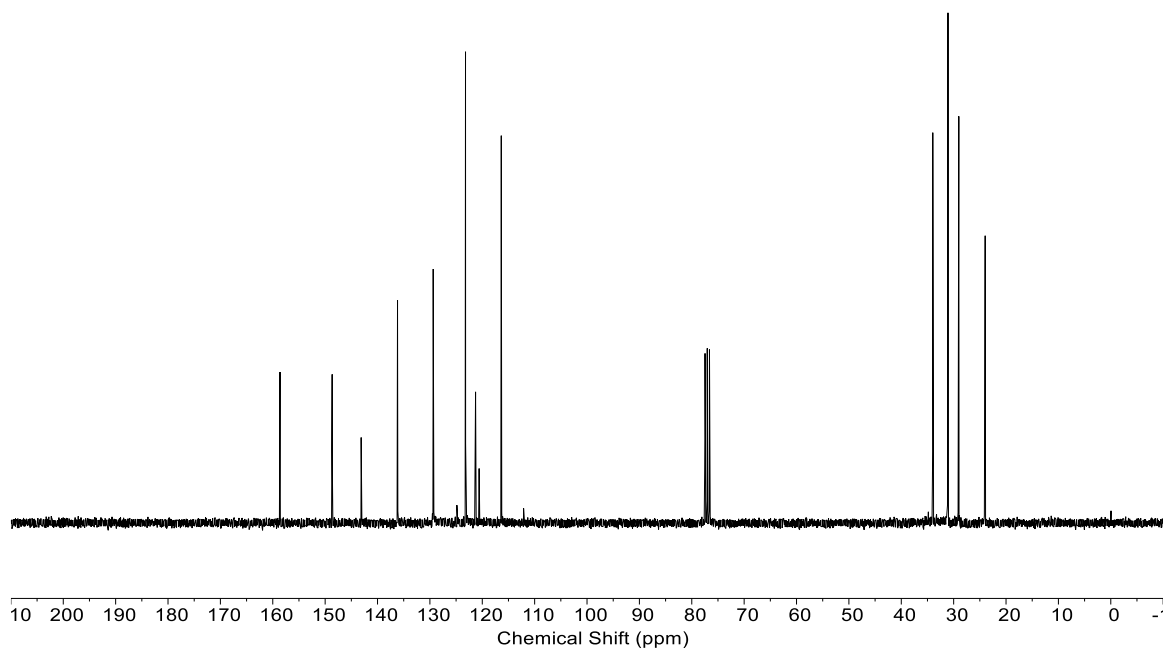
**S5.**  $^1\text{H}$  NMR spectrum of triflate **2.3**

Triflate (2.3)

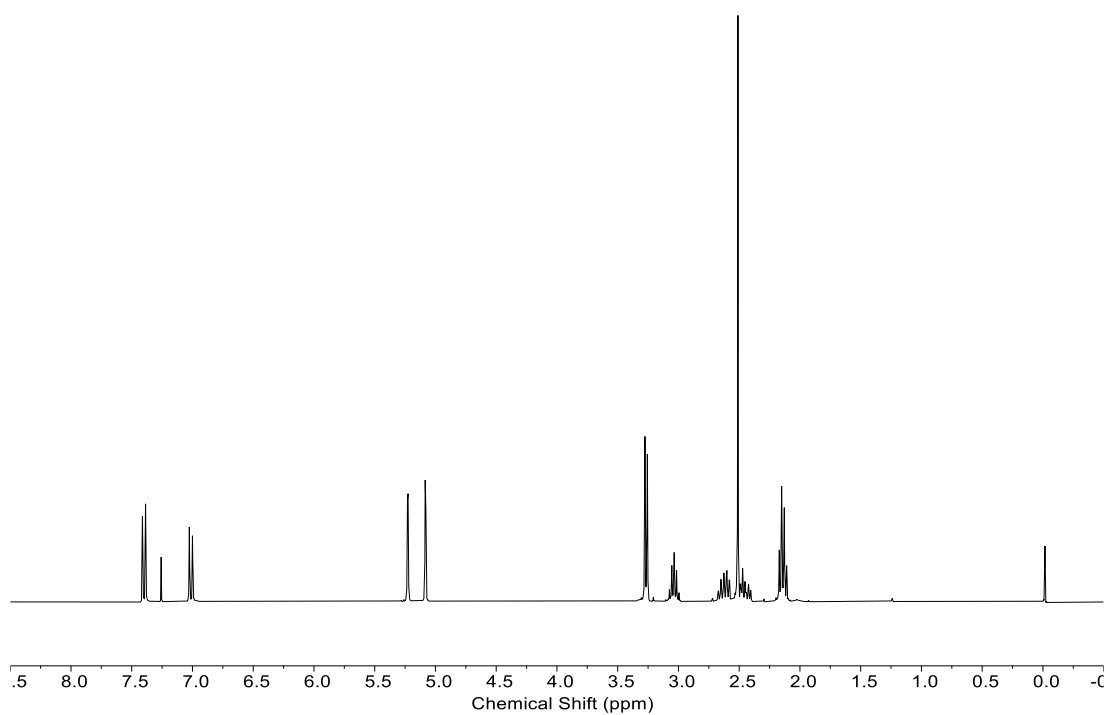


**S6.**  $^{13}\text{C}$  NMR spectrum of triflate **2.3**

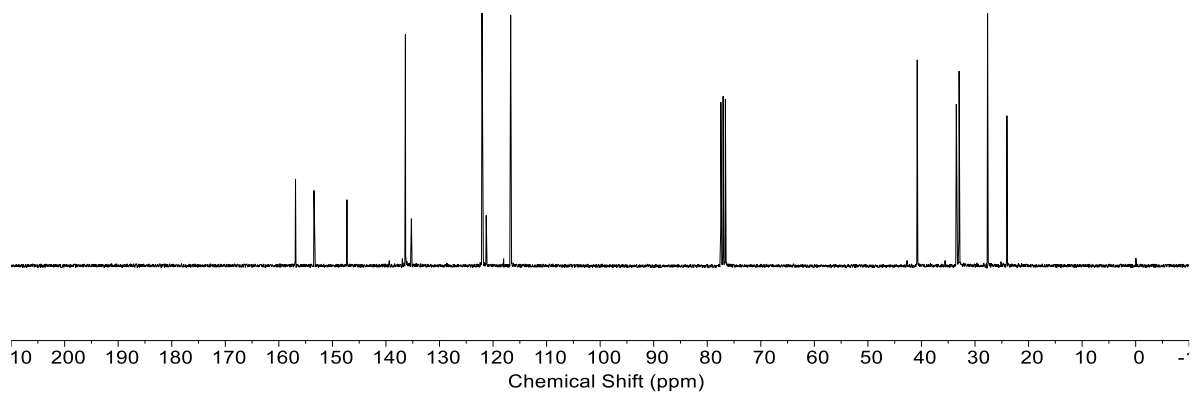
Triflate (2.3)



**S7.**  $^1\text{H}$  NMR spectrum of nitrile **2.2**  
Cyclized nitrile (2.2)

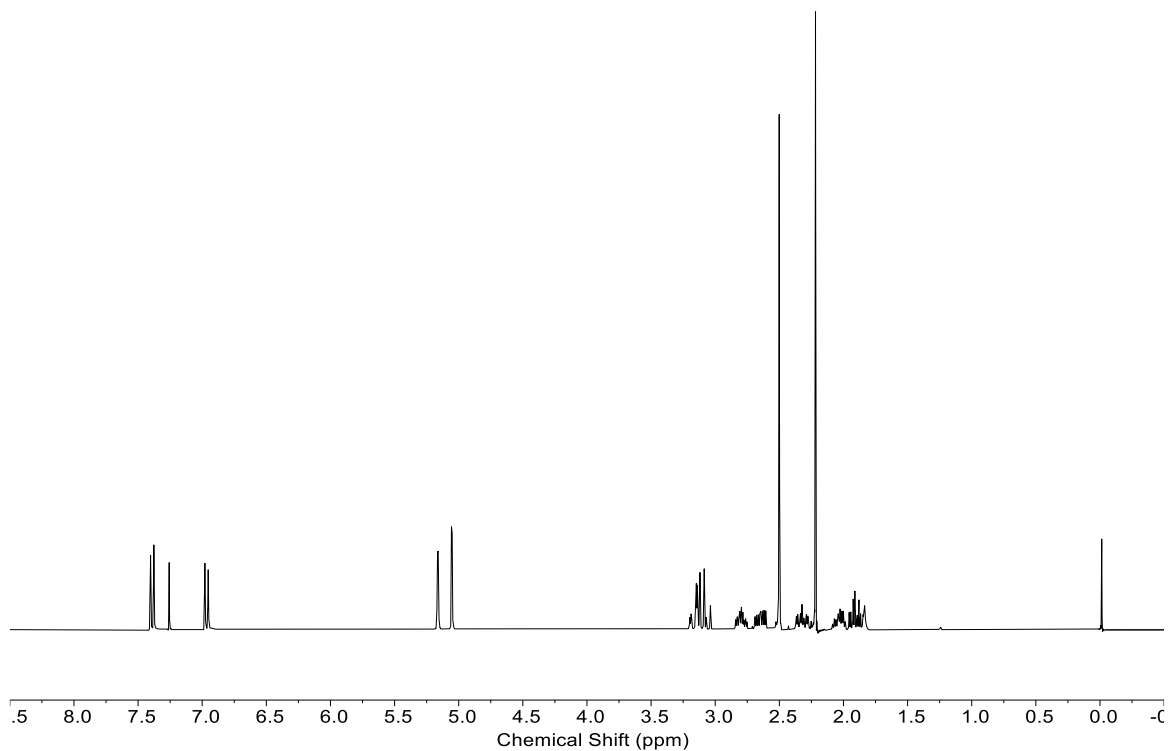


**S8.**  $^{13}\text{C}$  NMR spectrum of nitrile **2.2**  
Cyclized nitrile (2.2)



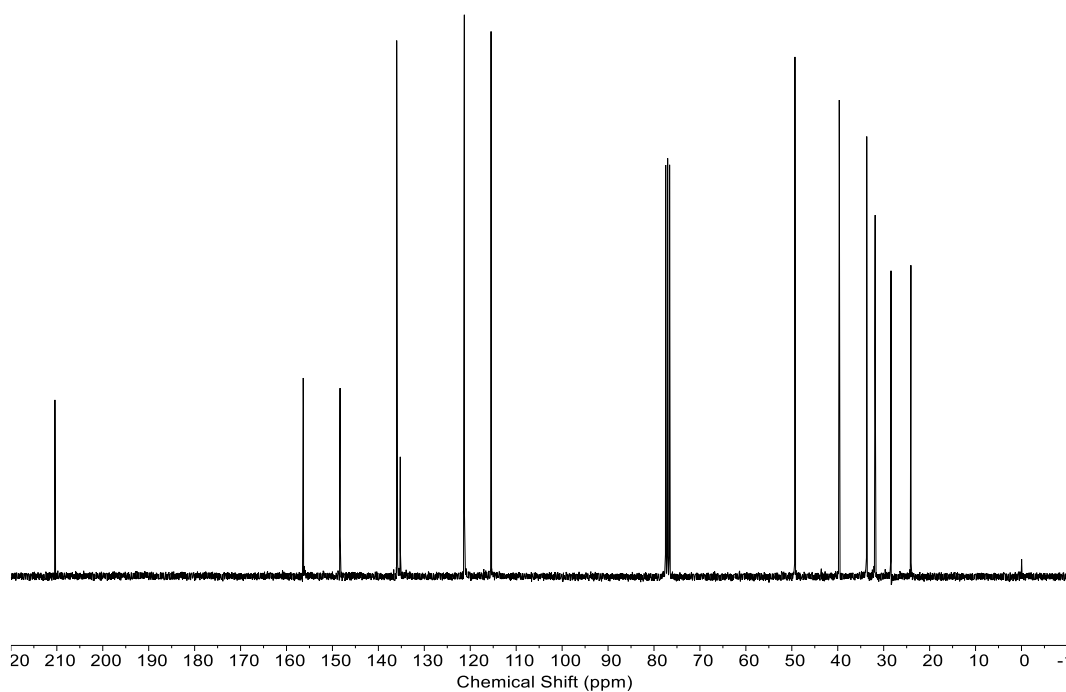
### S9. $^1\text{H}$ NMR spectrum of ketone 2.1

Alkene ketone (2.1)

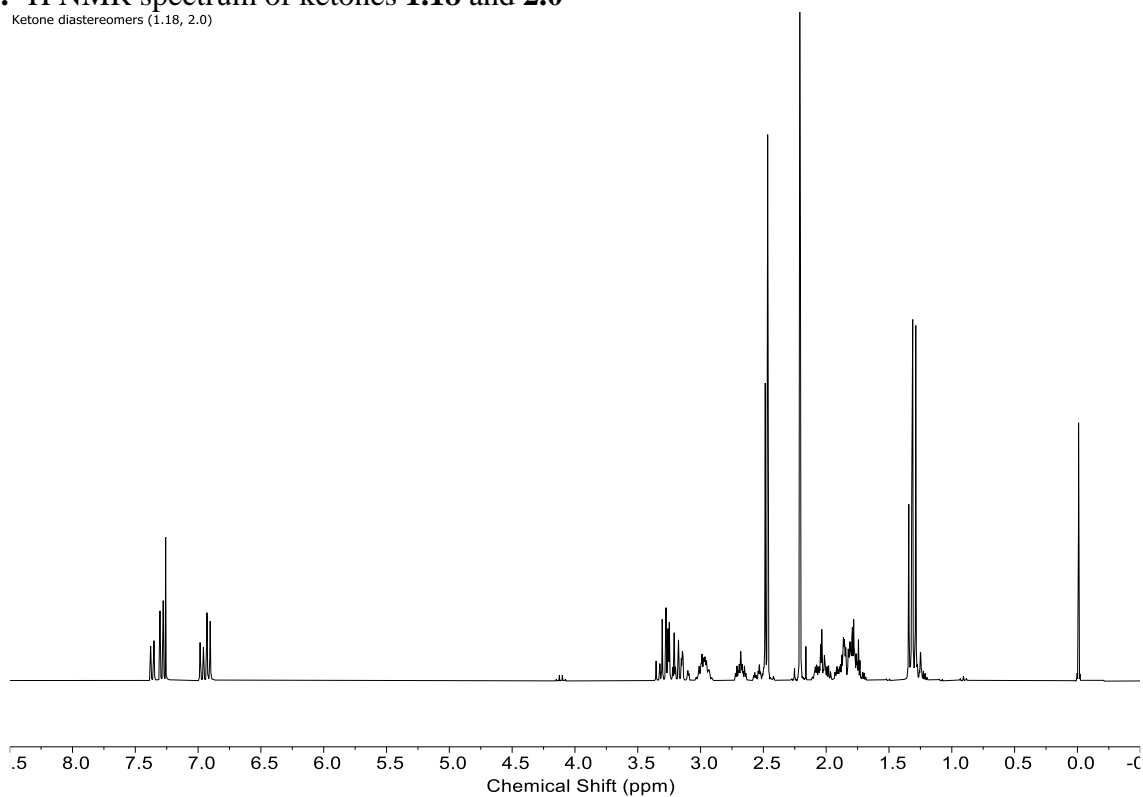


### S10. $^{13}\text{C}$ NMR spectrum of ketone 2.1

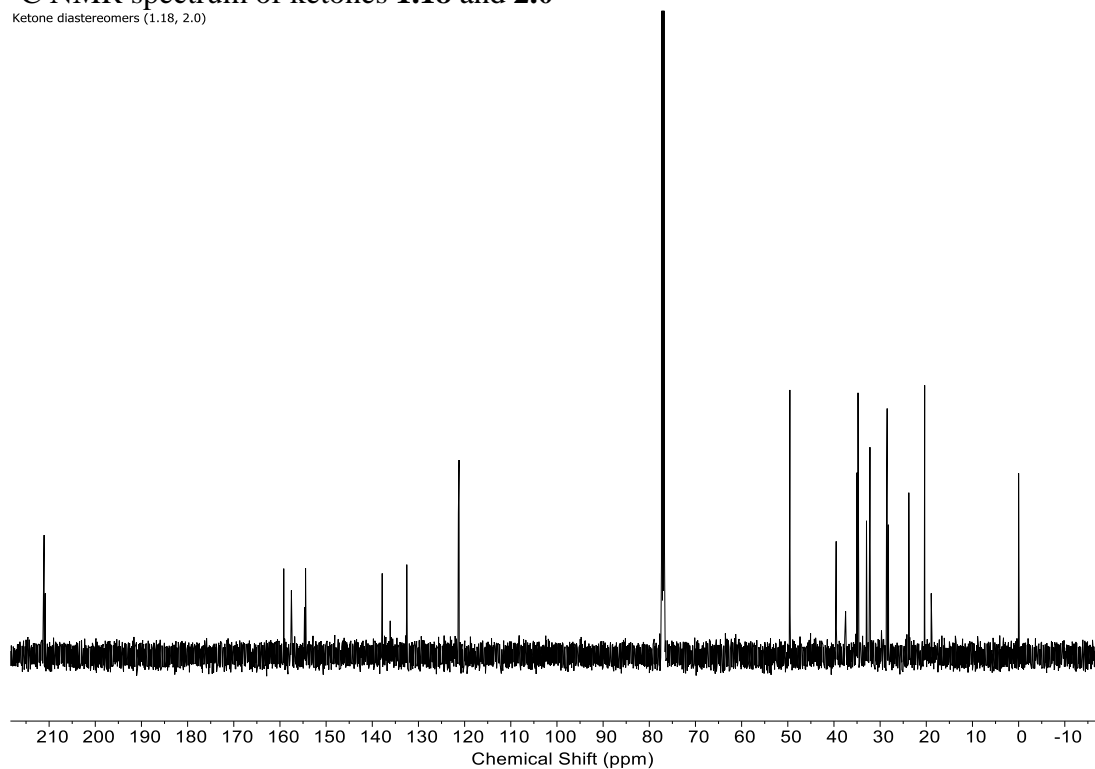
Alkene ketone (2.1)



**S11.**  $^1\text{H}$  NMR spectrum of ketones **1.18** and **2.0**  
Ketone diastereomers (1.18, 2.0)

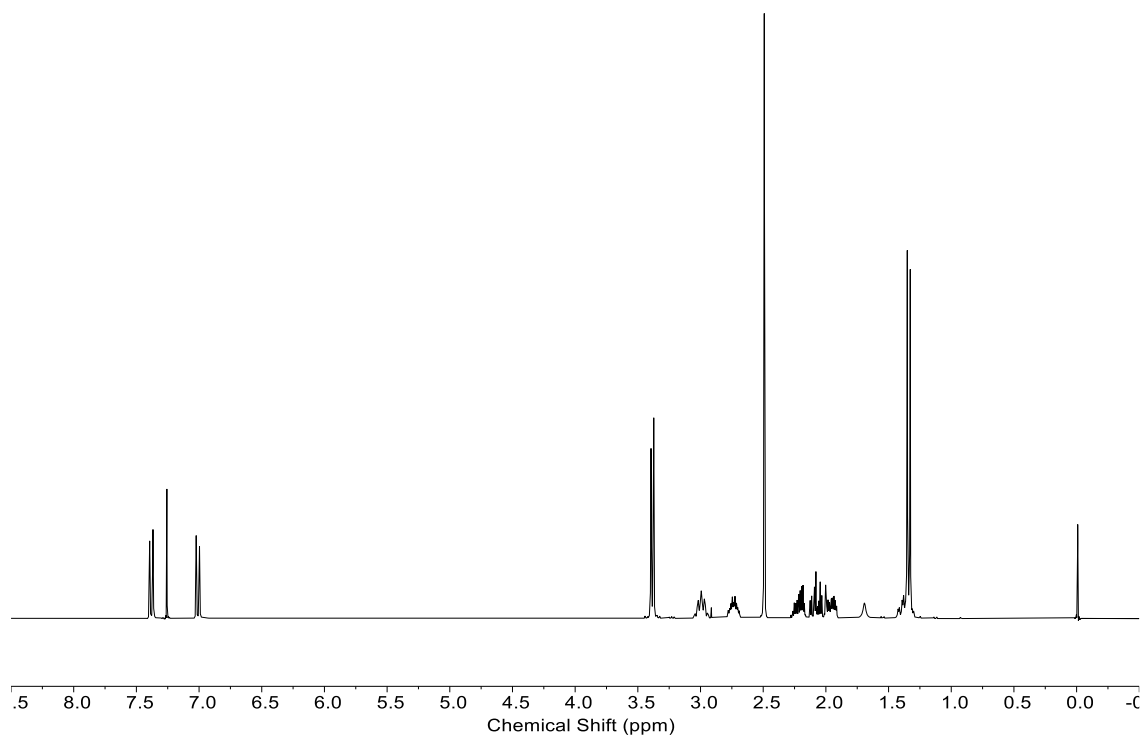


**S12.**  $^{13}\text{C}$  NMR spectrum of ketones **1.18** and **2.0**  
Ketone diastereomers (1.18, 2.0)



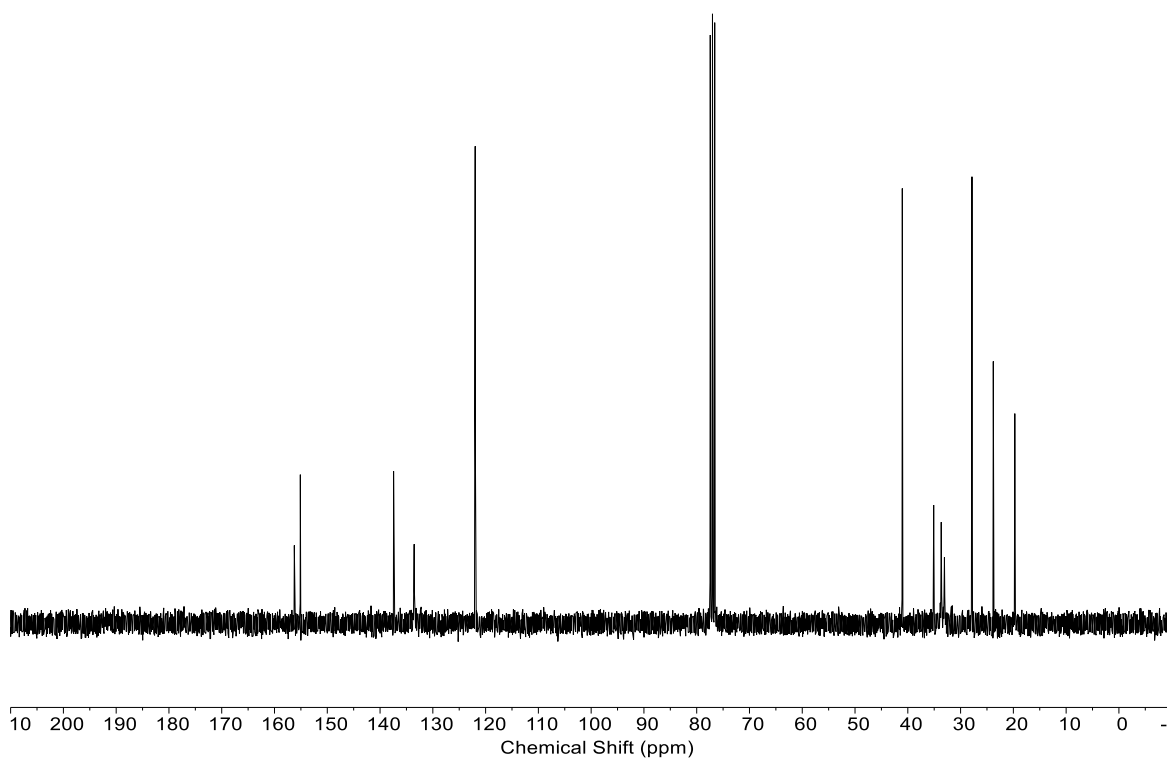
**S13.**  $^1\text{H}$  NMR spectrum of nitrile **2.8**

Nitrile (2.8)



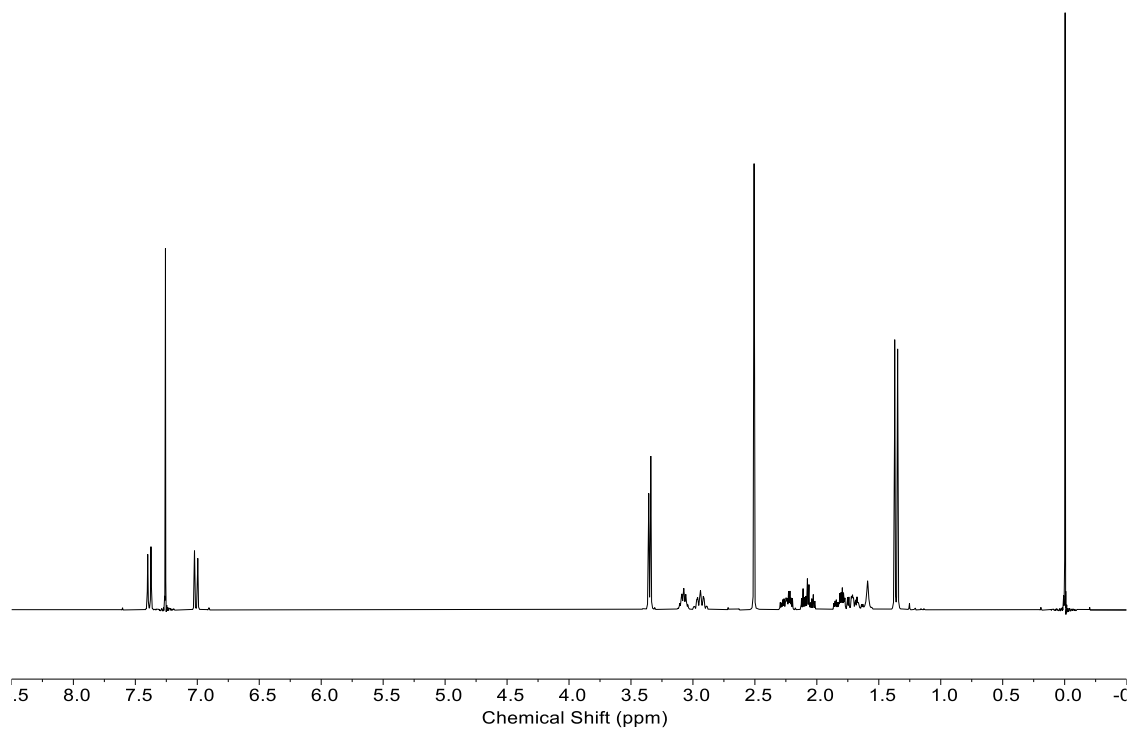
**S14.**  $^{13}\text{C}$  NMR spectrum of nitrile **2.8**

Nitrile (2.8)



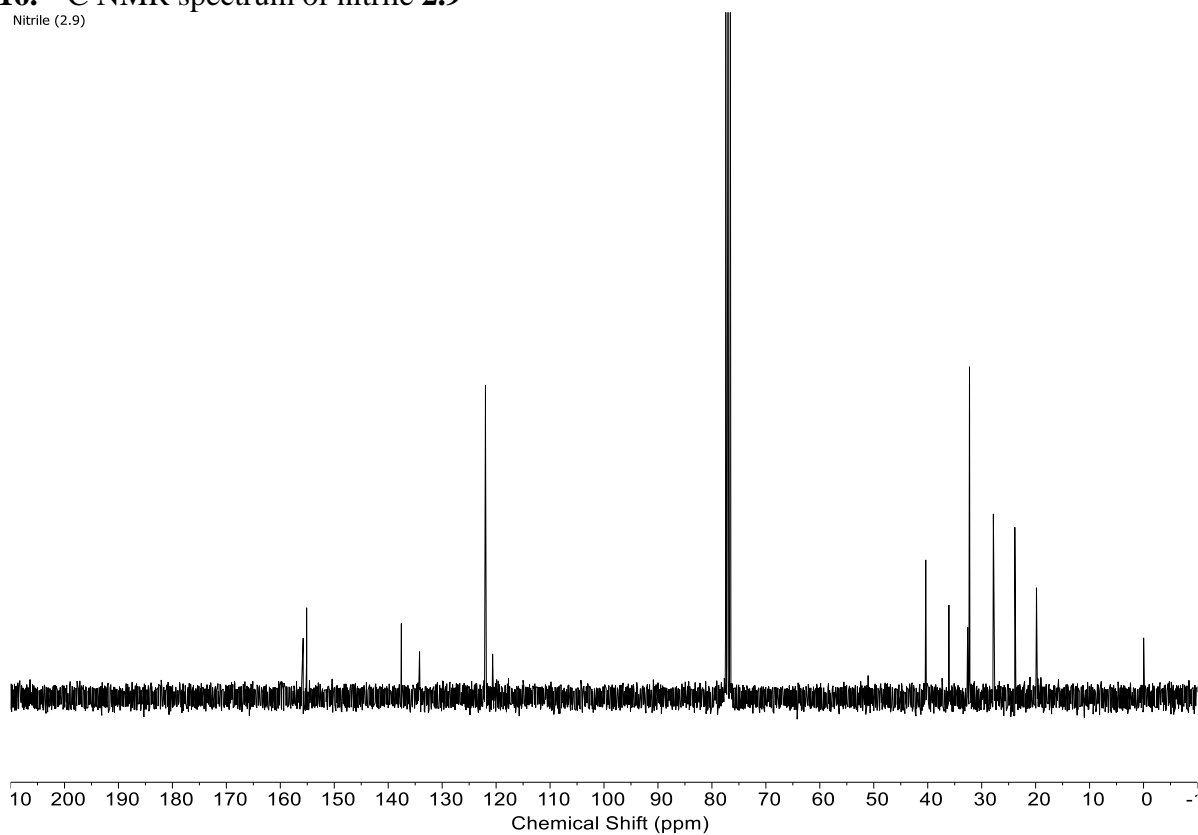
**S15.**  $^1\text{H}$  NMR spectrum of nitrile **2.9**

Nitrile (2.9)

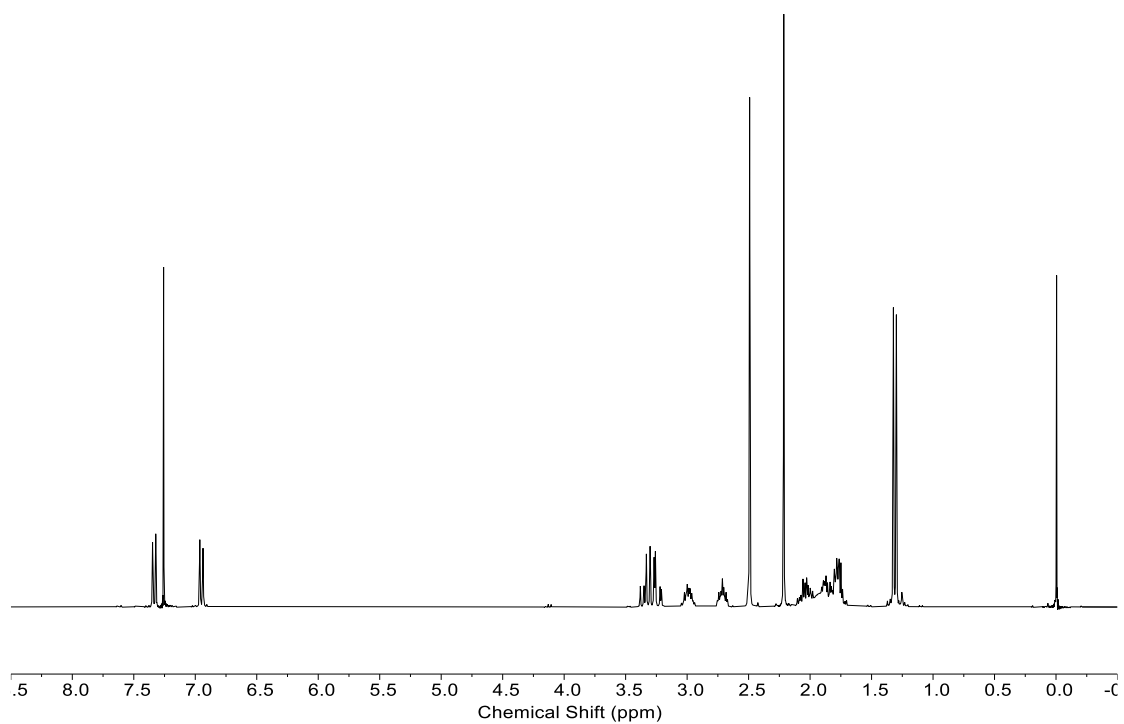


**S16.**  $^{13}\text{C}$  NMR spectrum of nitrile **2.9**

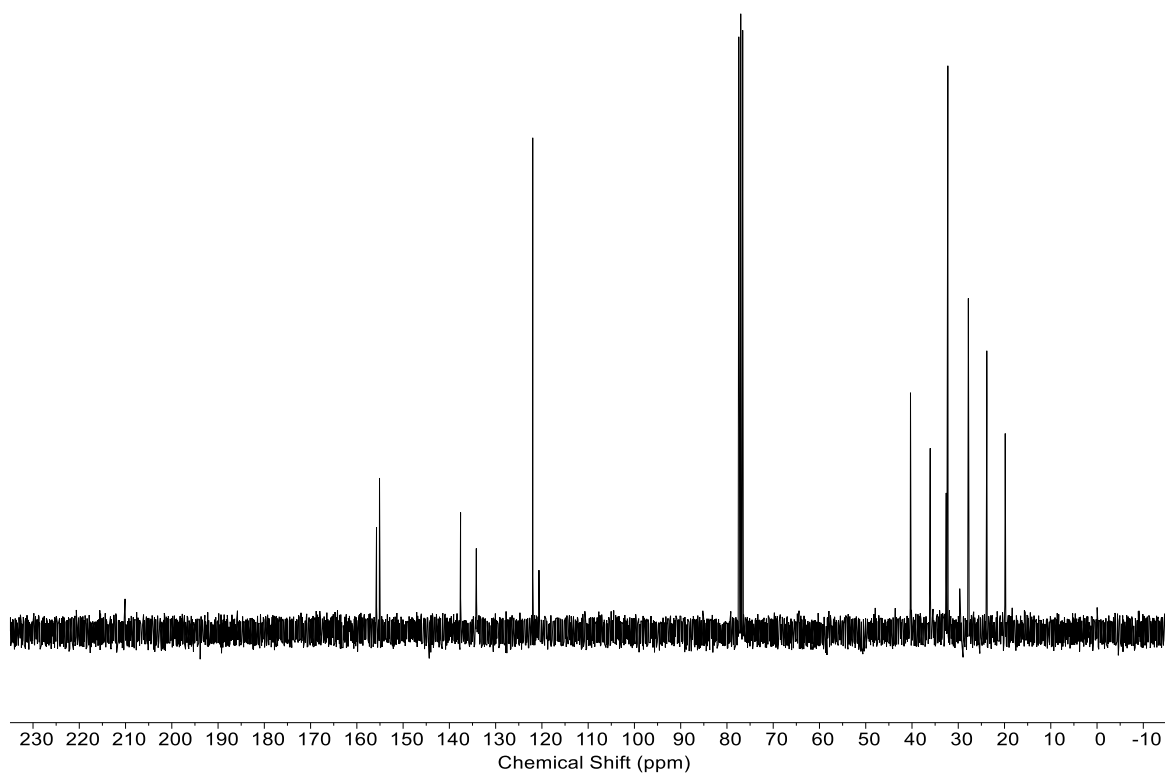
Nitrile (2.9)



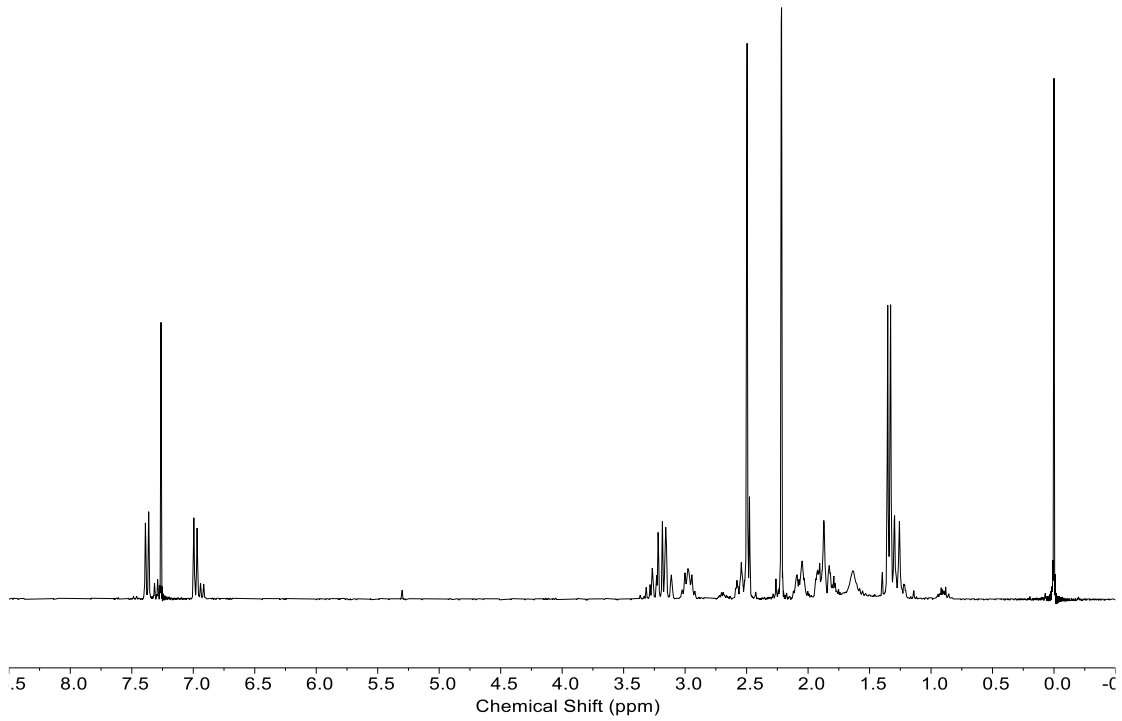
**S17.**  $^1\text{H}$  NMR spectrum of epi-rupestine D (**2.0**)  
epi-rupestine D (2.0)



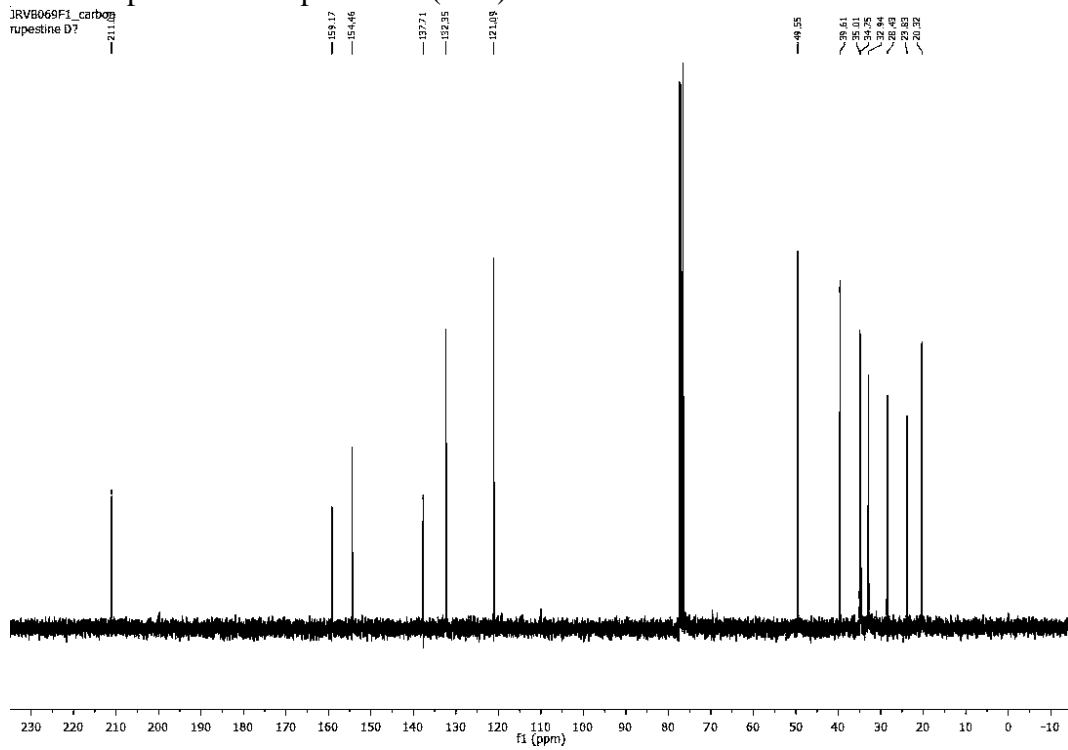
**S18.**  $^{13}\text{C}$  NMR spectrum of epi-rupestine D (**2.0**)  
epi-rupestine D



**S19.**  $^1\text{H}$  NMR spectrum of rupestine D (**1.18**)  
rupestine D 1.18)

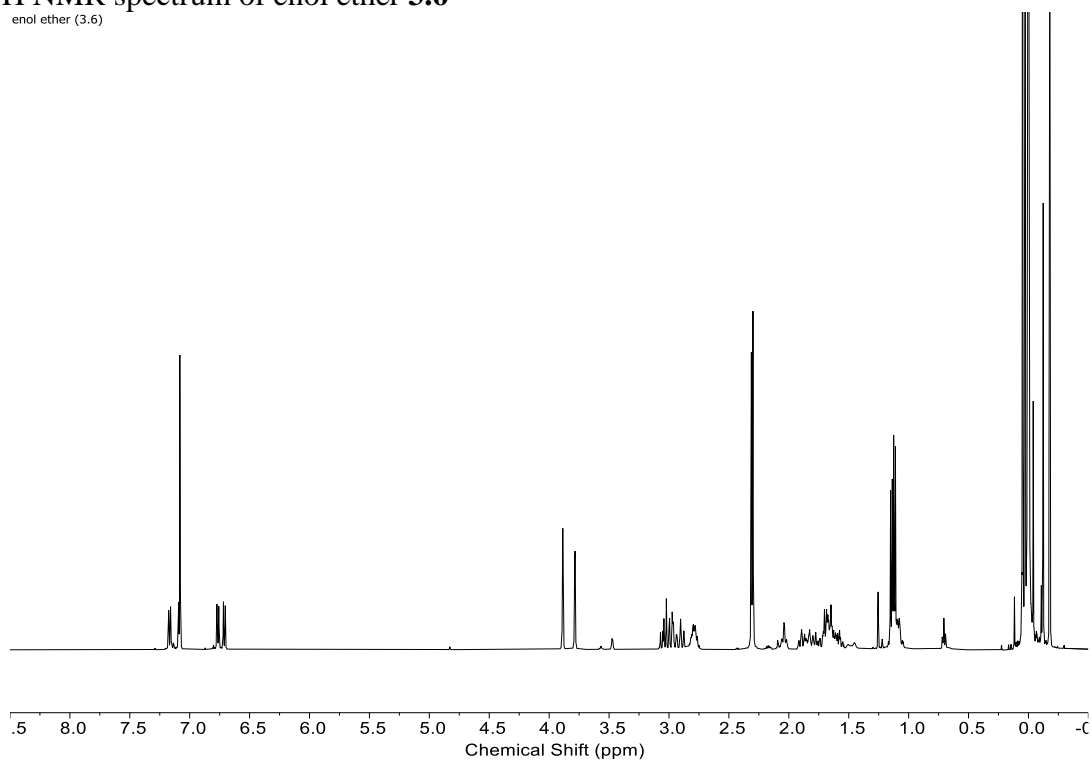


**S18.**  $^{13}\text{C}$  NMR spectrum of rupestine D (**1.18**)



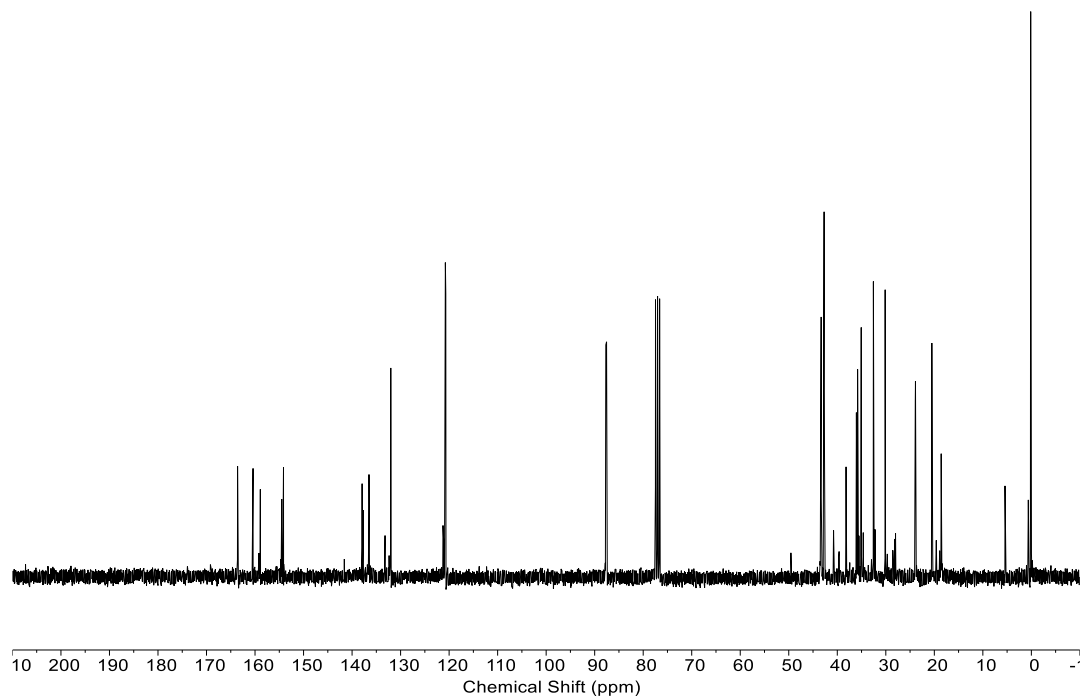
**S21.**  $^1\text{H}$  NMR spectrum of enol ether **3.6**

enol ether (3.6)



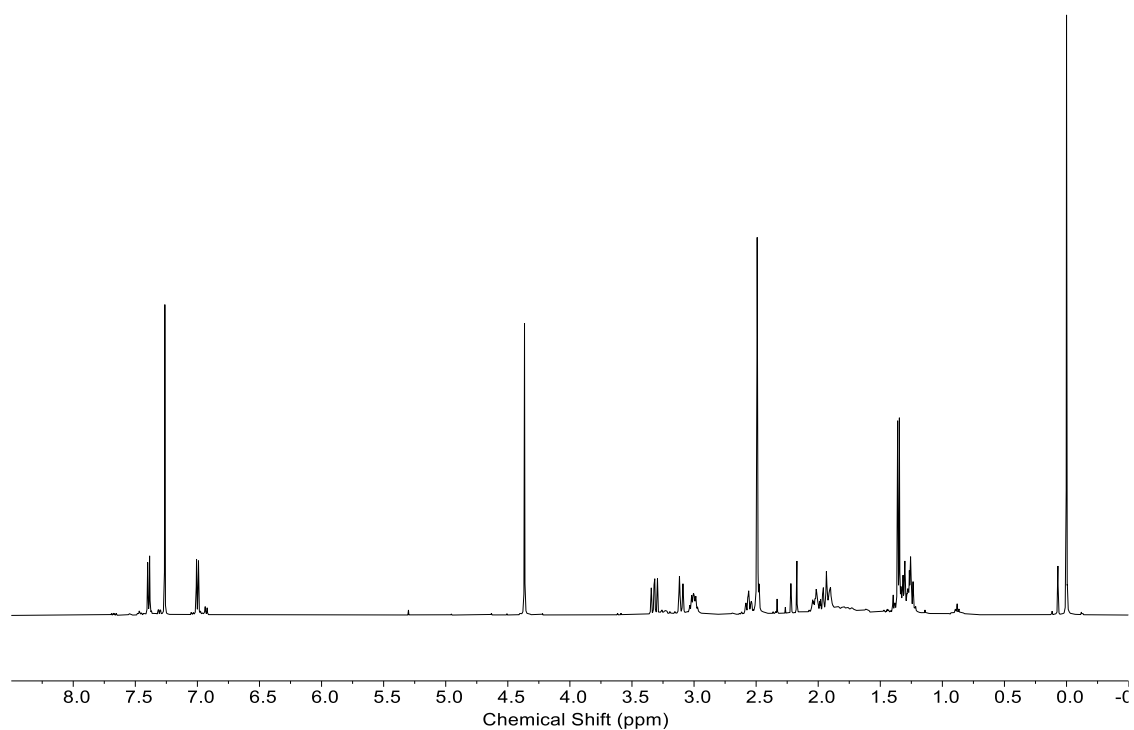
**S22.**  $^{13}\text{C}$  NMR spectrum of enol ether **3.6**

enol ether (3.6)



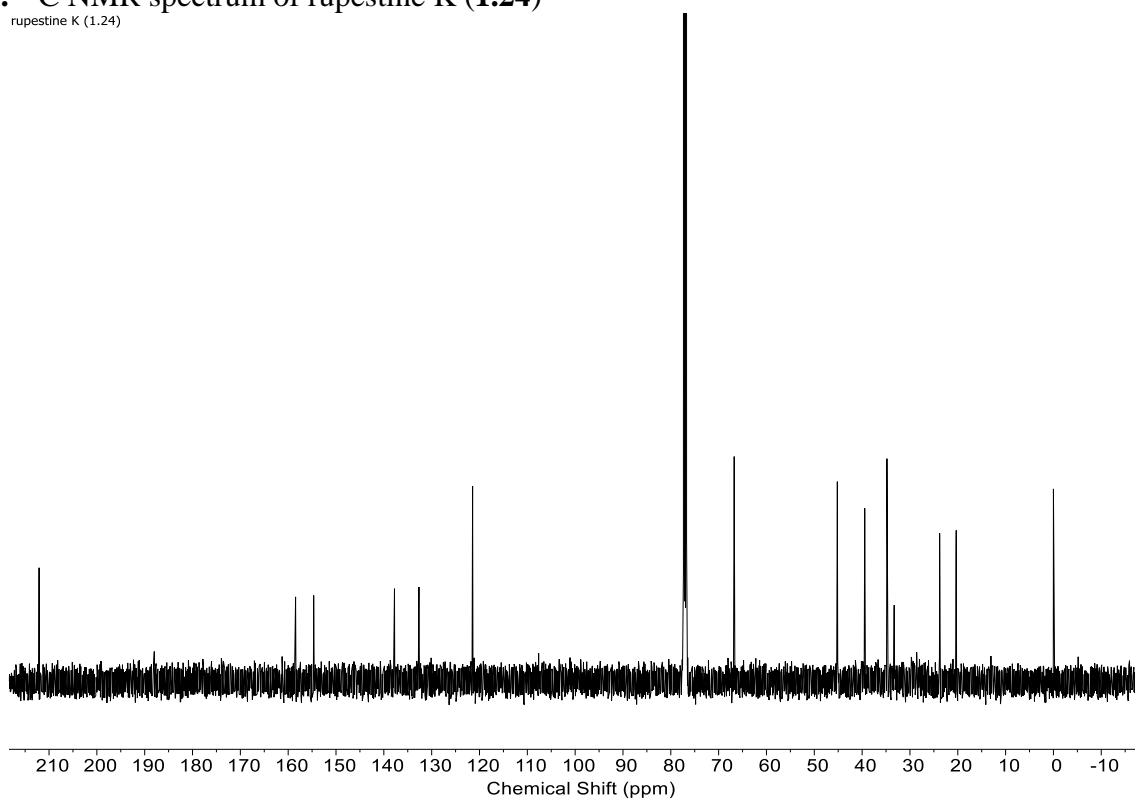
**S23.**  $^1\text{H}$  NMR spectrum of rupestine K (1.24)

rupestine K (1.24)

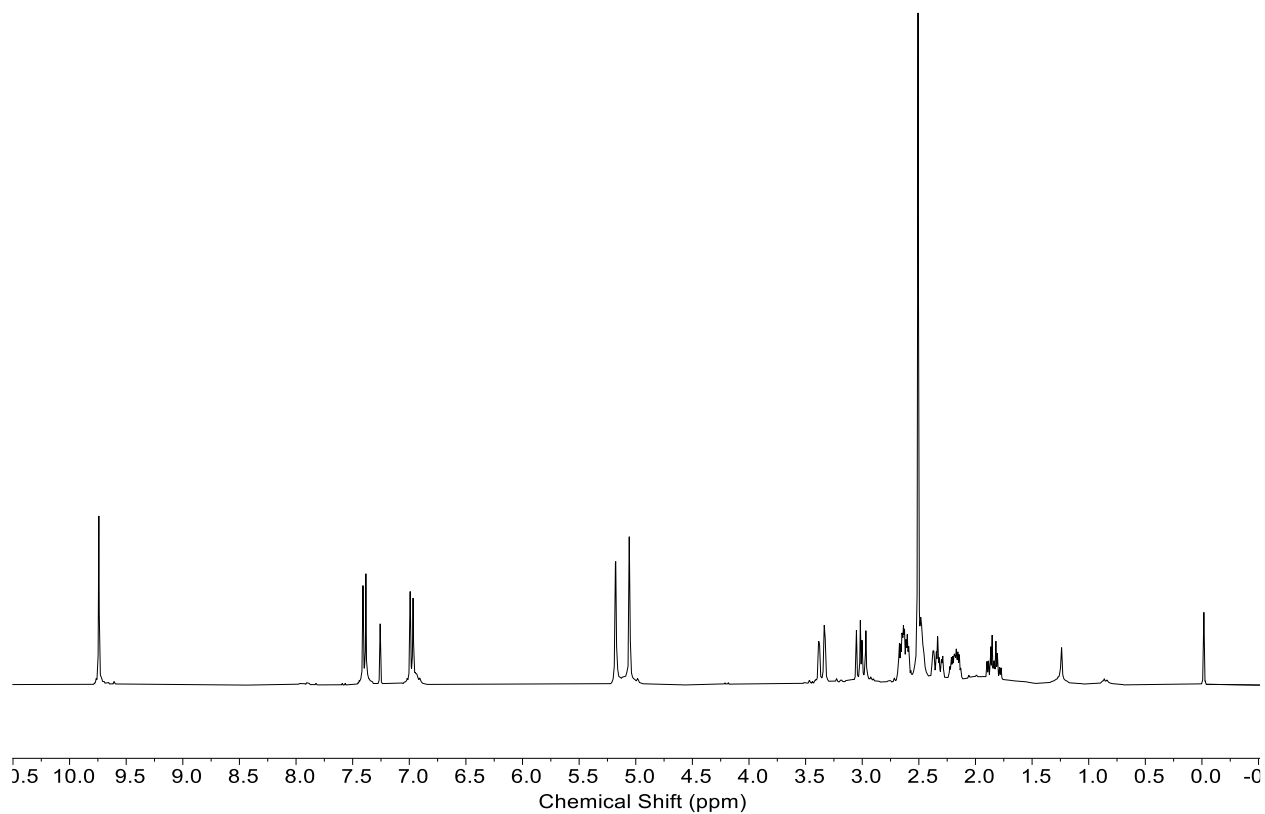


**S24.**  $^{13}\text{C}$  NMR spectrum of rupestine K (1.24)

rupestine K (1.24)



**S25.**  $^1\text{H}$  NMR spectrum of aldehyde **3.3**  
aldehyde



**S26.**  $^{13}\text{C}$  NMR spectrum of aldehyde **3.3**  
BJMB23pure\_carb

